Identification and characterization of a novel cell-envelope subcomplex crucial for A-motility in *M. xanthus*

Dissertation
zur Erlangung des Doktorgrades
der Naturwissenschaften
(Dr. rer. nat.)

dem Fachbereich Biologie
der Philipps-Universität Marburg
vorgelegt von

Beata Jakobczak
aus Gizycko, Polen

Marburg an der Lahn, Mai 2014

Die Untersuchungen zur vorliegenden Arbeit wurden von Oktober 2010 bis Dezember 2013 am Max-Planck-Institut für terrestrische Mikrobiologie unter der Leitung von Prof. Dr. Lotte Søgaard-Andersen durchgeführt.

Vom Fachbereich Biologie der Philipps-Universität Marburg als Dissertation angenommen am:

Erstgutachterin: Prof. Dr. Lotte Søgaard-Andersen

Zweitgutachterin: Prof. Dr. Erhard Bremer

Weitere Mitglieder der Prüfungskommission:

Prof. Dr. Uwe Maier

Prof. Dr. Andrea Maisner

Tag der mündlichen Prüfung:

Die während der Promotion erzielten Ergebnisse sind zum Teil in folgenden Originalpublikationen veröffentlicht worden:

The small G-protein MglA connects the motility machinery to the MreB actin cytoskeleton at bacterial focal adhesions
Edina Hot, Mathilde Guzzo, Damien Alcor, Adrien Ducret, Beata Jakobczak, Daniela Keilberg, Eric Macia, Sandra Lacas Gervais, Laura Faure, Peter Lenz, Michel Franco, Lotte Søgaard-Andersen, Tam Mignot (in submission).

GltBAC complex is an essential cell-envelope component of bacterial focal adhesions in gliding motility
Beata Jakobczak, Daniela Keilberg, Kristin Wuichet and Lotte Søgaard-Andersen (manuscript in preparation).

Table of contents

Abstract

Myxococcus xanthus is a rod-shaped, Gram-negative bacterium that has two different motility systems: the A- and the S-motility system. A-motility allows the movement of single cells, while S-motility is cell-cell contact-dependent and is similar to twitching motility in other bacteria. If genes of one of the motility systems are deleted, cells remain motile by the means of the remaining system. The exact mechanism of A-motility is not known, however it has been shown to be powered by the H^+ gradient across the cytoplasmic membrane through the AglRQS motor complex. One of the current A-motility models suggests that proteins involved in this system localize to multiple protein complexes referred to as FAs (Focal Adhesions) that are distributed along the cell body and fixed to the substratum in moving cells while a second model suggest a helical motor model. The FAs were suggested to span all subcellular compartments close to the gliding surface. So far, only few proteins essential for A-motility were found to localize to FAs. Notably, proteins localizing to the outer membrane have so far not been identified as components of FAs.

In this study, the function of four proteins that were previously identified as essential for A-motility, GltK, GltB, GltA and GltC was investigated. Bioinformatic predictions suggested that these four proteins localize to the periplasm and outer membrane making them interesting to study as potential candidates for anchoring FAs to the substratum. It was demonstrated that GltB, GltA and GltC are dependent on each other for stability. Furthermore, interaction studies and fractionation analysis strongly indicate that these three A-motility proteins form a complex in the periplasm and outer membrane. Colocalization studies with AglZ revealed that GltB and GltA localize to FAs. Moreover, our analyses on protein localization demonstrate that GltK, GltB, GltA and GltC are essential for the assembly of FAs. *Vice versa*, GltB and GltA incorporation in to FAs depends on other components of FAs including AglZ, AglQ and MglA. Thus, our experiments uncovered the first outer membrane subcomplex essential for the formation of FAs involved in A-motility in *M. xanthus*.

Zusammenfassung

Myxococcus xanthus ist ein Stäbchen-förmiges, Gram-negatives Bakterium und verfügt über zwei verschiedene Fortbewegungssysteme: das A- und das S-Bewegungssystem. Das A-Bewegungssystem erlaubt die Bewegung einzelner Zellen, wohingegen die S-Bewegung abhängig von Zell-Zell-Kontakten ist und der „twitching“ Bewegung anderer Bakterien, z.B. Pseudomonaden, ähnelt. Deletiert man Gene des einen oder anderen Bewegungssystems, bleiben die Zellen aufgrund des jeweils anderen Bewegungssystems beweglich. Der exakte Mechanismus, mit dem die A-Bewegung erfolgt ist weitgehend unbekannt, aber die Energiequelle ist der Wasserstoffionengradient durch die Zytoplasmamembran der von dem Motorkomplex, bestehend aus den Proteinen AglRQS, genutzt wird. Eines der derzeit zwei verschiedenen Modelle für das A-Bewegungssystem sieht vor, dass die beteiligten Proteine in mehreren Proteinkomplexen (FAs für „focal adhesion“-Komplexe) organisiert sind, die entlang der Längsachse der Stäbchen verteilt sind und während der Vorwärtsbewegung der Zellen mit der Oberfläche des Medium fest verbunden bleiben. Das andere Model basiert auf der Existenz eines helikalen Motors, der für die A-Bewegung verantwortlich ist. Basierend auf dem ersten Model wurde vermutet, dass die FAs vom Zytoplasma bis zur Oberfläche des Mediums alle subzellulären Kompartimente der Zelle umspannen. Bisher konnten erst wenige Proteine identifiziert werden, die in FAs lokalisieren (z.B. AglZ), aber darunter keine Proteine der äußeren Membran.

In dieser Arbeit wurde die Funktion der vier Proteine GltK, GltB, GltA und GltC, zuvor bekannt als essentielle Proteine des A-Bewegungssystems, untersucht. Bioinformatorische Vorhersagen wiesen darauf hin, dass diese Proteine sowohl im Periplasma als auch in der äußeren Membran lokalisieren könnten, somit erschienen diese Proteine als interessante Kandidaten, potentiell zuständig für die Verbindung der FAs zu der Mediumsoberfläche. Durch zahlreiche experimentelle Ansätze konnte nicht nur gezeigt werden, dass sich die Proteine GltB, GltA und GltC gegenseitig stabilisieren, sondern darüber hinaus auch miteinander interagieren und vermutlich einen Komplex im Periplasma und der äußeren Membran bilden. Kolokalisationsstudien mit dem

Protein AglZ zeigten, daß GltB und GltA mit AglZ kolokalisieren und somit ebenfalls in FAs lokalisieren. Darüber hinaus konnte gezeigt werden, dass alle vier Proteine GltK, GltB, GltA und GltC essentiell für die Assemblierung der FAs sind. *Vice versa*, ist die Lokalisierung von GltB und GltA in den FAs abhängig von anderen Komponenten der FAs, wie z.B. AglZ, AglQ und MglA. Somit kann man abschließend sagen, dass durch die vorliegende Arbeit die Identifizierung des ersten Unterkomplex der äußeren Membran, der essentiell für das A-Bewegungssystem von *M. xanthus* ist, gelungen ist.

Abbreviations

ATP/ADP	Adenosin tri-/diphosphate
BACTH	Bacterial Adenylate Cyclase-based Two-Hybrid
bp	base pairs
BSA	Bovine serum albumin
cDNA	Single-stranded complementary DNA
Cm	Chloramphenicol
CTT	Casitone Tris medium
DMSO	Dimethyl sulfoxide
DTT	Dithiothreitol
ECM	Extracellular matrix
EM	Electron microscopy
EPS	Exopolysaccharides
FAs	Focal adhesions
FRAP	Fluorescence recovery after photobleaching
GDP/GTP	Guanosine di- /Guanosine triphosphate
h	hours
IM	Inner membrane
IPTG	Isopropyl β-D-1-thiogalaktopyranoside
Km	Kanamycin
LPS	Lipopolysaccharides
min	minutes
OM	Outer membrane
PMF	Proton motive force
pN	piconewton
SDS-PAGE	Sodium dodecyl sulfate polyacrilamide gel electrophoresis
sec	seconds
Sec	Secretion
sfGFP	superfolder green fluorescent protein
T4P	Type IV pili
TIRF	total internal reflection fluorescence
YFP	Yellow fluorescent protein
WT	Wild type

1 Introduction

1.1 *Myxococcus xanthus*

Myxococcus xanthus is a rod-shaped, Gram-negative soil bacterium that belongs to the delta-subgroup of the proteobacteria. *M. xanthus* cells can't swim in liquid media, but are able to move by two genetically distinct motility systems, the A- and S-motility system on solid media (Kaiser, 1979b). Interestingly, the cells of *M. xanthus* have the ability to reverse their direction of movement. Reversals depend on a polarity switch, which results in inversion of the cell poles so that the lagging cell pole becomes the leading cell pole and *vice versa*.

The *M. xanthus* life cycle is complex and includes phases of vegetative growth and starvation-induced development, and both phases depend strongly on directed cell movements on solid surfaces (Figure 1). In favorable environments *M. xanthus* cells prey on nutrients from decomposing soil and detritus as well as on other organisms by producing and secreting antibiotics and lytic enzymes (Shimkets, 1999b, Reichenbach, 1999). The *M. xanthus* genome encodes multiple proteases, nucleases, lipases and antibiotics that are involved in the digestion of nutrients and microorganisms (Rosenberg *et al.*, 1977). Predation on other microorganisms includes close contact between *M. xanthus* cells and macromolecules which leads to rhythmic cell movements referred to as rippling (Reichenbach, 1999). Rippling is observed as waves of cells on a surface and is typically initiated prior to aggregation.

Many bacteria have evolved strategies that enable their survival in harsh environments. When *M. xanthus* cells are starved for nutrients they enter a developmental pathway, which begins with cell aggregation and results in the formation of fruiting bodies, inside which the rod-shaped cells differentiate into spores referred to as myxospores. Approximately 15% of the cell population undergo sporulation (O'Connor & Zusman, 1991b), while 80% of cells undergo programmed cell death (Wireman & Dworkin, 1977). The remaining 5% of cells differentiate into peripheral rods. These cells show a different pattern of protein expression when compared to vegetative and aggregating cells (O'Connor & Zusman, 1991a) and form a monolayer of cells which surrounds fruiting bodies. After 24 to 72 h myxospores are formed and each fruiting body contains 10^5 to

10^6 spores (Shimkets, 1999a). During sporulation rod-shaped *M. xanthus* cells undergo a morphological change, which reshapes the cell into a sphere of ~2 µm in diameter (Dworkin & Voelz, 1962), at this time the spore coat material that is essential for cell integrity and heat and sonication resistance is synthesized and assembled at the spore surface (Sudo & Dworkin, 1969). It was reported that Nfs and Exo proteins are involved in the spore coat formation (Muller *et al.*, 2012). Finally, the last step of the *M. xanthus* life cycle is the germination process, which takes place when nutrients become available.

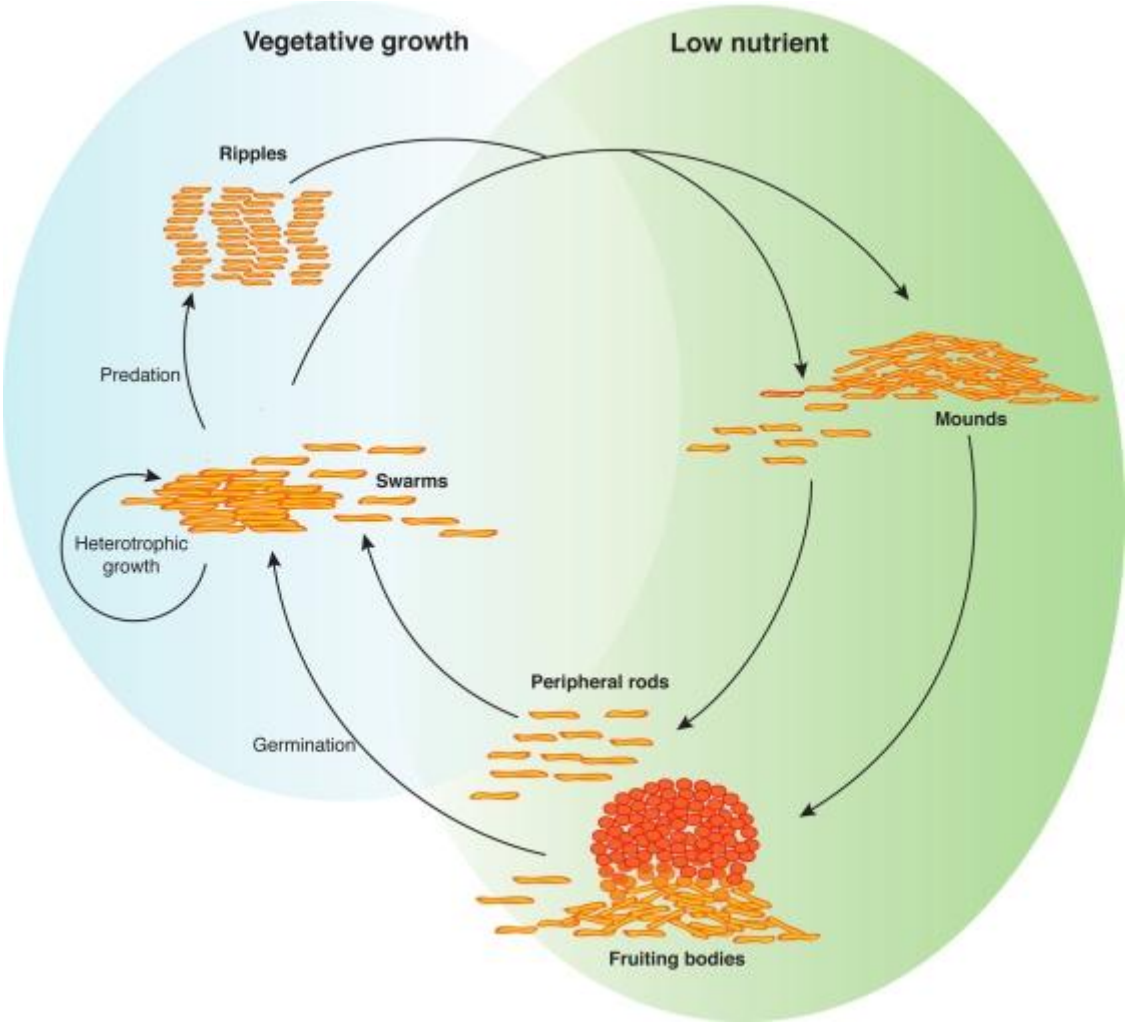

Figure 1. Lifecycle of *M. xanthus*.
Schematic representation of the different stages of the *M. xanthus* life cycle. The figure is reproduced from Mauriello *et al.* (2010).

1.2 Gliding motility of bacteria

Motility in bacteria is involved in processes such as chemotaxis, predation, virulence, colony growth, expansion, biofilm formation and development (Berleman & Kirby, 2009, Kearns, 2010, Miyata, 2010, Zusman *et al.*, 2007). Bacteria have evolved more than one mechanism to move on surfaces. Swarming motility involves rotation of flagellar filaments and is common for example in *Proteus mirabilis*, *Vibrio parahaemolyticus* and *Seratia marcescens* (Harshey, 1994). “Twitching motility” is based on polar retractile T4P (type IV pili) commonly found in *Pseudomonas, Vibrio* and *Neisseria* species (Henrichsen, 1983, Mattick, 2002a, Herrington *et al.*, 1988, Mignot, 2007). Other bacteria such as *M. xanthus*, *Flavobacterium johnsoniae* and some *Mycoplasma* spread over surfaces by a process known as gliding motility (Hoiczyk, 2000, McBride, 2000, Spormann, 1999). The gliding motility machineries are highly divergent in comparison to the T4P and flagellar systems, which are highly conserved and broadly distributed among bacteria (Pelicic, 2008, Baron *et al.*, 2007). The proteins known to be involved in gliding motility in these three species are unrelated, indicating that each system evolved independently (Jarrell & McBride, 2008).

Mycoplasma mobile is a Gram-positive pathogenic bacteria that lacks a peptidoglycan layer (Razin *et al.*, 1998). It is able to glide on glass at an average speed of 2.0 to 4.5 µm/s exerting a force up to 27 pN. The movement occurs in the direction of a membrane protrusion that is formed close to a cell pole. Rapid freeze-fracture deep-etch replica EM revealed that the gliding machinery is located in the neck area at the base of a membrane protrusion in the form of leg like structures that extend from the membrane as shown using (Figure 2A). The gliding machinery is supported by cytoskeletal structures reminiscent of a jellyfish, that are composed of a bell and tentacles (Nakane & Miyata, 2007). Gliding of *Mycoplasma mobile* was suggested to rely on the movements of the “leg” protein extending from the cell surface that would bind to, pull on, and release from sialylated oligosaccharides that are fixed on the substratum (Miyata, 2010) (Figure 2C). Three proteins Gli123, Gli349 and Gli521 were characterized as gliding proteins. While Gli349 was proposed to play the role of a leg (Uenoyama *et al.*, 2004), the Gli521 was predicted to play

the role of a gear (Seto *et al.*, 2005). In contrast, Gli123 was suggested to localize to the membrane and recruit Gli521 (Uenoyama & Miyata, 2005). Movements of the string-like leg structures are powered by ATP hydrolysis carried out by the P42 motor protein.

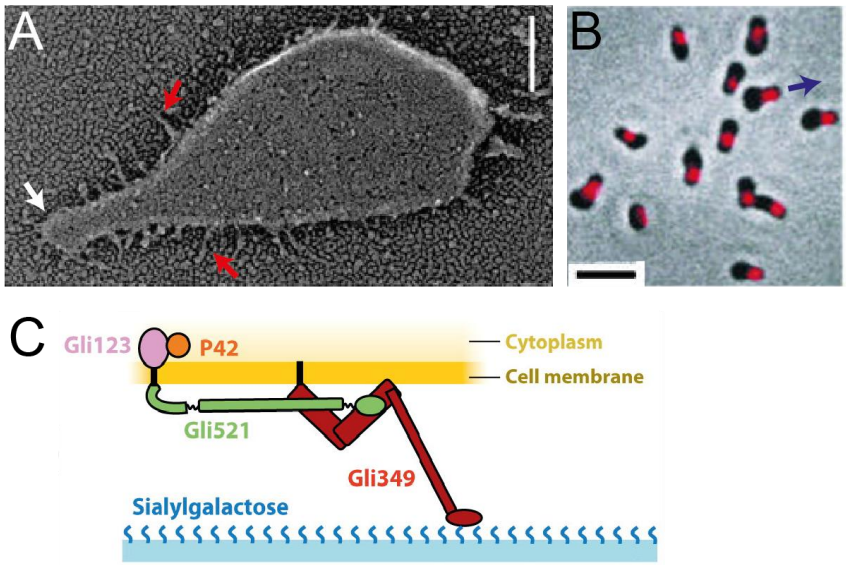

Figure 2. Structures involved in gliding motility of *Mycoplasma mobile*.
(A) Rapid freeze-fracture deep-etch replica EM image of *M. mobile* cell. Red arrows: string-like leg structures, white arrow: head-like protrusion. Scale bar: 100 nm. The figure is reproduced from Miyata *et al.* (2004). (B) Localization of Gli349 visualized by immunofluorescence. Scale bar: 2 µm. Blue arrow indicate gliding direction. (C) Gliding motility model. Gliding surface is marked with blue line with fixed sialylgalactose sugar chains. The figure is reproduced from Uenoyama *et al.* (2004).

Gliding motility in the Gram-negative bacterium *Flavobacterium johnsoniae*, was proposed to depend on different mechanism in comparison to that of *M. mobile*. Gliding motility of *F. johnsoniae* is powered by PMF (proton motive force) (Nakane *et al.*, 2013). It involves the rapid pole to pole movement of filaments composed of the adhesion protein SprB as well as RemA on the cell surface along a closed helical loop track (Figure 3B) (Shrivastava *et al.*, 2012). SprB and RemA are exported by a type IX secretion system to the cell surface and anchored in the OM (outer membrane) (Shrivastava *et al.*, 2013). These two protein filaments bind strongly to polysaccharides on the substratum, so that in moving cells the filaments become localized to the rear of the cell. After reaching the lagging cell pole, they loop around it and start to move toward the forward pole with a velocity of 3.4 µm/s, while these filaments are not fixed anymore to the substratum. The velocity of the SprB and RemA filaments

moving in opposite directions is constant with respect to the cell. TIRF (total internal reflection fluorescence) microscopy suggested that SprB move along a left-handed helical path resulting in a left-handed cell rotation (Nakane *et al.*, 2013).

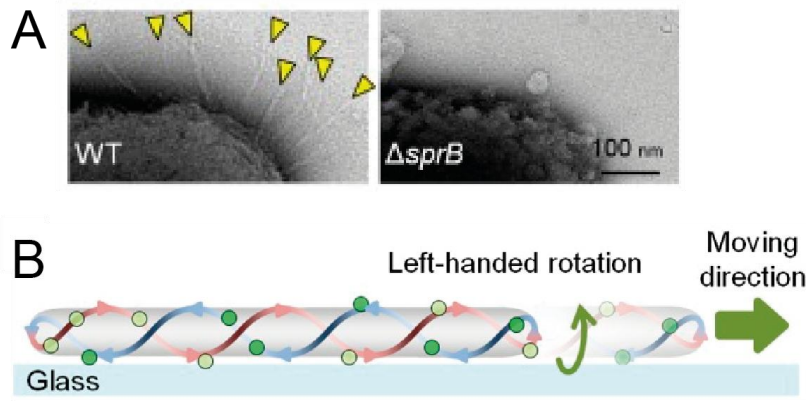

Figure 3. Structures involved in gliding motility of *Flavobacterium johnsoniae*. (A) Images of polar region of negatively stained WT and *sprB* deletion mutant *F. johnsoniae* cells. Yellow arrow heads indicate SprB filaments. (B) A working model for gliding motility. Green circles indicate two different states of the SprB and RemA adhesins. Dark green circles: proteins adhere to the surface and move towards the lagging cell pole, light green circles: proteins move toward the leading cell pole. The figure is reproduced from Nakane *et al.* (2012).

Another example of gliding motility is A-motility found in *M. xanthus,* which will be described later in greater detail. *M. xanthus* has two genetically distinct motility systems: the A-motility and S-motility system. *M. xanthus* cells can reach the speed of 2-4 μm per minute, which is slow in comparison to *E. coli* (~50 μm per second) (Baker *et al.*, 2006) or *F. johnsoniae* (5-10 μm per second) (McBride, 2001). If genes required for only one of the motility systems are deleted, the cells remain motile by means of the other system. An A^+S^+ strain shows normal motility (WT) and can spread over hard agar surface and display flares on soft agar plates. A^+S^- mutants spread only on plates with 1.5% agar, where single cells can be seen at the colony edges under high magnification, while on plates with 0.5% agar the mutant does not form flares. In contrast, A^-S^+ mutants are defective in single cell movement; A^-S^+ cells can glide only on soft agar where the groups of cells emerge from colonies forming long flares, while on hard agar the cells are non-motile. An A^-S^- mutant is completely non-motile on hard or soft agar.

1.3 S-motility in *M. xanthus*

S-motility, known as social motility, refers to a group cell movement that is favored on soft moist surfaces (Shi & Zusman, 1993). Social motility is cell-cell contact dependent and based on the extension, adhesion, and retraction of T4P. T4P are commonly found in bacteria and function in a variety of processes including pathogenesis (Craig *et al.*, 2004), biofilm formation (O'Toole & Kolter, 1998), cellular motility (Mattick, 2002b), protein secretion (Hager *et al.*, 2006) and DNA uptake (Dubnau, 1999). S-motility is equivalent to twitching motility in *Pseudomonas, Vibrio* and *Neisseria* species (Henrichsen, 1983, Mattick, 2002a, Herrington et al., 1988). *M. xanthus* cells are surrounded by fibril material which consists of ECM (extracellular matrix) material (Behmlander & Dworkin, 1991). EPS (exopolysaccharides) are integral part of ECM and play a crucial role in S-motility, they are anchors for T4P retraction (Li *et al.*, 2005b). In addition, LPS O-antigen is essential for S-motility; however the exact role is still not known (Bowden & Kaplan, 1998). The cell movements involve pili to binding to the EPS on the surface of a neighboring cell or on the substratum and then retracting. This retraction generates a force up to 150pN per pilus, which is sufficient to pull the cell body forward (Maier *et al.*, 2002, Clausen *et al.*, 2009).

The T4P machinery in *M. xanthus* consists of ten Pil proteins clustered in one genomic region, in addition to Tgl and TsaP that are found elsewhere in the genome (Figure 4) (Pelicic, 2008, Friedrich *et al.*, 2014, Siewering *et al.*, 2014). *M. xanthus* cells display 5-10 T4P (Kaiser, 1979a). T4P are polymers composed of mature pilin protein, PilA. PilA is synthesized as a preprotein and secreted via the Sec system (Francetic *et al.*, 2007). In the next step it is processed by the PilD prepilin peptidase (Nunn & Lory, 1991) and subsequently anchored in the IM (inner membrane). The pilus fiber can be up to several micrometers in length and have diameter of 5 to 8 nm (Craig & Li, 2008). The pilus fiber penetrates the OM via the PilQ complex, while PilC likely acts as a platform in the IM, from which pili are extended (Skerker & Berg, 2001, Nudleman *et al.*, 2006). The PilMNOP complex was suggested to align the IM and OM complex of T4P machinery (Scheurwater & Burrows, 2011). The extension of T4P is promoted by the ATPase PilB, while T4P retraction is promoted by the ATPase PilT (Jakovljevic *et al.*, 2008). Tgl is an OM lipoprotein that is essential for PilQ

oligomerization. Furthermore, TsaP is a peptidoglycan binding protein that is important for the surface display of T4P (Siewering *et al.*, 2014).

Recent studies presented evidence that the type IV pilus machinery in *M. xanthus* cells is assembled in an outside-in manner at the leading cell pole, based on analysis of localization and protein stability dependencies as well as on direct protein interactions (Friedrich *et al.*, 2014). In the first step of T4P assembly, Tgl stimulates the OM insertion and oligimerization of PilQ. In the second step, PilQ recruits PilP, an IM lipoprotein, and TsaP by direct interactions (Siewering *et al.*, 2014). PilP in turn recruits PilN and PilO to the IM (Friedrich et al., 2014). In the last step, PilM is recruited to the T4P complex by a direct interaction between PilM and cytoplasmic domain of PilN. Furthermore, PilC is likely recruited by PilO. The outside-in manner of type IV pilus machinery assembly could prevent T4P extensions when the complex is not fully formed.

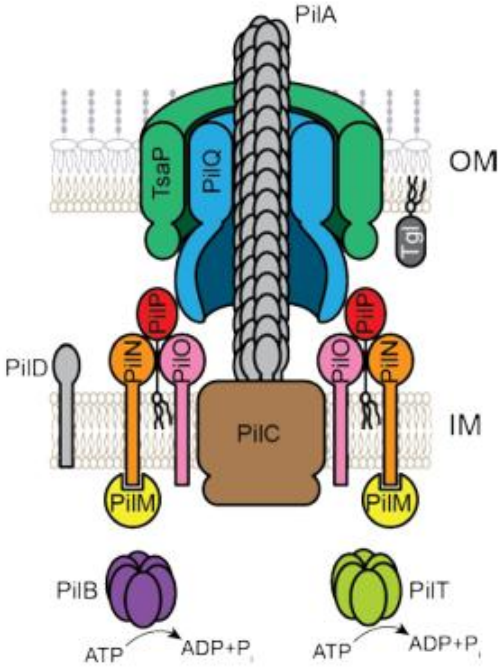

Figure 4. The type IV pili complex of *M. xanthus*.
Proteins are not drawn to scale. OM, IM stands for outer membrane and inner membrane, respectively. The figure is modified from Friedrich *et al.* (2014).

The T4P components are divided into two classes of proteins: stationary and dynamic. Stationary proteins localize to both cell poles although the assembly of T4P takes place only at the leading cell pole. Tgl and PilA are the exceptions to the polar localization, recent studies showed that these two proteins localize evenly around the cell envelope (Friedrich *et al.*, 2014). Dynamic proteins such as PilB and PilT switch the cell poles during reversals,

and localize in a bipolar asymmetric pattern. While PilB localizes at the leading cell pole, PilT localizes predominantly at the lagging cell pole. However, periodic accumulation at the leading cell pole is observed (Bulyha *et al.*, 2009).

1.4 A-motility in *M. xanthus*

The second motility system of *M. xanthus* is A-motility and is required for the movement of single cells. In contrast to S-motility, it is observed on hard, dry surfaces. Although research on A-motility, which will be called from now on gliding motility, is ongoing for over two decades, the exact mechanism is still not known. Over this time several models were proposed to explain the mechanism as well as uncover the function for known gliding motility components.

The first gliding motility model suggested that the cell movement is propelled by an active slime secretion from an apparatus located at the lagging cell pole pushing the cell forward (Jahn, 1924). Another model involved the secretion of a polymer displaying polyelectrolyte gel properties (Wolgemuth *et al.*, 2002b). It was proposed that this polymer would be synthesized in the IM and transported through the cell membrane in a dehydrated form and gradually become hydrated outside the cell. This hydration process was expected to create a force and push the cell forward. However, recent studies showed that slime is not secreted at the lagging cell pole, but at multiple sites along the cell body and does not power gliding motility but rather facilitate adhesion of the cell body to the gliding surface (Mignot *et al.*, 2007, Ducret *et al.*, 2012).

Currently there are two main models for gliding motility that are being investigated: the motor cargo model and the focal adhesion model (Figure 5). In the first model IM protein complexes deform the peptidoglycan and OM in order to create traction, whereas the motility complexes would span the entire cell envelope continuously in the second model.

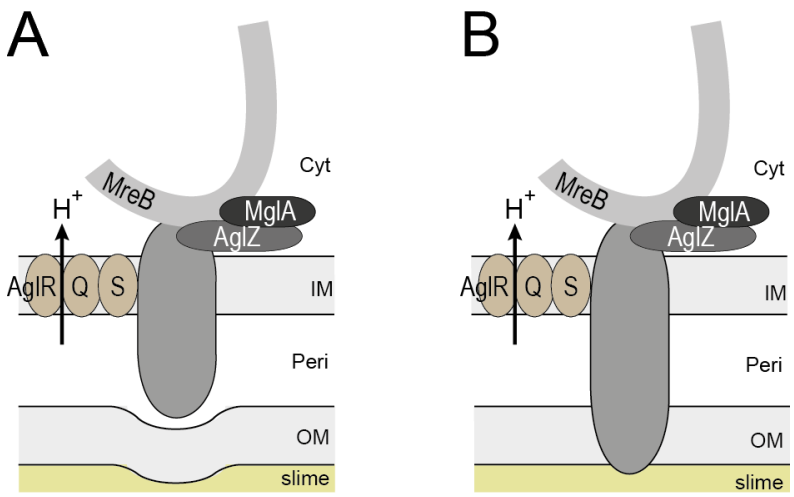

Figure 5. Two models of gliding machinery.
The motor proteins AglRQS, AglZ, small G-protein MglA and the MreB actin cytoskeleton are shown. The grey oval box represents proteins involved in the formation of motility complexes. (A) The motor cargo model. The motility complexes are built in the inner membrane and periplasm and push on the outer membrane. (B) The focal adhesion model. The motility complexes span the cell envelope and interact with the gliding slime.

1.4.1 Motor cargo model

The motor cargo model was proposed by Nan *et al.* (2011) based on the localization of the GltD protein in the cells. GltD is a periplasmic protein encoded in the G1 cluster, which will be described later. In cells expressing GltD-mCherry a helical localization pattern of GltD-mCherry was observed by analysis and deconvolution of z-stacks (Nan *et al.*, 2011). It was proposed that GltD localizes in the pattern ofan endless helical loop which would span the entire length of the cell body. Nan *et al.* also noticed that the distance between the nodes of the GltD helix is almost identical to that found for the cytoskeletal protein, MreB in *M. xanthus* (Mauriello *et al.*, 2009). Furthermore time lapse movies suggested a clockwise rotation of the GltD-mCherry helix during cell movement that is dependent on the PMF and the polymerization of MreB. In addition, the calculated linear velocity of cells based on the GltD helix period (~4.4-9.6 μm/min) was consistent with the maximum velocity of gliding motility (~2-4 μm/min) (Sun *et al.*, 1999). Interestingly, TIRF microscopy of *M. xanthus* cells expressing GFP in the cytoplasm revealed a periodic modulation of the GFP signal intensity when looking on the cell surface. The periodicity of the GFP signal was similar to the periodicity of nodes of the GltD helix, which lead

to the conclusion that proteins moving on a helical track distort the cell envelope.

Recent studies on the localization of the motor protein AglR were in agreement with the data obtained for GltD. Using SIM (structured illumination microscopy) Nan *et al.* observed that AglR displays a looped continuous helix with a periodicity similar to the GltD helix (Nan *et al.*, 2013). Additionally, the velocity of the rotating GltD and AglR helices was almost the same, indicating that these two proteins belong to the same machinery (Luciano *et al.*, 2011, Nan *et al.*, 2013). By tracking AglR molecules Nan *et al.* discovered that AglR moves in two dimensions in *M. xanthus* cells suggesting a helical movement. Using TIRF microscopy AglR molecules were observed to slow down at the ventral turn of the track closest to the gliding surface. This decrease was dependent on the surface hardness, suggesting that the side of cell contact with the gliding surface creates a resistance for the motility complexes. Similarly to GltD, rotation of the AglR helix depends on the PMF and the MreB actin cytoskeleton. Additionally, deletion mutations of genes essential for gliding motility strongly affected directed and dynamic movements of AglR molecules along the helical loop. In a Δ*gltD* mutant, AglR molecules were stationary, while in a Δ*aglZ* mutant the direction of movement was very irregular.

Based on the presented data the motor cargo model was proposed (Figure 5A). This model describes that proteins involved in gliding motility form protein complexes that travel along a closed helical loop which spans the full length of the cell body similarly to the SprB and RemA involved in gliding motility of *F. johnsoniae*. These coordinated protein movements force a clockwise rotation of the cell body. The protein complexes, which are in a close proximity to the sides where the cell has contact with the gliding surface, slow down because of the surface resistance. At these sides the traffic jams of protein complexes are formed and push on the cell membrane. These distortions of the cell envelope exert force on the gliding surface, collectively resulting in directed cell movement.

1.4.2 Focal adhesion model

The focal adhesion model was proposed by Mignot *et al.* (2007). The first experiments that supported the focal adhesion model were carried out on cephalexin treated and nontreated cells. Cephalexin is an antibiotic which blocks cell division leading to the formation of long flexible cell filaments. Elongated cells displayed almost normal gliding motility, whereas S-motility was severely reduced suggesting that the gliding motility machinery is distributed along the cell body and not at the lagging cell pole (Sun *et al.*, 1999).

AglZ-YFP was shown to localize to multiple clusters distributed along the cell body, which stayed fix to the substratum in moving cells (Figure 6) (Mignot *et al.*, 2007). Furthermore the number of AglZ-YFP clusters was strongly dependent on the cell length. The dynamics of AglZ-YFP clusters suggested that new clusters are assembled at the leading cell pole and disassembled at the lagging cell pole. Observations of the AglZ-YFP cluster movements suggested that motility complexes might be connected to an internal cell cytoskeleton similar to eukaryotic focal adhesions. Detailed analysis of elongated cells revealed that the localization pattern of AglZ-YFP clusters is correlated with the cell shape. AglZ-YFP clusters were only observed in the cell between the sites of cell bends. Interestingly cell reversals showed an effect on the AglZ-YFP localization, the clusters became diffuse shortly before a reversal and then appeared at the new leading cell pole while the cell continued its movement into the new direction (Mignot *et al.*, 2007). Another evidence for distributed motor complexes is that the cell velocity is independent of the cell length. Moreover the force necessary to power the cell movement was proportional to the number of clusters in the filamentous cells, indicating that most probably the force is produced at these adhesion sites (Mignot *et al.*, 2007).

Studies carried out by Mauriello *et al.* (2010) on MreB revealed that the MreB polymerization is essential for the gliding motility and the formation of the AglZ-YFP clusters in the cells. Furthermore Luciano *et al.* suggested that three genomic regions referred to as the G1, G2 and M1 cluster constitute the gliding motility machinery, and are composed of components that localize to regions spanning all cell compartments. The focal adhesion model suggests that gliding

motility machinery is primarily assembled on the ventral side of the cell, close to the gliding surface based on z-stack analysis of cells expressing periplasmic GltD-mCherry (Luciano *et al.*, 2011).

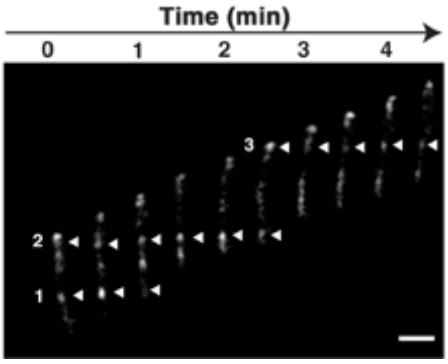

Figure 6. Dynamic localization of AglZ-YFP
The time lapse movie demonstrates AglZ-YFP localization in a moving cell over time. Fluorescence micrographs were taken every 30s. White triangles highlight the position of the observed AglZ-YFP clusters. Scale bar: 1um. The figure is reproduced from Mignot *et al.* (2007).

Based on all these data, a model for a gliding motility mechanism was proposed similar to the eukaryotic focal adhesions. It was hypothesized that proteins that are essential for gliding motility localize to motility complexes referred to as FAs (focal adhesions) that are stationary with respect to the substratum. FAs are thought to connect MreB with the slime polymers on the gliding surface spanning the whole cell envelope and localize in distributed clusters along the ventral side of the cell.

FA components in *M. xanthus*

The cytoplasmic part of the FAs includes MglA, AglZ and GltI complex connected to the MreB. The MreB is the bacterial actin homolog and it was shown to be required for rod cell shape (Wachi *et al.*, 1987, van den Ent *et al.*, 2001, Esue *et al.*, 2005). The MreB actin cytoskeleton in *M. xanthus* has been proposed to be in the form of a continuous helix, which would span the whole cell body (Mauriello *et al.*, 2010b). However, recent studies in *E. coli* and *B. subtilis* revealed that MreB rather forms short filaments which exhibit a patchy localization (Garner *et al.*, 2011). Experiments with the drug A22 showed that inhibition of MreB polymerization strongly reduced gliding motility (Mauriello *et al*., 2010b). A22 reduces MreB polymerization by binding to the nucleotide-binding pocket of MreB (Bean *et al.*, 2009). In addition, A22 caused the disassembly of FAs and inhibited assembly of the new FAs as seen by analysis of cells expressing MglA-YFP, AglQ-mCherry and AglZ-YFP fusions (Mauriello

et al., 2010b, Hot, in submission). Recent studies suggested that MreB is directly involved in the positioning of the FAs, because of its direct interaction with AglZ and MglA-GTP (active state of MglA) indicating that FAs are connected to the internal cytoskeleton (Mauriello *et al.*, 2010a, Hot, in submission). Additionally the transport of polystyrene beads bound to the outer surface of immobilized cells was found to depend on MreB polymerization (Sun *et al.*, 2011a). AglZ is a cytoplasmic protein and consists of an N-terminal pseudo-receiver domain and a C-terminal coiled-coil domain (Yang *et al.*, 2004a, Mignot, 2007). In WT (wild type) cells AglZ-YFP localizes to multiple clusters distributed along the cell body; however, this localization is strongly dependent on MreB, MglA, and proteins encoded in G1 cluster (Figure 5) (Yang *et al*., 2004a, Mauriello *et al*., 2010a, Nan *et al.*, 2010a). A gliding motility defect caused by an *aglZ* in-frame deletion can be restored by a double deletion of *frzE* and *aglZ,* suggesting that AglZ is a regulatory protein of the gliding motility system.

Proteins encoded in the G1 and the G2 clusters were suggested to constitute the structural elements of FAs (Luciano *et al.*, 2011). The G1 cluster encodes for GltJ, GltI, GltH, GltG, GltF, GltE and GltD proteins (Figure 7A). Using fractionation experiments GltE and GltG were identified as IM proteins while GltH as an OM protein (Luciano *et al.*, 2011). Furthermore GltF-mCherry was detected in membrane fraction whereas GltD was found to localize to the periplasm (Nan *et al.*, 2010b) (Figure 7B). Based on bioinformatics GltJ was suggested to localize to the IM whereas GltI to the cytoplasm. GltD and GltF were found to localize to multiple clusters distributed along the cell body similarly to AglZ-YFP using fluorescence microscopy. Interestingly, BACTH experiments showed a direct interaction between GltG and the motor protein AglR, suggesting that the motor complex asscoiates with FAs by specific interactions with GltG (Luciano *et al*., 2011). The G2 cluster defined by bioinformatic analysis consists of GltK, GltB, GltA and GltC (Figure 10). Transposon mutagenesis screens identified that *gltK* and *gltC* are essential for gliding motility (Yu & Kaiser, 2007, Youderian *et al.*, 2003). In parallel, construction and analysis of in frame deletion mutants confirmed that G2 proteins are essential for single cell movement (Daniela Keilberg, unpublished

data). GltC encoded in G2 cluster together with GltD, GltE and GltG encoded in G1 cluster as well as AglR, AglQ, AglS encoded in M1 cluster all share a similar taxonomic distribution, and furthermore, are encoded in a single genomic region in some Deltaproteobacteria, Gammaproteobacteria and Betaproteobacteria (Luciano *et al.*, 2011). This suggests that gliding motility machinery in *M. xanthus* is the derivative of the core complex present in other species of Proteobacteria, which has evolved and expanded from one to three separate clusters G1, G2 and M1 found in different genomic regions.

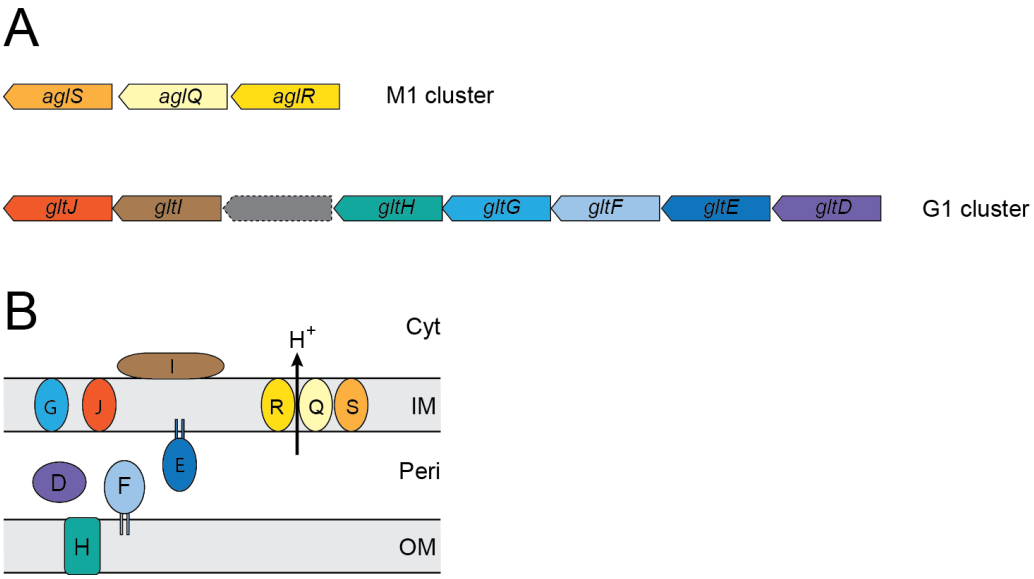

Figure 7. Genetic organization of the M1 and G1 cluster.
(A) Genetic organization of genes composing the M1 and G1 clusters. The arrows indicate the direction of transcription as well as show the gene names. (B) Protein products of M1 and G1 cluster are represented accordingly to bioinformatic and fractionation data. The color code for protein and genes is the same. The letters R, Q, S, J, I, H, G, F, E and D stands for gene names visible in the A panel. Cyt, IM, Peri and OM stands for cytoplasm, inner membrane, periplasm and outer membrane, respectively.

The common sources of energy for motility are PMF and ATP hydrolysis. To distinguish between these two options *M. xanthus* cells were treated with different drugs and analyzed in terms of motility. The application of carbonyl cyanide-m-chlorophenylhydrazone (CCCP), which destroys PMF, resulted in non-motile cells (Sun *et al.*, 2011b). The PMF is caused by pH difference or voltage difference across the IM. To distinguish between these two options nigericin and valinomycin were used. While nigericin reduces the pH gradient, valinomycin has a negative effect on the membrane potential. The results showed that valinomycin has no effect on gliding motility whereas nigericin

abolished single cell movement, strongly supporting that the energy, which powers the gliding motility machinery, comes from a pH gradient across the membrane.

The gliding motility motor consists of the three proteins AglQ, AglR and AglS, encoded in one genomic region referred to as the M1 cluster (Figure 7). AglS and AglR were found by transposon mutagenesis screens to be required for gliding motility (Youderian *et al*., 2003). Construction of in-frame deletions and subsequent motility assays revealed a gliding motility phenotype in cells lacking these three proteins. The in-frame deletion of *aglQ* results in either non-motile FAs, as seen by analysis of an AglZ-YFP fusion (Sun *et al*., 2011b) or loss of FAs, as observed in cells expressing GltD-mCherry (Luciano *et al.*, 2011). A single amino acid substitution in the residue of AglQ (D28N), which is essential for binding H^+ within the channel, results in stable, but non functional $AglQ^{D28N}$. Cells carrying $AglQ^{D28N}$ are non-motile. Analysis of cells expressing $AglQ^{D28N}$-mCherry revealed that FAs assembly still takes place in these cells indicating that the proton channel AglQRS powers the force generation in gliding motility (Sun *et al*., 2011b). Interestingly, the AglQRS motor complex was suggested to function not only with the gliding motility machinery but also with the Nfs/Exo machinery which is involved in the assembly of rigid spore coat during sporulation process (Wartel *et al.*, 2013).

Bioinformatic analysis revealed that motor proteins are homologous to MotA/TolQ/ExbB (AglR) and MotB/TolR/ExbD (AglQ and AglS) (Sun *et al*., 2011b). While MotA/MotB proteins build the stator part of the flagellar rotary motor, the TolQ/TolR complex is important for the OM integrity and cell division. ExbB and ExbD are part of the TonB-dependent energy transduction system (Raymond *et al.*, 2003, Postle & Kadner, 2003). All three protein complexes form proton channels in the IM. Moreover, in all three systems the proton channels are the motors that harvest the energy from the proton flux, and this energy is converted to a mechanical output as the motors are hooked up to a partner protein. The energy from the proton flux is converted to changes in protein conformation. AglQRS is the first bacterial motor able to move in a directed manner between subcellular regions since AglQ-mCherry was shown to localize to multiple clusters which were fixed to the substratum and move

towards the lagging cell pole in the moving cells (Sun *et al.*, 2011b). This system most probably works by a similar mechanism as the MotA/MotB, TolQ/TolR and ExbB/ExbD.

The assembly and disassembly of FAs depends on small GTPase MglA, which is an essential component of FAs. MglA, a Ras-like small G protein in a cytoplasmic complex with AglZ regulates assembly and disassembly of FAs. An in-frame deletion mutant of *mglA* has a defect in both motility systems of *M. xanthus* (Hodgkin & Kaiser, 1979). MglA was shown to localize to distributed clusters along the cell body, which were fixed to the substratum in motile cells suggesting that MglA is an integral component of FAs (Patryn *et al.*, 2010). Furthermore MglA was shown to interact directly with AglZ and MreB (Mauriello *et al*., 2010b, Hot, in submission), and was predicted to interact with GltI. These three proteins MglA, AglZ and GltI depend on each other for FAs localization. Only the active form of MglA, MglA-GTP is able to interact with MreB and to stabilize FAs by promoting their assembly at the leading cell pole. In cells lacking *mglA,* FAs have not been observed (Hot, in submission). MglA-GTP converted to MglA-GDP at the lagging cell pole does not interact with MreB and dissociates from the FA complexes resulting in the disassembly of FA. The new FAs are assembled at the leading cell pole where MglA-GDP is converted to its active form MglA-GTP, and recruitment of the FA components can occur.

1.4.3 Gliding slime

Another significant element of gliding motility is the gliding slime which was proposed to be secreted at FA sites underneath the cell body and to promote adhesion of FAs to the substrate (Ducret *et al*., 2012). Slime is composed of carbohydrates which can be selectively stained with ConA (concanavalin A), a fluorescent-derived lectin. The gliding slime is up to 1000-fold thinner then the bacterial cell, and because of that, the isolation of pure slime is a challenge at the present moment. Moreover, it was shown that in-frame deletion mutants of *aglQ, gltD* and *gltE* that have defects in gliding motility still secrete slime indicating that most probably another yet unknown complex of proteins is involved in slime secretion. The mutants of *wza* (component of capsular EPS export machinery), *difA* (regulates EPS

production) and *sasA* (involved in LPS O-antigen production) were found to still deposit slime trails indicating that slime is also not Wzy-dependent. However, our knowledge on slime is very limited, thus it is crucial to discover the slime deposit machinery as well as the slime composition.

1.5 Cellular reversals

Directed cell movement in *M. xanthus* is controlled by reversals. During a reversal, a cell stops and resumes the movement in the opposite direction. This event is tightly regulated by components of the Frz system as well as by MglA, MglB and RomR (Figure 8). Mutations or deletions of genes that are required for reversals result in a hypo- or hyper-reversal phenotype, and these cells are unable to form fruiting bodies (Zusman, 1982, Li *et al.*, 2005a). Reversals correspond to an inversions of the cell polarity, when the old lagging cell pole becomes a new leading cell pole and *vice versa* (Blackhart & Zusman, 1985).

1.5.1 Frz chemosensory system

The Frz system consists of seven proteins that show high similarities to chemotaxis proteins (McBride *et al.*, 1989): FrzCD, a cytoplasmic chemoreceptor; FrzA and FrzB, CheW-like coupling proteins; FrzE, a CheA-CheY-like fusion protein; FrzF, a methyltransferase; FrzG, a methylesterase; and FrzZ, a dual-response regulator protein. *M. xanthus* cells lacking Frz proteins display abnormal cellular reversal periods that lead to defects in motility and development, suggesting that directed cell movements are required for predation and fruiting body formation. *Frz* mutants reverse rarely, however some mutations in *frzCD* cause hyper-reversals (Blackhart & Zusman, 1985, Bustamante *et al.*, 2004). Based on this data, the Frz chemosensory system was proposed to control reversals of *M. xanthus*.

Previous studies suggested that signal to reverse is sensed by FrzCD, which in turn leads to autophosphorylation of the histidine kinase FrzE. It was shown experimentally by Astling *et al*. that differential FrzCD methylation by FrzF can regulate the Frz pathway (Astling *et al.*, 2006). The phosphoryl group

is then transferred from FrzE to FrzZ and down to the response regulator RomR, however the exact pathway is still not known (Figure 8) (Bustamante et al., 2004, Inclan *et al.*, 2008, Inclan *et al.*, 2007, Keilberg *et al.*, 2012, Zhang *et al.*, 2012).

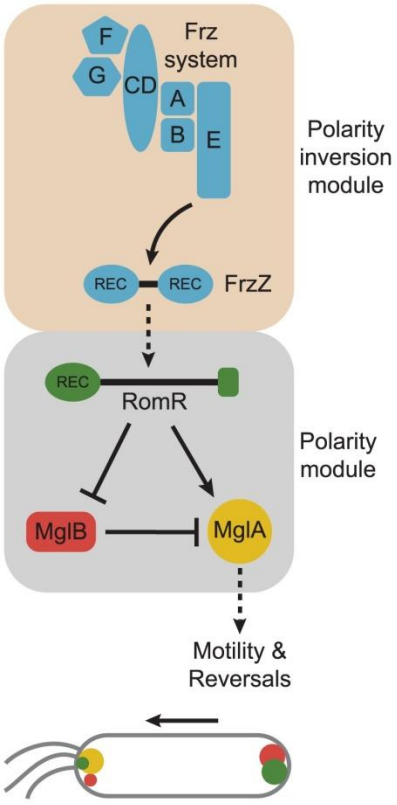

Figure 8. Model of the regulatory cascade.
Frz proteins are represented as F, G, CD, A, B, E and FrzZ. The polarity module consists of RomR, MglB and MglA. Arrows and T-bars indicate direct interactions. The dashed lines indicate that the mechanism of the interaction is not known. The bottom panel represents a cell with localization pattern of MglB, MglA and RomR, and marked pili at the leading cell pole, which moves in a direction pointed with an arrow. The figure is reproduced from Keilberg *et al.* (2012).

1.5.2 The polarity module consists of the proteins RomR, MglB and MglA

The signal received by the Frz system is transduced to RomR, which interacts directly with both MglA and MglB regulating their unipolar localization (Keilberg *et al*., 2012). The cell reverses when MglA and MglB switch the poles; however, the exact mechanism is still not known. This phenomenon also causes other proteins to switch cell poles such as PilB and PilT (Bulyha *et al.*, 2009) or AglZ and AglQ (Mignot *et al*., 2007, Sun *et al*., 2011b), which are involved in the S-motility and gliding motility, respectively. This change in polarity allows for the assembly of motility machineries at the new leading cell pole.

MglA is an output protein which regulates both motility systems and cell reversals. MglA belongs to the Ras family GTPases, which are commonly

involved in signal transduction and cell migration in eukaryotic cells (Charest & Firtel, 2007). MglA is a small G protein that displays two substrate-bound forms in *M. xanthus* cells. In an active state MglA is in a GTP-bound form (MglA-GTP) and localizes to the leading cell pole. MglB is a GTPase-activating Protein (GAP) of MglA and localizes to the lagging cell pole, where it stimulates GTP hydrolysis causing MglA-GTP to convert to the inactive, GDP-bound form, MglA-GDP. MglA-GDP in contrast to the active form is diffuse in the cell. The exchange from MglA-GDP to MglA-GTP is hypothesized to be carried out by an unknown guanine nucleotide exchange factor (GEF) at the leading cell pole. It was shown that a Q→A substitution results in a locked GTP active state of MglA. MglA^{Q82A} is able to interact with MglB but does not hydrolyze GTP leading to a bipolar localization pattern of MglA^{Q82A}-YFP in addition to a large non-polar cluster oscillating between the cell poles (Miertzschke *et al.*, 2011). When the non-polar cluster of MglA^{Q82A}-YFP, which is fixed to the substratum, reaches the lagging cell pole, the cell reverses (Miertzschke et al., 2011). Thus, a MglA^{Q82A} mutant shows a hyperreversal phenotype. In addition, it was shown that in a Δ*mglB* mutant MglA accumulates at the lagging cell pole resulting in a bipolar MglA localization. On the other hand in a Δ*romR* mutant MglA localizes diffusively. Moreover *mglB* mutant have an effect on cell reversals resulting in hyperreversals (Keilberg et al., 2012, Zhang et al., 2012).

MglA was proposed to recruit motility proteins to their sites of action to regulate cellular reversals and motility. MglA was shown to interact directly with FrzS and AglZ which are essential for S-motility and gliding motility, respectively. FrzS was recently suggested to regulate social motility by controlling EPS production (Berleman *et al.*, 2011), while AglZ is a component of FAs, the gliding motility machinery. MglA, SofG and BacP regulate the proper localization of the PilB and PilT ATPases that are essential for extension and retraction of T4P (Bulyha *et al.*, 2013). SofG, similar to MglA, is a small GTPase which interacts directly with the bactofilin BacP. While SofG targets both ATPases to one cell pole, MglA sorts them to the opposite cell poles.

Link between Frz system and MglAB is RomR, a response regulator, which consists of an N-terminal receiver domain and a C-terminal output domain (Leonardy *et al.*, 2007). It localizes in a bipolar asymmetric pattern with

the big cluster at the lagging cell pole. RomR localization is dynamic and changes during cell reversals. The activity of RomR is likely regulated by phosphorylation of the conserved Asp residue in the receiver domain (Stock *et al.*, 2000). It was shown that a D→E mutation, which likely mimics a phosphorylated state (Domian *et al.*, 1997) of RomR, causes a hyperreversal phenotype while a D→N mutation, which cannot be phosphorylated, causes a hyporeversal phenotype (Leonardy et al., 2007). These data suggest that phosphorylation of the receiver domain is important for the dynamics of RomR and release of MglA from the pole what regulates cellular reversals (Leonardy *et al*., 2007). RomR is essential for both motility systems. Further genetic epistasis experiments showed that RomR functions between the Frz system and MglA/MglB complex. The most recent studies revealed that RomR is a polar targeting determinant of MglA (Keilberg et al., 2012, Zhang et al., 2012). Interestingly, RomR was found to act together with MglB to regulate MglA-GTP (active state of MglA in a GTP bound form) localization to the leading cell pole at the same time defining MglB localization to the lagging cell pole. Based on these data it was concluded that RomR is essential for the correct MglB and MglA unipolar localization to opposite cell poles (Keilberg *et al.*, 2012, Zhang *et al*., 2012).

1.6 Eukaryotic focal adhesions

The focal adhesion model in *M. xanthus* was based on focal adhesions characterized in eukaryotes. Migration of eukaryotic cells involves multiple structural and regulatory proteins, which are tightly coordinated during the cell movement. Eukaryotic cells can move over surfaces using a mechanism that includes assembly of focal contacts at the front of the cell. This process is initiated by the integrins aggregating at focal adhesion sites (Miyamoto *et al.*, 1995a, Miyamoto *et al.*, 1995b). Focal contacts are multimeric protein complexes and have low affinity to the substratum. During cell migration they stay fixed to the substratum. Later they can either undergo maturation and be converted to fibrillar adhesions or be disassembled. Fibrillar adhesions are located towards the center of a cell and mainly composed of thin actin cables (Zaidel-Bar *et al.*, 2003, Katz *et al.*, 2000). Fibrillar adhesions are transformed to

focal adhesions at the rear of the cell. Small GTPases play major roles in regulation of focal adhesions assembly and formation of actin stress fibers (Ridley & Hall, 1992). Focal adhesions have strong affinity to the substratum and provide a link between cell surface and the intracellular actin cytoskeleton. The focal adhesions can be either left on the substratum or disassembled under control of varied effectors such as epidermal growth factor (Xie *et al.*, 1998).

In the 1970s interference reflection microscopy was used to characterize focal adhesions in fibroblasts, which are the most common cells of connective tissue in animals. A major component of focal adhesions are integrins, which span the cell membrane and bind ligands available on the gliding surface. Cytoplasmic domains of integrins interact with numerous regulatory and cytoskeletal proteins that are involved in integrin affinity and cytoskeletal interaction. In addition, some components of focal adhesions are signaling and structural molecules that form a complex network, which interacts with integrins. Most of these proteins regulate actin cytoskeleton dynamics as well as provide a linkage between integrins and actin filaments. Additional essential components of focal adhesions are: adapter proteins, which recruit numerous proteins resulting in complex formation; protein kinases, which participate in integrin-mediated signaling; and phosphatases, which maintain the balance of phosphorylation levels.

1.7 Nfs cluster

The *nfs* locus (necessary for sporulation) comprises eight genes *nfsA-H,* which are upregulated during sporulation (Muller *et al.*, 2010). Nfs proteins are close homologs to some components of FAs (Luciano *et al*., 2011). Mutants in the *nfs* loci have a defect in sporulation process and are unable to complete morphogenesis from a rod into spherical spores (Muller *et al*., 2012). Further studies using EM (electron microscopy) revealed that the spore coat in *nfs* mutants is amorphous and does not exhibit a dense polymer layer that is tightly sealed to the spores, as observed for WT. These results indicate that the composition of the spore coat polymer, referred to as Exo polymer, exported by the Exo-machinery is impaired (Muller *et al*., 2012). To further investigate the function of the Nfs proteins the spore coat material from WT and certain

deletion mutants was isolated and analyzed in terms of its composition. The *M. xanthus* spore coat material consists of N-acetylgalactosamine, Glc (glucose), GalNAc (N-acetylglucosamine), xylose, rhamnose, mannose and galactose. Interestingly, the ratio of terminal carbohydrate residues to multiple linked residues in Glc and GalNAc molecules differ in *nfs* in-frame deletion mutants and WT, indicating that the Nfs proteins are directly or indirectly involved in the regulation of the Exo polymer composition (Holkenbrink, PhD thesis). Furthermore Nfs proteins were suggested to form a complex in the cell envelope based on bioinformatic and fractionation data (Figure 9). NfsABC were characterized as OM proteins, while NfsDEG as IM proteins using *E. coli* cells in which proteins were produced heterologously and a sucrose density gradients method (Holkenbrink, PhD thesis).

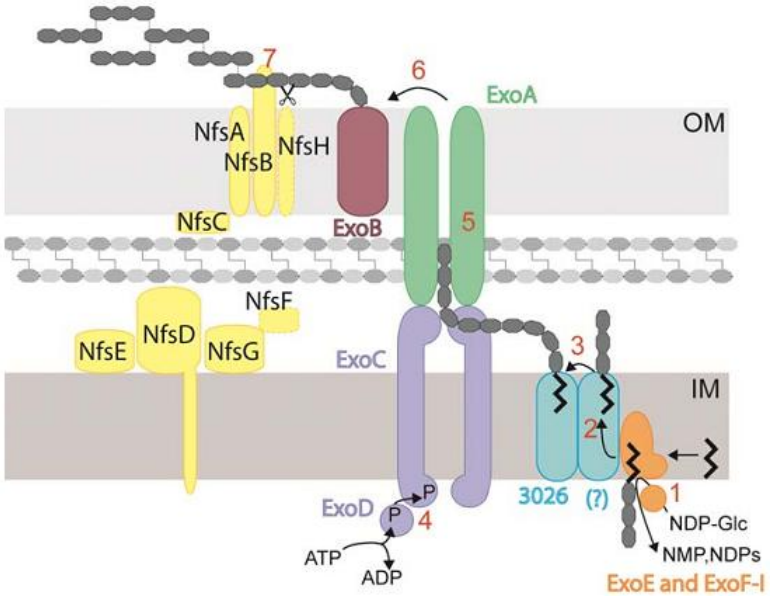

Figure 9. Model of the spore coat assembly machinery.
Nfs proteins are represented in yellow. Exo proteins build the machinery in the cell envelope that exports polysaccharide chains outside the cell. These chains are converted by Nfs machinery (1-7). The figure is reproduced from Holkenbrink PhD thesis (2013).

Nfs proteins were suggested to act together with the Exo proteins which are involved in the export of spore coat material during sporulation (Muller *et al.*, 2012). The Exo locus encodes for nine proteins which are also upregulated during sporulation (Licking *et al.*, 2000). Based on protein homology, the components of the Exo cluster are predicted to encode a Wzy-dependent polysachcaride export machinery (Cuthbertson *et al.*, 2009, Kimura *et al.*,

2011). Analysis of *exo* mutants revealed that the spore coat material is not present on the spore surface and that the mutants are strongly affecting sporulation. In both cases, the *nfs* and *exo* mutants are not able to form viable spores. Furthermore Wartel *et al*. showed that Nfs complex moves around the spore surface. The movement of Nfs complex depends on activity of AglQRS motor, while its directionality depends on secretion of the Exo polymer (Wartel *et al*., 2013, van Teeffelen *et al.*, 2011).

1.8 Scope of the study

M. xanthus cells can glide over surfaces using the A-motility system also called gliding motility. The two current models of gliding motility vary in many aspects. While one of the models describes the motility complexes as FAs spanning the whole cell envelope, the other one presents the motility complexes as traffic jams, which push on the peptidoglycan and OM. Although the most recent studies have revealed many interesting facts about the gliding motility machinery and its components, the exact mechanism is still not known.

In this study, we investigated the function of four proteins GltK, GltB, GltA and GltC encoded in the G2 cluster that are essential for gliding motility. Based on bioinformatic data these four proteins are candidates for OM associated components of the gliding motility complexes. To better understand gliding motility and distinguish between the two proposed models we used molecular biological and biochemical methods to investigate the cellular protein localization and protein-protein interactions. We also analyzed the localization patterns of the G2 proteins in the absence of individual gliding motility proteins using fluorescence microscopy. Finally, to find out how the motility complexes are assembled in the cell we also examined localization of AglZ and AglQ in the absence of the G2 proteins.

2 Results

2.1 G2 cluster

2.1.1 Bioinformatic analysis of the G2 cluster

To study the role of the G2 cluster in A-motility, also called gliding motility, we started with a bioinformatics approach to gain knowledge of all of the proteins encoded in the G2 cluster. The G2 cluster consists of four genes *gltK, gltB, gltA* and *gltC* (Figure 10) (Luciano *et al*., 2011). Two of them, *gltK* and *gltC,* were identified by a transposon mutagenesis screen to be required for gliding motility (Youderian *et al*., 2003, Yu & Kaiser, 2007). According to taxonomic distribution of genes constituting G1, G2 and M1 clusters and genetic characterization of G1 and G2 clusters, *gltK* and *gltC* together with *gltB* and *gltA,* are part of the gliding motility machinery complex (Luciano *et al*., 2011).

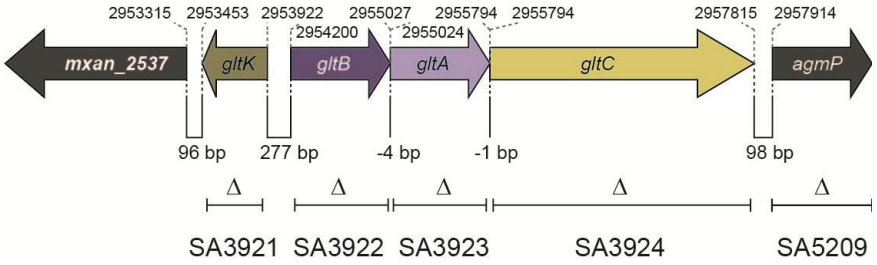

Figure 10. Genetic organization of the G2 cluster region.
Numbers on the top indicate coordinates of the genes in the *M. xanthus* DK1622 genome. Numbers on the bottom indicate distances between genes in bp. SA numbers correspond to deletion strains of indicated genes. The arrows representing genes indicate the direction of transcription, are drawn to scale, and also show the locus names: *mxan_2537*, *gltK* (*mxan_2538*), *gltB* (*mxan_2539*), *gltA* (*mxan_2540*), *gltC* (*mxan_2541*) and *agmP* (*mxan_2542*).

The first of these genes, *gltK*, encodes a protein that belongs to the group of contact dependent gliding motility proteins and was previously n amed CglC (Pathak & Wall, 2012). This previous *cgl*-gene designation was given to genes that encode OM proteins, which are transferred between the cells. This process requires physical contact with donor cells containing the corresponding WT gene (Wei *et al.*, 2011, Pathak *et al.*, 2012). Luciano *et al*. renamed all of the G1 and G2 genes *glt* (**gl**iding **t**ransducer) to homogenize the nomenclature. GltK is predicted to be anchored in the OM because it is

transferred between the cells (Pathak & Wall, 2012). GltK includes a type II signal peptide (Pathak & Wall, 2012).

Because previous work suggested that GltK is membrane-associated, we wanted to predict the cellular localization of the remaining G2 proteins. The genes *gltB*, *gltA* and *gltC* encode proteins with a type I signal peptide as determined by SignalP 4.1 Server (Petersen *et al.*, 2011). Bioinformatic analysis revealed that GltB and GltA are homologous with 50.1% similarity based on EMBOSS Needle (Rice *et al.*, 2000). GltB and GltA were further analyzed using the TMHMM Server v. 2.0 (Krogh *et al.*, 2001) and JPred 3 Server (Cole *et al.*, 2008) and their secondary structures are dominated by β-sheets. Furthermore, based on results using HHomp Server (Remmert *et al.*, 2009), GltB and GltA are predicted to contain a domain homologous to the OM domain of OmpA from *E. coli* and therefore should localize to the OM. Consistent with previous bioinformatic analyses, GltC is predicted to contain TPR-repeats (Luciano *et al*., 2011), characteristic of multiprotein assemblies, and unlike the other G2 proteins, is predicted to localize to the periplasm (Table 1) (Blatch & Lassle, 1999).

Table 1. G2 proteins.

locus	Gene name (s)	Length (aa)	Domain & No. of aa/Signal peptides & No. of aa	Predicted localization
MXAN2538	*agmO, cglC, gltK*	171	None / SpII 17aa	OM lipoprotein
MXAN2539	*gltB*	276	OmpA(OM) 180aa / SpI 19aa	OM ß-barrel
MXAN2540	*gltA*	257	OmpA(OM) 190aa / SpI 21aa	OM ß-barrel
MXAN2541	*agnA, gltC*	674	TPR 335aa / SpI 24aa	periplasm

OM: outer membrane; SPI: Type I signal peptide; SpII: Type II signal peptide; TPR: Tetratricopeptide repeat; OmpA: Outer membrane protein A; aa: amino acids

Proteins encoded in the G2 cluster are homologous to proteins expressed from three other gene clusters, the G3, G4 and G5 clusters (Figure 11). Furthermore, the *glt* genes are more similar to the *nfs* genes transcribed in G3 cluster than the homologs of the G4 and G5 clusters, based on the

phylogenetic analysis of GltD-E-G homologs (Figure 11) (Luciano *et al*., 2011). The Nfs/G3 cluster genes encode proteins that are involved in the formation of an envelope complex necessary for compact spore coat production in *M. xanthus* (Muller *et al*., 2010, Muller *et al*., 2012). Furthermore, recent data indicated that AglQRS gliding motor complex encoded in the M1 cluster is also involved in the sporulation pathway and associates with the Nfs complex to form sporulation-specific machinery (Wartel *et al*., 2013). This led to the hypothesis that the Nfs and Glt complexes are paralogous complexes which draw energy from the same AglQRS motor.

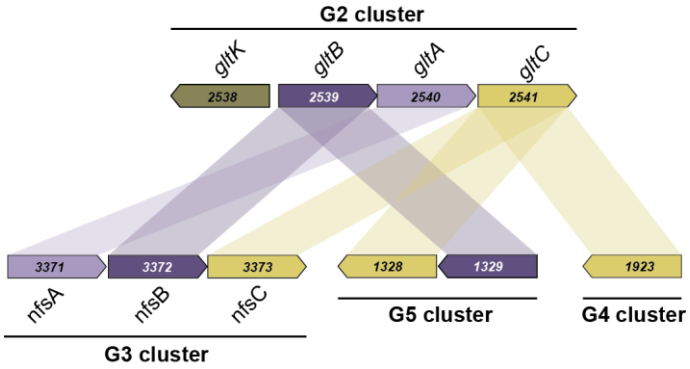

		Homologs (Identity % /Similarity %)			
		G2 cluster	G3 cluster	G4 cluster	G5 cluster
G2 cluster	GltK				
	GltB	(50.1%/50.1%) GltA	NfsB (18.3%/27.3%)		mxan_1329 (21.3%/34.2%)
	GltA	(50.1%/50.1%) GltB	NfsA (24.8%/36.5%)		
	GltC		NfsC (18.6%/35.2%)	mxan_1923 (15.0%/26.8%)	mxan_1328 (22.1%/38.8%)

Figure 11. G2 cluster homologs.
Genetic organization of genes composing the G2, G3, G4 and G5 clusters. Homologous genes are highlighted in the same color. Gene homology was determined using EMBOSS Needle (K Wuichet). Degree of homology as % identity and % similarity is listed in the table.

Following this idea, GltBAC might have similar function to NfsABC complex, although in regulating gliding slime production and/or composition instead of regulating spore coat production. In contrast, the G4 cluster, upstream of motility/polarity control proteins *mglA* and *mglB,* which shares

some homology with the G2 cluster, is not essential for gliding motility (D. Keilberg, personal communication). Finally, the G5 cluster consists of the five genes *mxan_1327-mxan_1331 and* is not thought to be required for gliding motility since an insertion mutant of *mxan_1327,* did not impact gliding motility or S-motility (Luciano *et al*., 2011). Overall, these comparisons with the G3, G4 and G5 clusters suggest that gene duplication lead to the evolution of new gene functions and machinery specialization.

2.1.2 *gltB*, *gltA* and *gltC* genes belong to one operon

Based on the bioinformatic data, we decided to test whether *gltB, gltA and gltC* constitute an operon, excluding *gltK,* which is transcribed in the opposite direction in the genome (Figure 12). Total RNA and gDNA were independently isolated from WT *M. xanthus* cells and cDNA was synthesized from the total RNA as described in 4.4.6. The same primer pairs were used for PCR reactions performed with gDNA, RNA and cDNA. In this experiment, PCRs performed with RNA and the intergenic fragment between *gltK* and *gltB* served as negative controls. In agreement with the divergent organization of *gltK* and *gltB*, no product was generated in the PCR reaction performed using cDNA as a

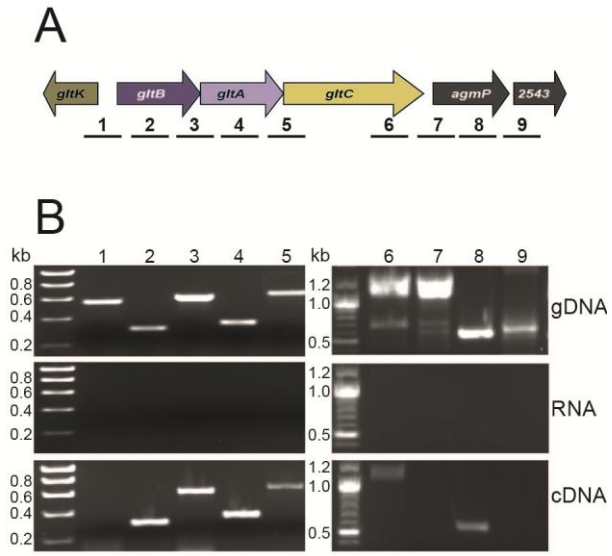

Figure 12. *gltB, gltA* and *gltC* are transcribed together.
(A) Black bars below the schematic representation of the G2 cluster region correspond to PCR products: numbers 1, 3, 5, 7, and 9 represent intergenic fragments, while numbers 2, 4, 6, 8 are intragenic fragments. (B) Analysis of PCR products by agarose gel electrophoresis. In all cases (gDNA, RNA, cDNA) the same primer pairs were used. The numbers designate fragment sizes as determined by the size of the marker bands (leftmost lane of all six gels).

template. Similarly, in the PCR reaction using RNA as a template, no detectable products were amplified, indicating that the RNA was not contaminated with DNA. In contrast, intergenic fragments of *gltB/gltA* and *gltA/gltC* could be amplified using cDNA as template. Further intergenic fragments of *gltC/agmP* and *agmP/mxan_2543* did not give any products when using cDNA in the PCR reaction. These results show that *gltB, gltA* and *gltC* are transcribed in one unit and suggest that the three encoded proteins function together.

2.1.3 GltK, GltB, GltA and GltC are essential for gliding motility

To verify results from the transposon mutagenesis screen, in frame deletions for each of the four genes transcribed from the G2 cluster were generated and motility assays were performed (Daniela Keilberg, unpublished). Concentrated cell suspensions were spotted on 0.5% CTT containing 0.5% or 1.5% agar that favors either group (S-motility) or single cell movement (gliding motility) respectively (Figure 13). After an overnight incubation at 32°C, bacterial colonies were analyzed in terms of motility. WT (DK1622) colonies, in which cells are able to move using both systems, spreading single cells could be observed on hard agar as well as groups of cells forming long flares at the edge of the bacterial colonies on soft agar. The strain impaired in S-motility (DK1300, A^+S^-) showed no cell movement on 0.5% agar, but single cells were still able to move by gliding motility on hard agar. In contrast, a strain with a defect in gliding motility (DK1217, A^-S^+) displayed flares on the soft agar, but no motile cells on hard agar. Similar to an A^- mutant, Δ*gltK*, Δ*gltB*, Δ*gltA* and Δ*gltC* mutants displayed normal cell behavior on the soft agar, but showed smooth colony edges on 1.5% agar, suggesting that cells are not able to move by gliding motility.

To investigate the extent of G2 cluster region, an in frame deletion mutant of *agmP* (*mxan_2542*), the gene downstream of *gltBAC,* was also tested for motility defects. The results from the motility assays showed that *agmP* is not essential for either of the motility systems; *agmP* colonies spread identically to WT colonies on both types of agar (Figure 13A). The upstream gene *mxan_2537* was previously studied and like *agmP,* it was not required for gliding motility (D. Wall, personal communication).

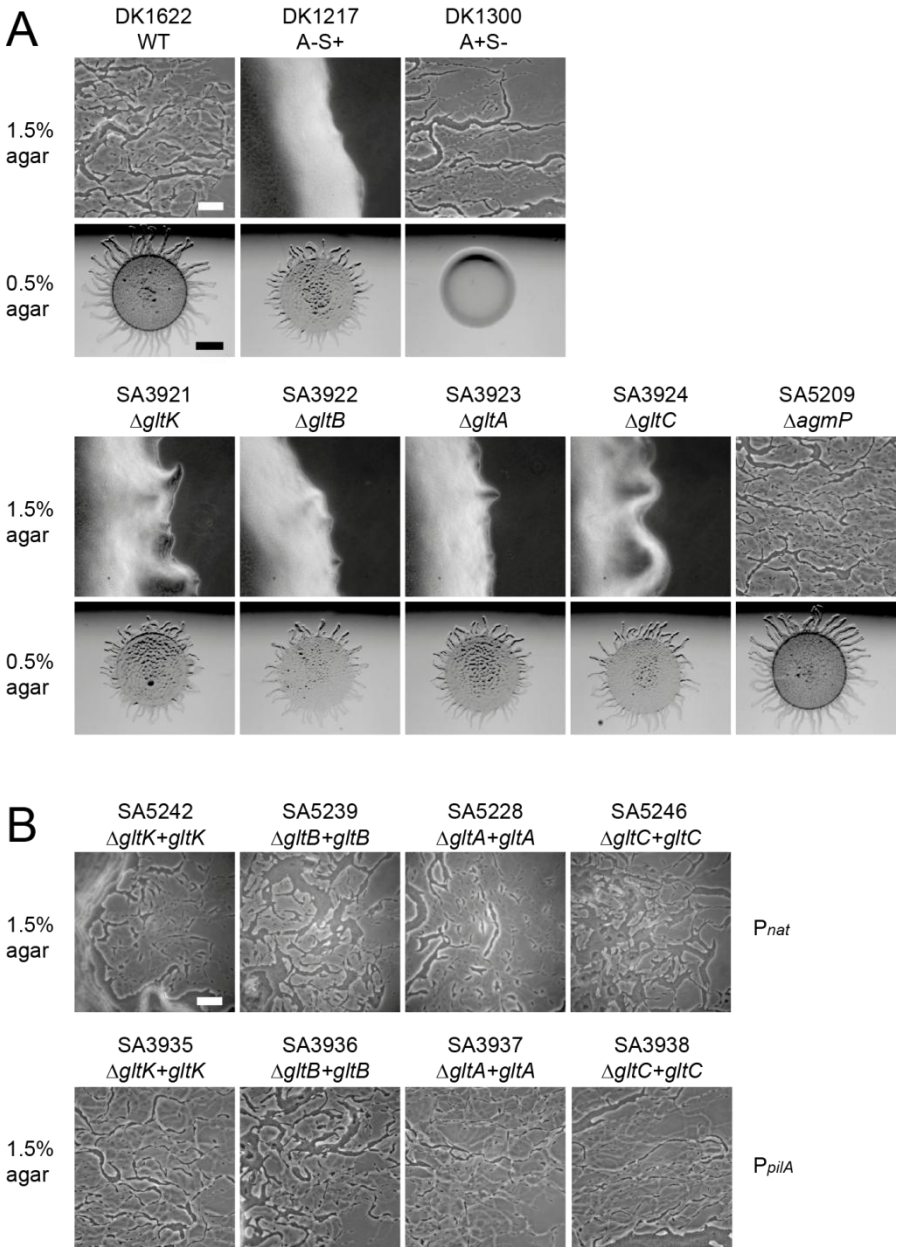

Figure 13. Genes encoded in the G2 cluster are essential for gliding motility.
Motility assay on soft (0.5% w/w) and hard (1.5% w/w) agar which favors T4P-dependent and gliding motility, respectively. Images of the colony edges were taken after 24h incubation at 32°C. (A) The upper panel shows the controls, DK1622 as a positive control, DK1217 and DK1300 as a negative control for gliding motility and S-motility, respectively. In frame deletion mutants are shown in the bottom panel. (B) Images for the complementation strains are shown only for gliding motility. Proteins were expressed from the native (P_{nat}) or *pilA* (P_{pilA}) promoter. SA numbers indicate for strain number. Scale bar for gliding motility = 50 µm.Scale bar for S-motility = 2 mm.

To exclude polar effects, complementation strains were generated by introducing the corresponding WT gene copy under the control of the native or *pilA* promoter (Keilberg PhD thesis) at the Mx8 *attB* site. Based on the data from operon mapping, two native promoters were used in this experiment; the *gltK* native promoter (a 277bp fragment upstream from the *gltK* open-reading frame) and the *gltBAC* native promoter (a 277bp fragment upstream from the *gltB* open-reading frame). The complementation strains were analyzed on 0.5% CTT plates containing 1.5% agar to test gliding motility. Microscopy analysis revealed that single cells were spreading at the edges of the bacterial colonies indicating that the gliding motility defect in all four mutants was complemented. Thus, the observed gliding motility phenotypes resulted from the lack of any one of the *glt* genes and were not due to polar effects (Figure 13B).

In order to test the protein levels in the complementation strains, we tested cell lysate by Western blot, using antibodies specific to each protein (Figure 14). In the case of GltK, the protein level in the complementation strain, using native promoter, was very low in comparison to the WT. Interestingly, we observed that the protein expression from the *gltBAC* native promoter resulted in GltB and GltA overexpression while GltC accumulation was decreased in comparison to the WT. These observations indicate that the position on the (long) mRNA influences protein expression in WT cells. However, in the case of GltK and GltC the low level of proteins in the cells were sufficient to restore the gliding motility defect. Moreover, in the case of GltB and GltA high level of proteins did not have dominant negative effect on gliding motility. In contrast, complementation strains with *pilA* promoter in place of native promoter revealed protein overexpression in the case of all four proteins encoded in G2 cluster (Figure 14B), none of these strains showed defects in gliding motility. In total, we concluded that concentration of G2 proteins in the cell is not so relevant to have active gliding motility.

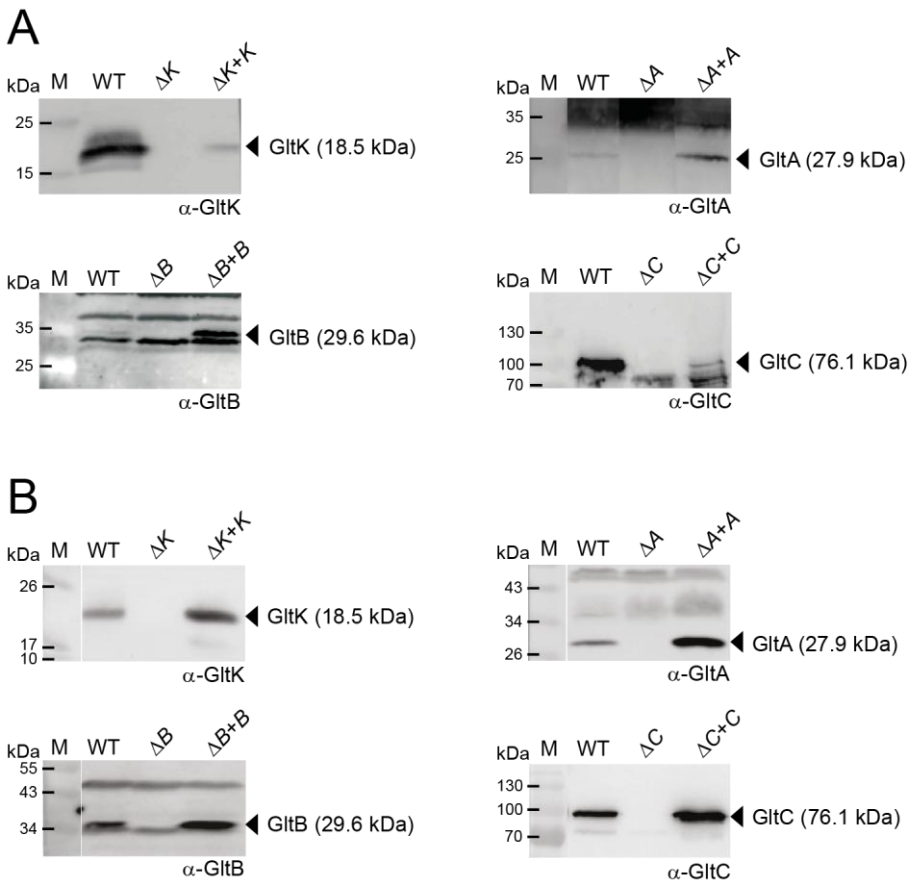

Figure 14. Immunoblot analysis of G2 cluster complementation strains.
Cell extracts of WT, deletion mutants and complementation strains were analyzed by Western blot using protein-specific antibodies. Each sample was concentrated to density of 2.5×10^9 cells/ml. Black triangles indicate correct protein bands with indicated calculated molecular weights in brackets. M indicates molecular marker, while black bars correspond to molecular masses in kDa. K, B, A and C stands for genes *gltK, gltB, gltA* and *gltC,* respectively. The first lane in each blot represents WT lysate, the second lane lysate of the relevant in-frame deletion mutant and the last lane the relevant complementation strain. (A) The complementation strains express proteins under control of the native promoter at the Mx8 *attB* site. (B) The complementation strains express proteins under control of the *pilA* promoter at the Mx8 *attB* site.

2.2 GltB, GltA and GltC form a complex in the cell envelope

2.2.1 GltK, GltB, GltA and GltC localize to the cell envelope

All four G2 proteins are encoded within one gene cluster and based on the domains and signal peptides identified by bioinformatics analyses as well as operon mapping, three of the proteins are predicted to localize to the OM, and one is predicted to be in the periplasm. Building on bioinformatic studies and operon mapping, we hypothesized that the G2 proteins form a subcomplex in the cell envelope. To check this hypothesis we tested the sub-cellular localization of GltK, GltB, GltA and GltC by analyzing different cell fractions. We

probed cell extract from whole cell lysate and from soluble and membrane fractions by Western blot using antibodies specific to each of the G2 proteins as well as antibodies specific to PilB, PilC and PilQ, which served as controls of cytoplasmic, IM and OM cell fractions, respectively. Cell fractions were prepared as described in 4.5.7. Immunoblot analysis revealed a membrane localization of GltK. Similarly, the two predicted OM proteins GltB and GltA were detected in the membrane fraction. None of these proteins were found in the soluble fraction. In contrast, GltC was found to accumulate in the soluble fraction, containing both cytoplasmic and periplasmic proteins, but not in the membrane fraction (Figure 15). In accordance with bioinformatic data that suggested that GltC contains a type I signal peptide, we assume a periplasmic and not a cytosolic localization of GltC in the cell although this assay cannot differentiate between the two cases (Table 1).

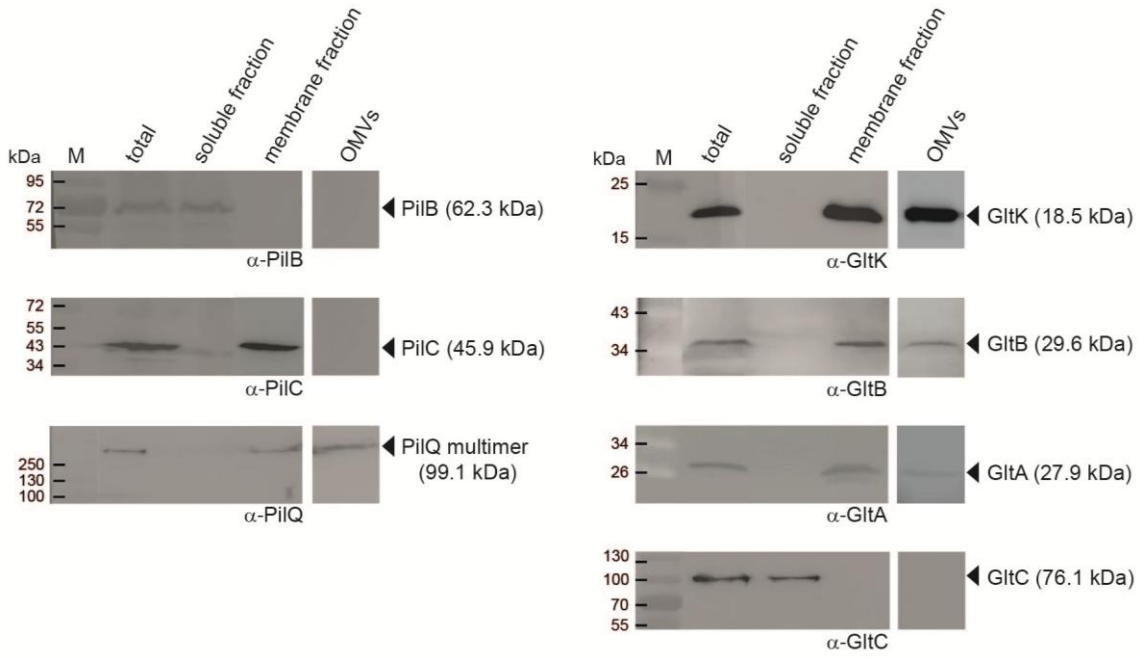

Figure 15. Envelope localization of the G2 proteins.
Western blots using antibodies raised to the indicated proteins. PilB, PilC and PilQ were used as control markers of the soluble, inner membrane and outer membrane cell fractions, respectively. OMVs served as outer membrane fraction due to difficulties in separating inner from outer membrane. Samples of different cell fractions were analyzed by Immunoblots. M indicates the molecular marker.

The next step was to test whether the three membrane associated proteins are inner- or outer-membrane proteins. Because of some difficulties in separating membranes using detergents, we decided to harvest outer

membrane vesicles (OMVs) that are derivatives from the OM. One of the G2 proteins (GltA) was previously identified as a protein found in OMVs (Kahnt *et al.*, 2010). Here, we detected GltA in the membrane fraction as well as in OMVs. Similarly, Western blots using specific antibodies revealed that GltB and GltK localize to OMVs. Because GltK is a lipoprotein and has been shown to be transferred between *M. xanthus* cells, we suggested that it is attached to the OM. Furthermore the localization of GltB and GltA in OMVs is consistent with the bioinformatic data, which proposed a secondary structure dominated by multiple β-sheets, a secondary structure common in integral OM β-barrel proteins.

2.2.2 GltB, GltA and GltC are interdependent in terms of protein stability

Given the absence of gliding motility in strains lacking any of the G2 genes, we sought to understand where the G2 proteins fit with the known gliding motility machinery and hypothesized that they interact with the known components of the FAs. Often, complex-forming proteins interact directly and are interdependent in terms of stability. Following this idea, we next aimed to test whether GltK, GltB, GltA and GltC depend on each other for stability. To do so, we used immunoblots to test the stability of the G2 proteins in the absence of each other. Briefly, cells grown to exponential phase were harvested, lysed and proteins in the lysate were separated by SDS-PAGE. The protein levels of the G2 proteins in the cell extracts were determined by immunoblots using specific antibodies.

First we tested GltK, a predicted lipoprotein, which was detected at levels comparable to WT in the Δ*gltB*, Δ*gltA* and Δ*gltC* mutants, suggesting that lack of these genes did not affect the stability of GltK (Figure 16). GltK was not detected in its own deletion mutant confirming the specificity of the antibodies. Next, we examined the OM proteins GltB and GltA. GltB accumulated to WT levels in the absence of *gltK* or *gltC*. In contrast, a lack of *gltA* resulted in loss of GltB, suggesting that GltA is essential for GltB stability. Furthermore, GltA was found to accumulate in a *gltK* deletion strain at levels comparable to WT. Similarly, a *gltC* deletion mutant resulted in no effect on GltA accumulation suggesting that neither GltK nor GltC is essential for GltA stability. In Δ*gltB* and

Δ*gltA* cell extract, GltA was not detectable indicating that GltB stabilizes GltA in the cells. Finally GltC, a periplasmic protein with TPR repeats was found to accumulate in the absence of *gltK* at levels comparable to WT using specific GltC antibodies. However, GltC was not stable in the cells lacking *gltB* and *gltA*, as we were not able to detect GltC in cell extracts originating from these two deletion mutants.

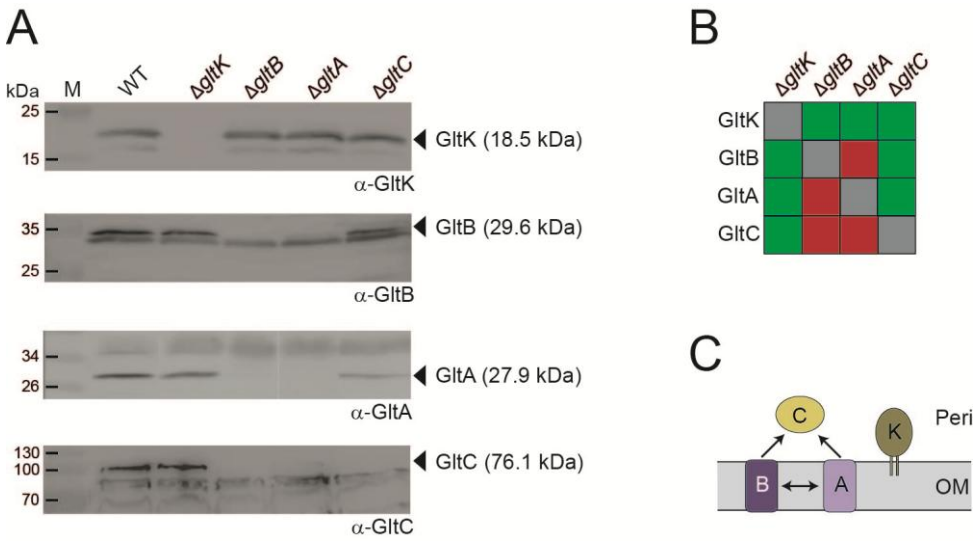

Figure 16. GltB and GltA are required for stability of G2 proteins.
(A) Immunoblot analysis of cell extracts from WT and in-frame deletion mutants of each gene of the G2 cluster Δ*gltK*, Δ*gltB,* Δ*gltA,* Δ*gltC*. M corresponds to the protein marker with the corresponding molecular weights of the protein marker indicated to the left. The black arrows indicate the correct band of the protein with the calculated molecular weight in parentheses. The primary antibodies used are listed underneath each corresponding immunoblot. (B) Summary of protein stability dependency. Grey indicates no protein accumulation in the corresponding in-frame deletion mutant, green indicates no changes in protein stability, and red indicates no protein accumulation (C) A model representing protein stability dependencies among G2 proteins. K, B, A and C stands for GltK, GltB, GltA and GltC respectively. OM:outer membrane; Peri: periplasm. Arrow head indicates direction of influence.

In summary, GltK accumulates independently of the other G2 proteins, but GltB and GltA play important roles in the stability of the remaining G2 proteins. The absence of *gltC* in the cell did not result in any changes in accumulation of GltB, GltA or GltK, suggesting that GltC requires interaction partners for stability, but it is not essential for the accumulation of other proteins encoded in the G2 cluster. These data strongly suggest that GltB, GltA and GltC form a complex.

2.2.3 GST-GltB and GltC-His form oligomers while MalE-tagged proteins exist as monomers

The results from the fractionation experiment and the protein stability analysis strongly suggested that the GltBAC proteins form a complex in the cell envelope. To verify our hypothesis about this complex, our next goal was to check for direct protein-protein interactions *in vitro* by a pull-down assay using purified proteins. Presumably due to the OM localization of GltK, GltB and GltA, the corresponding His-tagged fusions in *E. coli* showed a tendency to accumulate in the pellet fraction during the purification process, suggesting that these proteins were aggregating non-specifically. Protein purification under denaturing conditions and subsequent refolding of the protein by dialysis could lead to improper three-dimensional protein structure, which could affect protein-protein interactions and/or protein activity; thus, we tested the solubility of the proteins fused to different tags. We have no assay to check for continued protein function, but assumed that soluble proteins would be more likely to be active. Interestingly the best candidate turned out to be the MalE tag. The use of this tag can be problematic because it can cause protein aggregation resulting from the incorrect folding of the proteins due to cytoplasmic conditions. Thus, purified proteins were analyzed by size exclusion chromatography to exclude non-functional aggregated proteins.

To produce purified soluble protein for further experiments, GltK (MalE-GltK), GltB (MalE-GltB, GST-GltB), GltA (MalE-GltA), GltC (MalE-GltC, GltC-His_6) and a negative control (MalE) were purified (Figure 17A). The signal peptides found on each of the G2 proteins were not included in the overexpression constructs to prevent secretion over the *E. coli* IM after protein induction. All proteins were overexpressed under control of the T7 promoter from *E. coli* Rosetta 2 cells carrying the T7 polymerase under the IPTG-inducible *lac*-promoter and purified under native conditions as described in 4.5.1. The purified proteins were loaded on a gel filtration column in order to analyze the potential oligomeric states of the proteins and check for aggregation. This step was purely diagnostic, and the later experiments were carried out with elution fractions of purified proteins obtained from amylose column and not with aliquots obtained from the gel-filtration column.

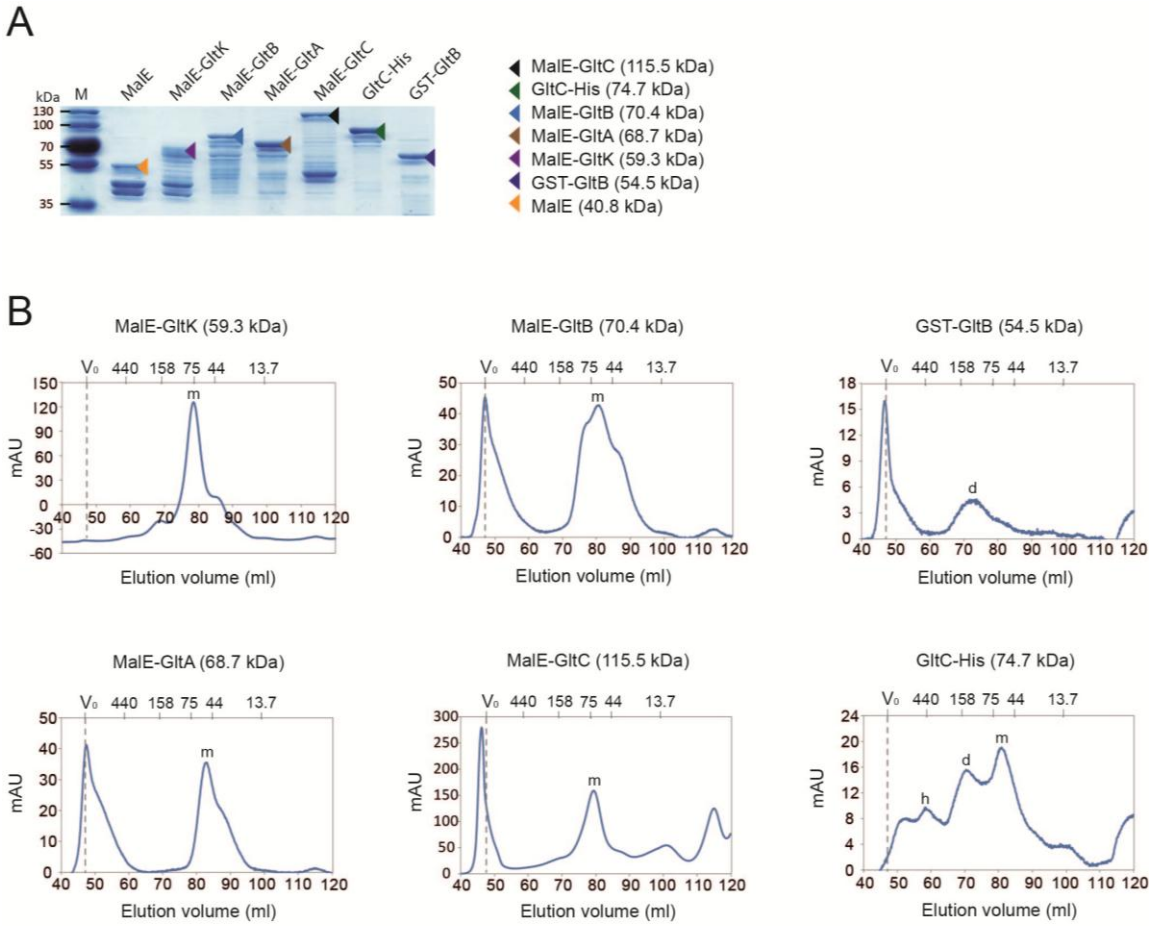

Figure 17. *In vitro* analysis of G2 proteins.
(A) SDS-PAGE analysis of purified proteins. The proteins were stained with Page Blue. The molecular marker is indicated as M. Each arrow indicates the purified protein with a size as expected from its aa sequence, with the calculated molecular mass indicated to the right, visible additional bands are putative degradation products. (B) Diagrams representing results from size-exclusion chromatography experiments (Hi Load 16/600 Superdex 200 prep grade). Molecular size markers are indicated at the top in kDa. Peaks marked with small letters m, d, h corresponds to monomer, dimer and hexamer, respectively.

MalE-GltK eluted from the column as one peak only, corresponding to a monomeric state (Figure 17B). The three other MalE tagged proteins, MalE-GltB, MalE-GltA and MalE-GltC, eluted as one peak, corresponding to the expected mass of protein monomers, as well as in void volume. In contrast, the elution profile for GltC-His_6 showed three peaks corresponding to the masses of monomers, dimers and hexamers, while GST-GltB eluted with a size corresponding to dimers as well as in void volume (Figure 17B). The GST tag was previously reported to exist as a stable dimer, suggesting that GST-GltB dimerization might result from the interaction between the GST tags (Tudyka & Skerra, 1997).

Tag selection which would make a protein of interest soluble proved to be very challenging. Ultimately, all obtained soluble fusion proteins that were analyzed on the gel-filtration column and showed to not elute only in the void volume, which would indicate aggregation, were predicted to be fully functional. These purified proteins were used in the subsequent pull down experiments.

2.2.4 GltB, GltA and GltC interact directly

We tested for direct interactions between GltK, GltB, GltA and GltC using the purified proteins in pull down experiments, as described in detail in 4.5.8. Briefly, we incubated two proteins together with amylose matrix for one hour, and one of those proteins included a MalE-tagged protein that served as the bait and GST-GltB or GltC-His as prey proteins. The matrix was packed into a column and washed (5x10 ml CB1 buffer), and then proteins were eluted with a buffer containing 10 mM maltose. The experiment was performed in two series: in the first series we tested for a direct interaction between GltC-His_6 and each of the three other G2 proteins (MalE-tagged); in the second series we checked for interactions between GST-GltB and each of the other G2 proteins (MalE-tagged). As negative controls, we included MalE and GST-GltB or MalE and GltC-His reactions. For each protein pair we analyzed the mixture of proteins before loading on the amylose matrix (L), the flow through (FT), the last wash (W) and the eluate (E) by immunoblot using antibodies specific to the bait and prey for each tested pair (Figure 18).

The results from the first series of experiments with GltC-His_6 showed that in the negative control GltC-His did not interact with the MalE tag (Figure 18A). As in the negative control, GltC-His_6 did not elute with MalE-GltK, but did elute with MalE-GltB and MalE-GltA, suggesting that GltC interacts directly with GltB and GltA, but not with GltK (Figure 18A). In the second series of pull down assays testing for direct interactions with GltB, the analysis of samples deriving from the mixture of GST-GltB and MalE tag, which served as a negative control, revealed no direct interaction between GltB and the MalE tag itself. As in the experiments carried out with GltC-His_6, no interaction between MalE-GltK and GST-GltB was detected. In contrast, GST-GltB and MalE-GltA were each detected by immunoblot in the elution fraction when incubated together. This

shows that GltB, GltA and GltC interact directly with each other (Figure 18). The finding that GltB, GltA and GltC interact is in agreement with data obtained from the protein stability analysis, which showed that these three proteins depend on each other for stability. The interaction studies support the previously stated hypothesis that GltBAC proteins form a complex in the cell envelope. A summary of direct protein interactions is presented in Figure 18C.

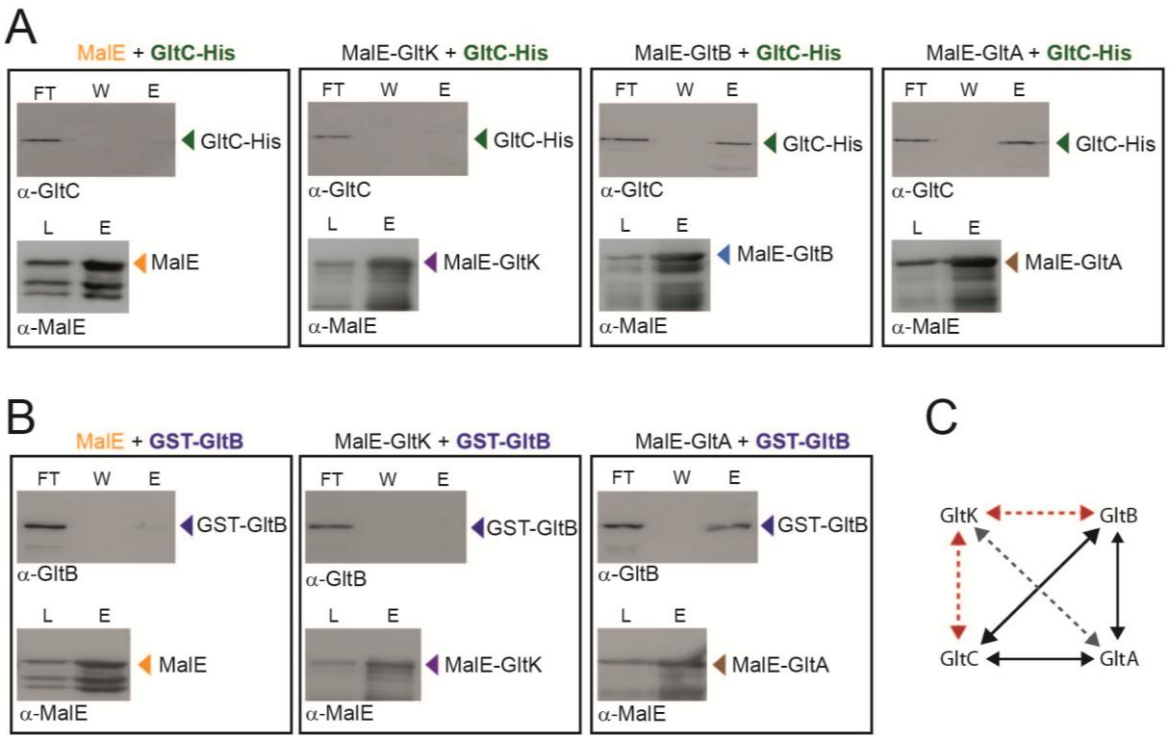

Figure 18. GltB, GltA and GltC interact directly.
MalE, MalE-GltB, GST-GltB, MalE-GltA, MalE-GltC and GltC-His have been expressed and purified from *E.coli* Rosseta 2 cells. The purified proteins have been used in pull down assays to check for direct protein interactions. In the experiment amylose matrix was used. The protein mixtures before loading on column (L), the flow through (FT), the last washing step (W) and the elution (E) were checked by immunoblots using respective antibodies. (A) GltC-His interacts directly with MalE-GltB and MalE-GltA. Green triangle indicates the protein band of GltC-His with calculated molecular weight of 74.7 kDa. (B) GST-GltB interacts directly with MalE-GltA. Blue triangle indicates the protein band of GST-GltB with calculated molecular weight of 54.5 kDa. (C) Summary of direct protein interactions. Red dashed lines: no interaction; grey dashed line: not tested; black lines: interaction.

2.2.5 BACTH

We performed Bacterial Two-Hybrid analysis (BACTH) to further analyze direct protein interactions of the G2 proteins *in vivo*. Due to transmembrane localization of GltB and GltA, we checked only for direct interactions between

GltK and GltC using BACTH. One of the significant advantages of BACTH system over pull down experiments are the native conditions which facilitate protein-protein interactions because the assay is carried out *in vivo* in *E. coli* cells. However, there are also disadvantages, one limiting factor being the low sensitivity of the system for detecting transient or weak protein interactions.

To test for direct interactions, *E. coli* BTH101 cells were transformed with two constructs, each harboring *gltK* or *gltC* fused either to the T18 or T25 fragment of adenylate cyclase. Each BACTH assay was performed as described in 4.3.5 and 4.4.11. In the BACTH system, interaction between two proteins of interest leads to functional complementation between the T18 and T25 fragments and, therefore, cAMP synthesis resulting in a Cya+ phenotype. cAMP turns on the expression of genes involved in lactose and maltose catabolism. One of them is β-galactosidase that hydrolyses X-Gal to galactose and 5-bromo-4-chloro-3-hydroxyindole, the second product oxidizes to insoluble product with an intensely blue color. The positive protein-protein interaction is visualized by a blue color of the bacterial colonies on indicator media containing X-Gal. T25-zip and T18-zip fusion proteins expressed from pKT25-zip and pUT18C-zip served as positive control because the dimerization of these zipper motifs results in strong Cya+ phenotype. In the negative control, empty plasmids were used, and the T18 and T25 fragments alone cannot interact, resulting in white colonies on the indicator medium.

We analyzed all possible options for interaction between GltK and GltC using the BACTH assay. However, no positive interactions between these two proteins were detected (Figure 19). Interestingly, GltK was found to interact with itself suggesting that GltK oligomerizes. In contrast, size exclusion chromatography did not reveal GltK multimers; however, for that analysis a MalE tagged version of GltK was used. The molecular mass of MalE is twice as big as that of GltK, and the tag could act as a barrier preventing the interaction of GltK with other protein molecules. The BACTH system failed to link GltK directly to GltC. This could be because interaction between GltK and GltC is weak or transient in nature. Another possibility is that GltBAC must first form a complex to interact with GltK. It can also not be excluded that additional

interaction factors are needed for GltK and GltBAC to interact, or they may not interact directly.

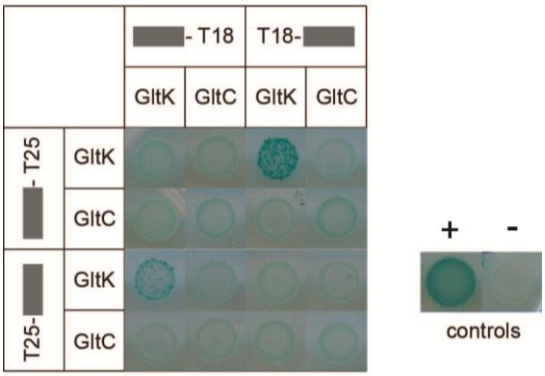

Figure 19. Analysis of interaction between GltK and GltC by BACTH.
Bacterial two hybrid assays were performed as described by Euromedex. GltK and GltC indicate proteins that are expressed from pUT18C, pUT18, pKNT25 or pKT25 vectors. GltK and GltC are fused to T18 or T25 fragments C- or N- terminally as is indicated by pictures in the row or column headings. Blue and white colonies indicate direct interaction and no interaction, respectively.

2.3 GltB, GltA and GltC localize dynamically in multiple clusters

One of the current gliding motility models proposes that proteins essential for gliding motility build the cell envelope spanning complexes on the ventral side of the cell called FAs (Luciano *et al*., 2011). AglQ and AglZ, well studied gliding motility proteins, localize to multiple clusters referred to as FAs, which are distributed along the cell body and stationary with respect to the substratum in moving cells (Mauriello *et al*., 2009, Sun *et al*., 2011b). Following these data we aimed to test whether the G2 proteins localize in the same pattern as the other gliding motility proteins previously localized to FAs.

To visualize the G2 proteins, we performed fluorescence microscopy and tested various expression strategies and fluorescent tags. Initial attempts to express C-terminally tagged mCherry fusion proteins from the *pilA* promoter resulted in protein overexpression in comparison to the WT and a diffuse envelope localization pattern. The next attempts involved a copper-inducible promoter and a sfGFP tag. Analysis of gliding motility of strains carrying such sfGFP fusions revealed that the fusion proteins were partially or fully nonfunctional. In contrast, mCherry fusions expressed under control of the copper-inducible promoter proved to be fully functional; however, the cells

showed high background signal probably due to the high copper concentration in the media. We also created and tested mutants with C-terminally tagged fluorescent fusion proteins at the native site in the genome and expressed from the native promoters; however, these trials resulted in non-functional proteins. The fluorescently tagged G2 proteins with the highest activity and most wt-like expression levels used the native promoter and mCherry tag fused C-terminally to the protein of interest and expressed from the Mx8 *attB* site. Unfortunately, we were not successful with any *gltK* construct, as multiple trials with different promoters and fluorescent proteins did not result in a functional fusion protein. We decided to continue our investigation of the localization of GltB, GltA and GltC, excluding GltK from the studies.

Strains expressing G2 protein mCherry fusions were analyzed by motility assays to test for active fusion proteins. Cell suspensions were spotted on hard agar, which favor gliding motility as defined by single cell movements. Results from this motility assay revealed that GltB-, GltA- and GltC-mCherry can successfully complement gliding motility defects caused by the deletion mutations of the respective genes, suggesting that the fusion proteins are fully functional (Figure 20).

Furthermore, immunoblots using specific antibodies confirmed that GltB- and GltA-mCherry accumulated in the WT and mutant backgrounds at levels comparable to the WT protein (Figure 21A,B). In contrast, immunoblot analysis of strains harboring GltC-mCherry revealed that the level of this fusion protein is severely reduced in comparison to WT (Figure 21C). These observations might be the result of the incorrect amount/section of DNA which was used as the promoter as we already observed that the levels of GltC expressed under control of native promoter at the Mx8 *attB* site is strongly reduced in comparison to WT in the complementation strains (Figure 14). As an additional control, Δ*gltB* and Δ*gltA* strains harboring *gltB*- and *gltA-mCherry* were analyzed for the presence of GltC and GltA or GltB, respectively, due to interdependence of G2 proteins in terms of stability. The GltB-mCherry fusion was shown to be sufficient for GltA and GltC accumulation in the cell. Similarly, GltA-mCherry was found to stabilize GltB and GltC in the cells, in agreement with data from the motility assays.

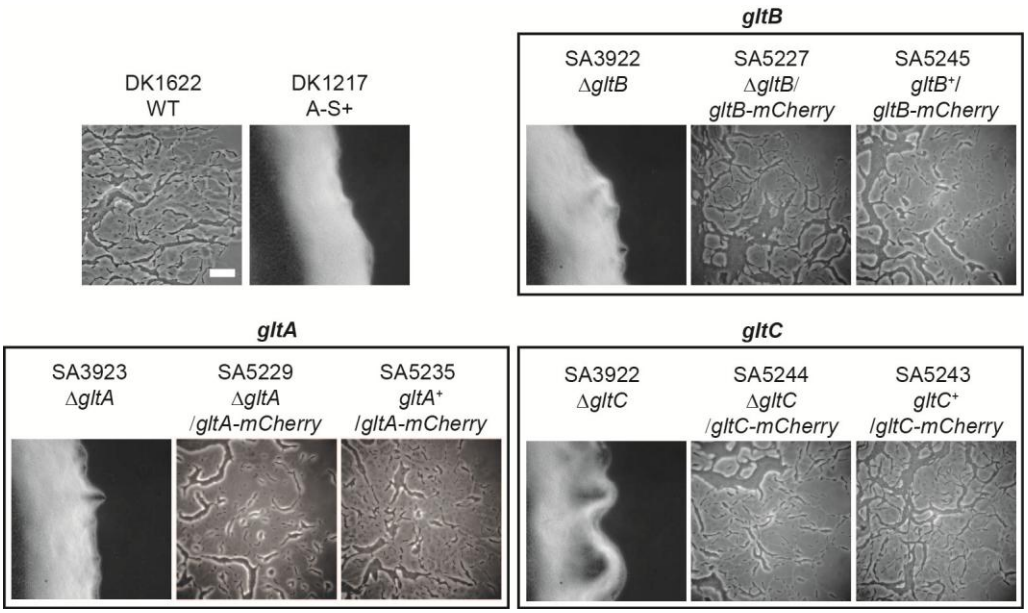

Figure 20. Analysis of *M. xanthus* strains harboring GltB-mCherry, GltA-mCherry and GltC-mCherry in terms of motility.
Single motility assay on hard agar (1.5% w/w). DK1622 and DK1217 strains served as positive and negative control, respectively. Images of bacterial colony edges were taken after 24h incubation at 32°C. SA numbers indicate for strain number. Scale bar = 50μm.

The microscopy analyses revealed multiple clusters of GltB- and GltA-mCherry that were distributed along the length of the cell body as previously observed for AglQ-mCherry (Sun *et al*., 2011b). Interestingly, GltB- and GltA-mCherry fusions could be additionally observed to localize evenly all around the cell envelope. In total, the cells revealed two patterns of protein localization: uniform membrane localization and membrane localization with multiple bright foci. The number of cells expressing GltB- and GltA-mCherry fusions, which showed clustered localization pattern of these proteins, differed when compared in WT and deletion background strains. In the case of GltB-mCherry, 81% of cells showed multiple bright foci in WT backround, while only 48% of cells showed the same localization pattern in the deletion background (Figure 22A). The opposite situation was observed for cells carrying GltA-mCherry fusion. In 71% of WT cells GltA-mCherry localized to multiple foci whereas in deletion background up to 93% of cells showed the same localization pattern (Figure 22B). These data indicate that protein levels are important for cluster formation. Moreover, fluorescence microscopy revealed that GltC-mCherry localized similarly to GltB- and GltA-mCherry fusions and formed multiple clusters distributed along the cell body (Figure 22C). While only 30% of WT cells

revealed multiple cluster localization of GltC-mCherry, up to 70% of cells lacking *gltC* showed the same localization pattern of GltC-mCherry. Unfortunately the low GltC-mCherry expression resulted in poorly visible signal from the fusion proteins under the microscope, which made it impossible to make any conclusions about putative envelope GltC localization.

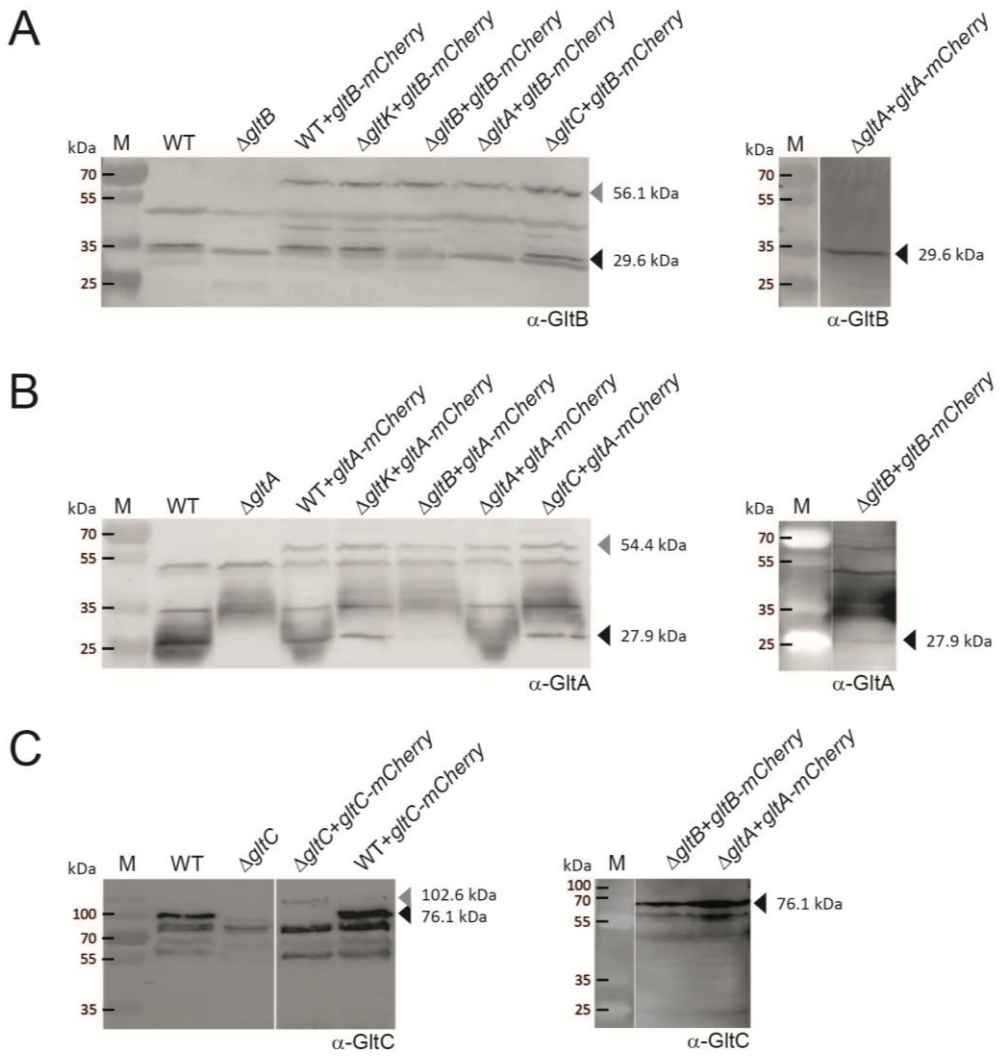

Figure 21. Immunoblot analysis of *M. xanthus* strains harboring GltB-mCherry, GltA-mCherry and GltC-mCherry fusions.
Immunoblot analysis of *M. xanthus* strains expressing mCherry fusion proteins under control of the native promoter from the Mx8 *attB* site. The band corresponding to the fusion protein is marked with a grey triangle, while native protein is marked with black triangle. Calculated molecular masses of the native and fusion proteins are indicated on the right side of the triangles.

The current gliding motility model proposes that the gliding machinery is located on the ventral side of the cell, close to the gliding surface. In a previous work, Luciano *et al*. analyzed the localization of periplasmic GltD by

investigating different z layers of the cells, which revealed that GltD clusters were clearly visible when the focal plane was focused closer to the substratum (Luciano *et al*., 2011). To test whether GltBAC clusters localize to the ventral side of the cell, we performed microscopy analyses on cells carrying GltB, GltA or GltC fusions to mCherry along the z-axis. In agreement with previously published data and the proposed gliding motility model, clusters were mostly visible when the focal plane captured the ventral cell surface close to the substratum (Figure 22). Similar observations were made for AglQ-mCherry; in focal planes dorsal to the substratum, the protein clusters disappear and only the envelope protein localization was visible (Figure 31).

To uncover the dynamics of the observed GltB- and GltA-mCherry clusters, we continued with time-lapse recording tracking the behavior of the clusters during cell movement. Interestingly, we discovered that GltB- and GltA-mCherry clusters behaved in the same manner as AglZ-YFP and AglQ-mCherry clusters. The observed clusters stay fixed to the substratum in moving cells. Additionally, we observed that new clusters appeared close to the leading cell pole and disappeared near the lagging cell pole, which is consistent with the current FA motility model. This supports that new FAs are assembled at the leading cell pole while old FAs are disassembled at the lagging cell pole.

Furthermore, during analysis of the time-lapse recordings, we observed that reversing cells lost FAs distributed along the cell body shortly before reversal, and new FAs appeared at the leading cell pole when the cell started to move in the opposite direction, supporting the notion that the polarity of gliding motility machinery was reversed and the motility complexes were assembled anew. Although GltC-mCherry was shown to complement the deletion strain’s motility defect, the fusion protein may not be fully functional based on the microscopic observations. Two types of GltC-mCherry clusters were observed: clusters that stayed fixed as the cell moved and clusters that moved with the cell. The bright clusters that were moving with the cell were visible not only at the mCherry channel, but also at other fluorescence channels, suggesting that these clusters were made up of non-functional proteins forming inclusion bodies. However, since some clusters stayed fixed relative to the substratum within moving cells, as observed in GltB- and GltA-mCherry microscopy

analyses, we hypothesized that these were functional fusions and that their localization indicated a connection with the gliding motility machinery. The data obtained from microscopy analyses strongly indicate that the GltBAC complex is a component of FAs (Figure 22).

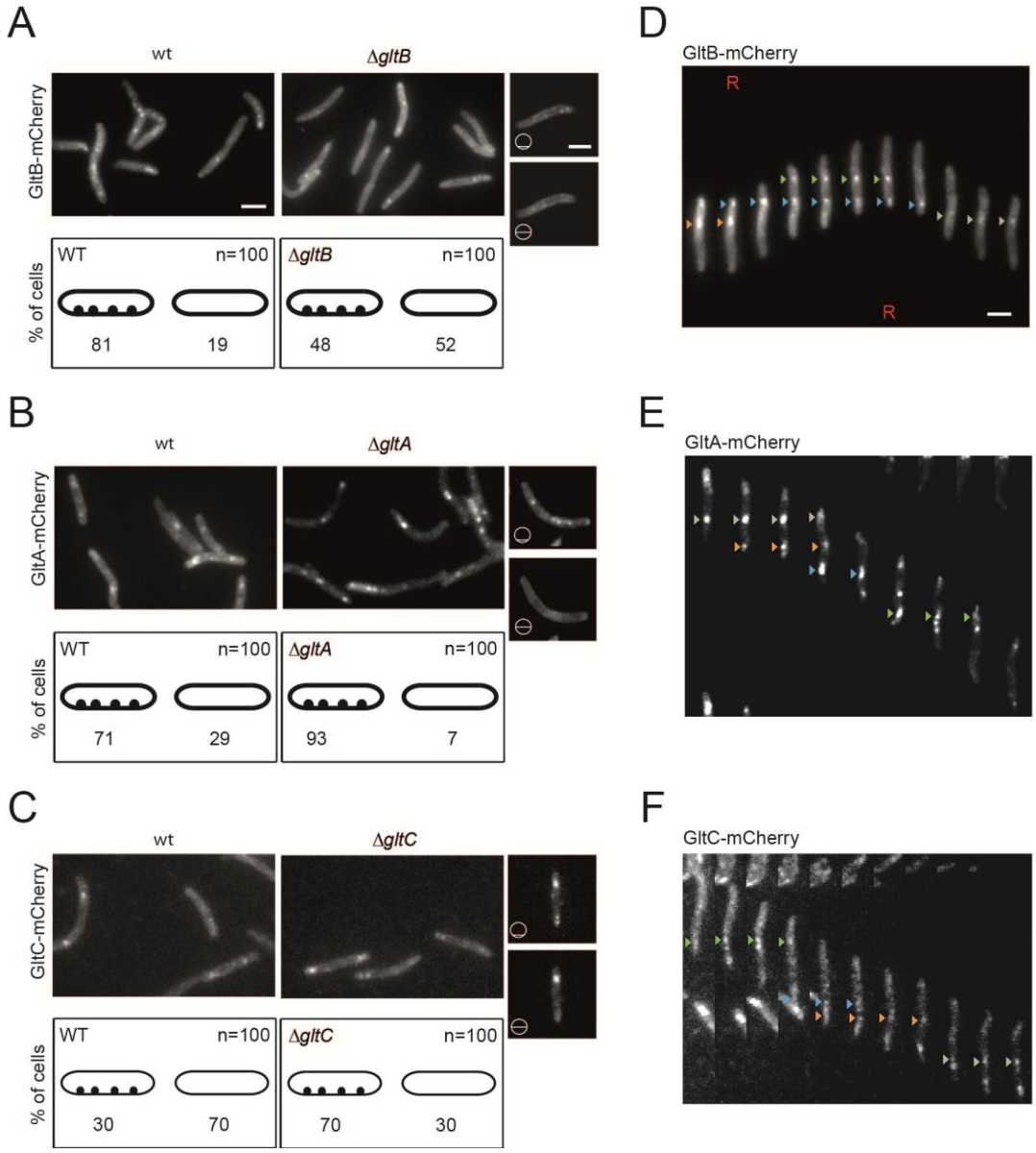

Figure 22. GltB, GltA and GltC localize dynamically in multiple clusters.
(A, B, C) Localization of GltB-mCherry, GltA-mCherry and GltC-mcherry in WT and mutant backgrounds. Glt proteins localize to the cell envelope and additionally to multiple clusters distributed along the cell body; schematics below the micrographs show quantifications of these localization patterns as observed in 100 cells. The right-most images show unprocessed fluorescent micrographs of 2 different z sections. The z positions are indicated by a barred circle. (D,E,F) Dynamic localization of GltB-mCherry, GltA-mCherry and GltC-mCherry in the deletion mutant backgrounds during cell movement. Matching colored triangles indicate the position of the same protein cluster during cell movement. R stands for cell reversal. Scale bar = 2 µm.

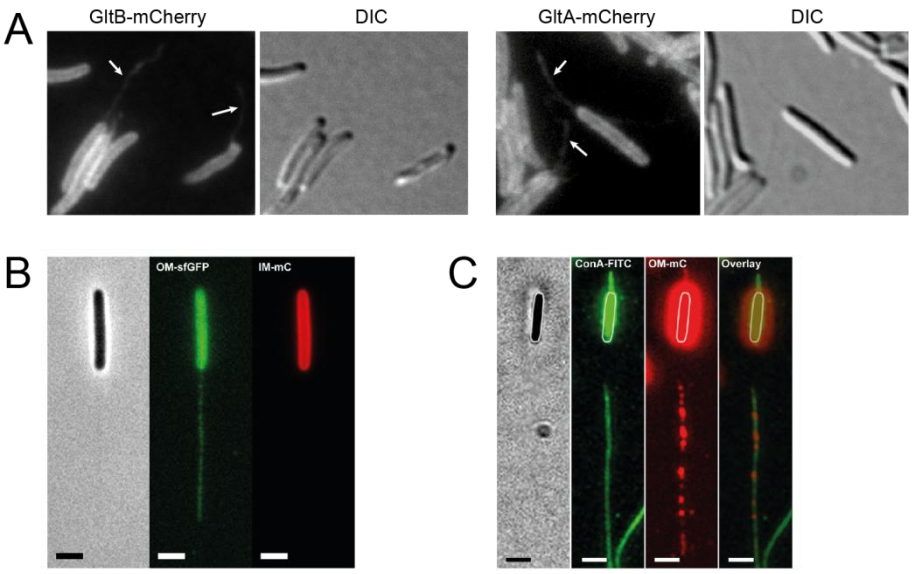

Figure 23. GltB-mCherry and GltA-mCherry fusions are deposited by *M. xanthus* cells.
(A) Fluorescent images representing GltB- and GltA-mCherry localization into the OMVs/lipid tubes. White arrows indicate deposited outer membrane material. (B) Visualization of deposited OMVs and lipid tubes by sfGFP. Scale bar = 1 µm. Figure modified from Ducret *et al.* (2013). (C) Visualization of deposited slime by staining with ConA-FITC and outer membrane material by mCherry fusion. Scale bar = 1 µm. Figure modified from Ducret *et al.* (2013).

During fluorescence microscopy, we observed that the cells expressing GltB- and GltA-mCherry fusions left fluorescent tracks behind them (Figure 23A). Previous studies suggested that cells deposit slime and outer membrane material (Ducret *et al.*, 2013). Unfortunately, such outer membrane material cannot be distinguished from lipid tubes, which have been suggested to be involved in protein transfer and OMVs (Wei *et al.*, 2014). However, it was shown that OMVs can form chain like structures which resemble the appearance of tubes. Furthermore, it was shown that the secreted slime trails colocalize with outer membrane material (Figure 23C). Fluorescent tracks of GltB- and GltA-mCherry resembled the tube-like structures previously identified by Ducret *et al*. These data indicate that indeed GltB- and GltA-mCherry localize to the OM and are deposited with the outer membrane material, which is in agreement with the data from the cell fractionation studies where GltB and GltA were found in the OMV fraction.

2.4 Gliding motility proteins show localization dependencies

2.4.1 Localization of GltB and GltA is affected in the absence of each individual G2 protein

Biochemical experiments revealed direct interactions between GltB, GltA and GltC. Furthermore, these three proteins appeared to stabilize each other, suggesting that they are most likely interdependent for correct localization in the cell. To further investigate the possible connections between the G2 proteins, we analyzed the localization of GltB- and GltA-mCherry in the absence of each individual protein encoded in G2 cluster. The findings help us understand how the G2 complex is assembled as well as the nature of the mutual influence of G2 proteins on each other. The strains carrying GltB- and GltA-mCherry fusions in Δ*gltK*, Δ*gltC* and Δ*gltA* or Δ*gltB* were prepared and analyzed by immunoblot and fluorescence microscopy. We did not analyze GltC-mCherry localization due to the tendency of the fusion protein to form inclusion bodies in the cells, which could be easily confused with FAs. The strains were constructed in the same way as the complementation strains.

To test if the fluorescent tags affect protein stability, immunoblot analysis was performed. GltB-mCherry was detected in the absence of *gltA* at levels comparable to WT. Similarly, GltA-mCherry was found in the cell extract of the *gltB* deletion mutant, suggesting that both fusions are stable despite the reported protein stability dependencies. Based on these data we concluded that mCherry stabilizes GltB and GltA even in the absence of the proteins that are essential for the accumulation of the untagged protein (Figure 21A, B). Furthermore both fusion proteins were detected at levels comparable to WT in the *gltK* and *gltC* deletion backgrounds (Figure 21).

Fluorescence microscopy revealed that the percentage of cells with multiple GltB- and GltA-mCherry clusters was severely reduced in a Δ*gltK* background in comparison to WT (Figure 24), the majority of cells demonstrated a diffuse envelope localization pattern, indicating a relationship between GltK and the GltBAC complex, and thus to FAs. Similarly the deletion of *gltC*, and *gltA* or *gltB* inhibited the ability of GltB- and GltA-mCherry, respectively, to localize to multiple clusters. This supports that each protein encoded in the G2

cluster is essential for the formation of GltB- and GltA-mCherry clusters, which are integral parts of GltBAC envelope complexes. Although GltK seemed not to be involved in the formation or stability of G2 complexes based on interaction and stability studies, microscopy analyses reveal that it is essential for the correct localization of GltB- and GltA-mCherry within the cells. These data support that GltK interacts directly or indirectly with the GltBAC complex for proper localization, but not for complex formation or protein stability.

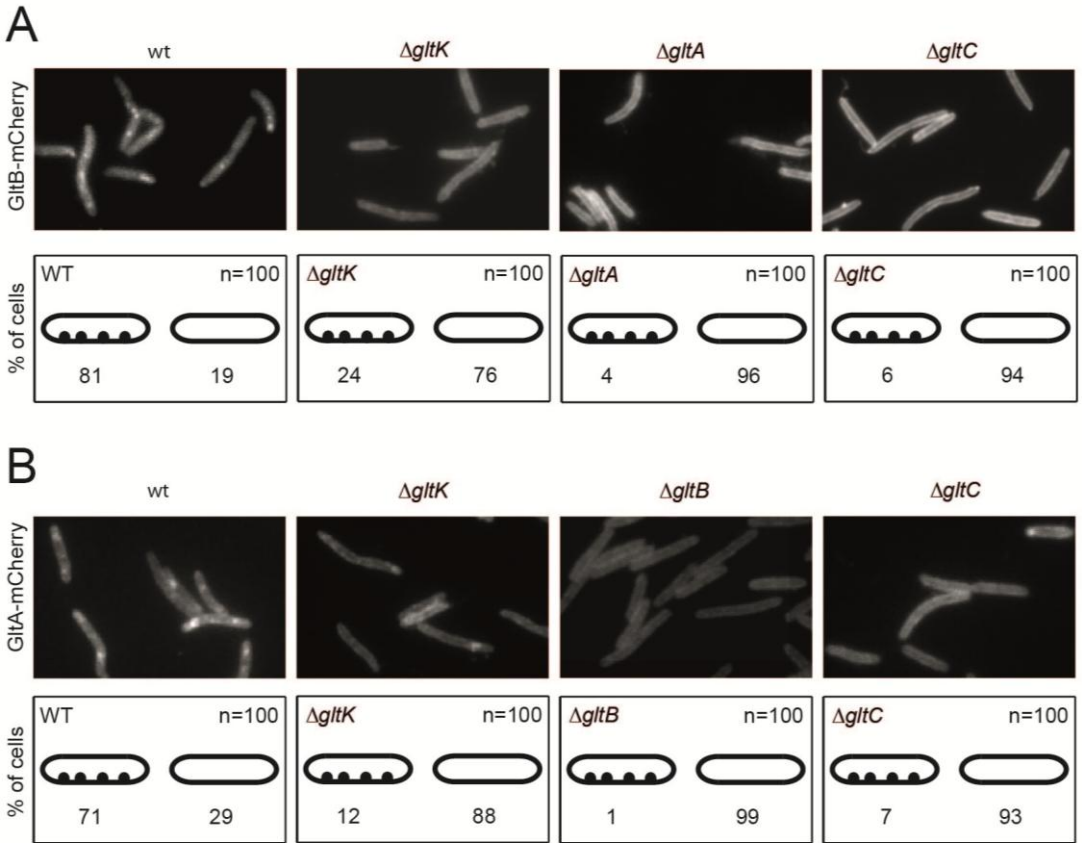

Figure 24. GltB and GltA require G2 proteins to form subcomplexes in the cell envelope.
GltB-mCherry and GltA-mCherry do not localize to multiple clusters in the absence of G2 proteins. Summary of results from fluorescence microscopy analysis of strains expressing (A) GltB-mCherry and (B) GltA-mCherry in different genetic backgrounds. Scale bar = 2 μm.

2.4.2 GltB and GltA accumulate independently of MglA, AglZ and AglQ

We have shown that the G2 proteins depend on each other not only for stability, but also for correct localization in the cells, confirming our hypothesis that GltA, GltB, and GltC form a complex in the periplasm and OM. Our next goal was to look for a connection between the OM proteins, GltB and GltA, and

other known FA components. To investigate whether the G2 proteins depend also on other gliding motility proteins, we aimed to test the effect of *aglZ, aglQ* and *mglA* deletion mutants on GltB and GltA accumulation in the cell by performing immunoblots with protein-specific antibodies. While MglA and AglZ are cytoplasmic regulatory proteins needed for gliding motility, AglQ is part of the IM motor complex that powers the gliding motility machinery (Sun *et al*., 2011b). The information about protein stability dependencies would give the valuable information about the potential hierarchical assembly of the gliding motility complex.

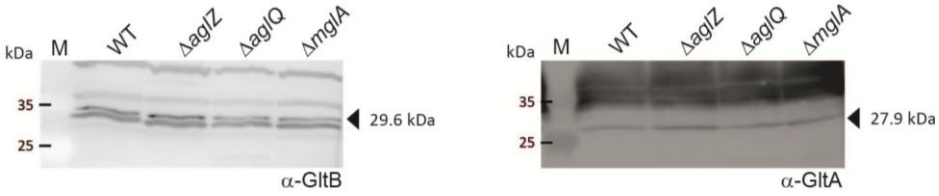

Figure 25. GltB and GltA accumulate independently of AglZ, AglQ and MglA in the cells.
Immunoblot analysis of GltB and GltA stability in *aglZ, aglQ* and *mglA* deletion mutants. The band corresponding to the protein is indicated by a black arrowhead and the calculated molecular mass.

Briefly, cells from exponentially growing cultures were harvested and resuspended in loading buffer to the OD_{550}=3.5. Cell extract samples of WT and three Δ*aglZ*, Δ*aglQ* and Δ*mglA* deletion mutants were resolved by SDS-PAGE and analyzed by immunoblot for the presence of GltB and GltA. By using specific antibodies, we could detect a protein band of GltB at levels comparable to WT in *aglZ*, *aglQ* and *mglA* deletion mutants (Figure 25). Furthermore, we discovered that the lack of *aglZ* did not affect the stability of GltA. Similarly, immunoblot analysis revealed that GltA accumulates in the cell at levels comparable to WT independently of AglQ and MglA (Figure 25). These data showed that GltB and GltA encoded in the G2 cluster most likely do not require other gliding motility proteins to accumulate in the cell.

2.4.3 Correct GltB and GltA localization depends on MglA, AglZ and AglQ

GltB- and GltA-mCherry fusions localize to multiple clusters distributed along the cell body that behave in the same manner as FAs, suggesting that the

G2 proteins are part of the gliding motility machinery. Although GltK is not required for GltBAC stability it is essential for cluster formation by GltB- and GltA-mCherry fusions. Similarly, MglA, AglZ and AglQ are not needed for GltBA stability (2.4.2). However, MglA, AglZ and AglQ might have an influence on GltB and GltA localization, which would suggest that these motility proteins act upstream of the G2 proteins, or that the G2 proteins and these other FA components form a single large complex. MglA and AglZ are part of the cytoplasmic portion of FAs and connect the FAs to the MreB actin cytoskeleton, while this work suggests that GltBAC are the most external part of FAs. MglA is involved in regulation of both motility systems in *M. xanthus* (Hartzell & Kaiser, 1991). Furthermore, MglA is essential for AglQ and AglZ cluster formation, suggesting that assembly of FAs depends on MglA (Hot *et al*., in submission). Moreover, AglZ is dependent on numerous gliding motility proteins for correct localization (Nan *et al*., 2010b). Further, AglQ is a motor protein involved in the gliding-associated, PMF-driven motor that powers gliding motility (Sun *et al*., 2011b). Given the importance of these proteins in FAs, we aimed to determine whether MglA, AglQ and AglZ affect localization of the G2 OM proteins involved in gliding motility, particularly GltB and GltA.

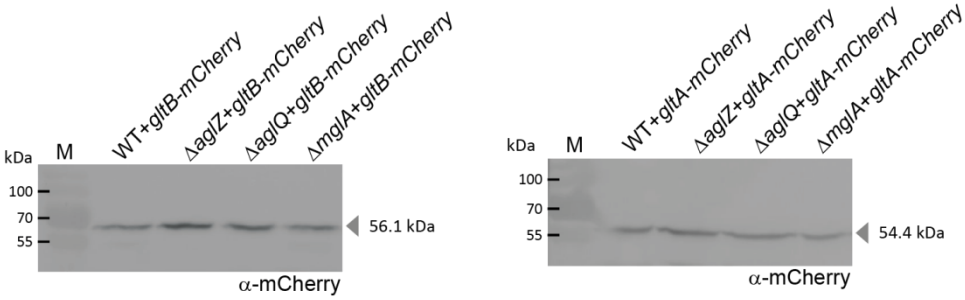

Figure 26. GltB-mCherry and GltA-mCherry fusions accumulates independently of *aglZ*, *aglQ* and *mglA* in the cells.
Immunoblot analysis of fusion proteins: GltB-mCherry and GltA-mCherry in different genetic backgrounds. Each loaded sample contained in total 3.75 × 10^7 cells/ml. The bands corresponding to fusion proteins are marked with grey arrowheads and calculated molecular masses.

To check whether these three genes, *aglZ, aglQ and mglA,* have an effect on the localization of GltB and GltA, in-frame deletion strains of *aglZ*, *aglQ* and *mglA* carrying GltB- or GltA-mCherry fusions were generated and analyzed by fluorescence microscopy. The strains were first analyzed by

immunoblot to verify that there was proper GltB- and GltA-mCherry fusion accumulation using mCherry specific antibodies. GltB-mCherry was detected at levels comparable to WT in the *aglZ*, *aglQ* and *mglA* deletion mutants (Figure 26). Similarly, GltA-mCherry accumulation in the cells lacking *aglZ, aglQ* or *mglA* was not affected. This is in agreement with data obtained from the protein stability analysis.

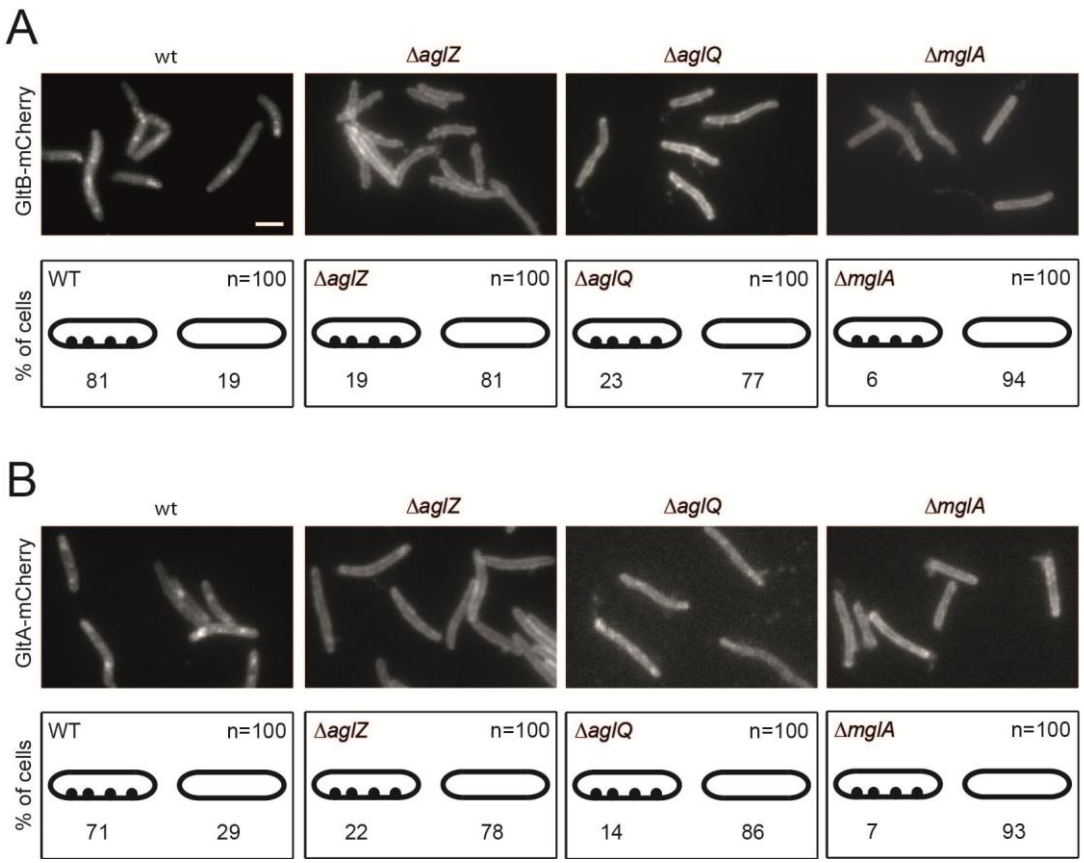

Figure 27. GltB and GltA require gliding motility proteins to form internal clusters in the cells.
Fluorescent images of GltB-mCherry (A) and GltA-mCherry (B) localization in different mutant backgrounds. Bottom schematics show quantification of localization patterns for 100 cells as characterized visually. Scale bar = 2 μm.

Since fluorescently labeled GltA and GltB accumulate normally, we proceeded with fluorescence microscopy. This revealed that *aglZ* is required for GltB-mCherry cluster formation (Figure 27A). An *aglZ* deletion strongly increased the number of cells with diffuse GltB-mCherry along the cell envelope. Similarly, *aglQ* and *mglA* were essential for GltB-mCherry to localize to multiple clusters distributed along the cell body. Furthermore, the GltA-mCherry fusion in an *aglZ* mutant formed multiple clusters only in a minority of

cells. Lack of *aglQ* and *mglA* resulted in a similar localization pattern of GltA-mCherry, indicating that multiple GltA clusters are not stable/assembled in the absence of other components of the FAs. These data suggest that GltB and GltA are recruited to the motility complexes by previously characterized components of the FAs, while in cells missing any of the FA components, GltB and GltA are distributed all around the cell envelope (Figure 27). These results fit with previously published data demonstrating that MglA is essential for the assembly of the envelope spanning motility complexes involving cytoplasmic, IM and OM proteins (Hot *et al*., in submission).

2.4.4 Localization of AglZ-YFP in the absence of G2 proteins

In order to understand how FAs are assembled, we next aimed to determine whether the localization of FA components like AglZ and AglQ is affected by deletion of genes transcribed from the G2 cluster. AglZ was the first protein reported to localize to FAs, moreover it interacts directly with both the actin-like MreB cytoskeleton and MglA in the cytoplasm (Yang *et al.*, 2004b, Mauriello *et al*., 2010b). Furthermore, AglZ interacts with the IM component of FAs, GltJ, suggesting that AglZ connects FAs to the MreB cytoskeleton (Nan *et al*., 2010b). MreB was suggested to be directly involved in positioning and assembly of motility complexes as its depolymerization delocalizes MglA, AglZ and AglQ (Mauriello *et al*., 2010b, Hot, in submission). However, the suggested hypothesis that motility machinery tracks along active MreB polymers is still under investigation. Studies on AglZ-YFP localization revealed that many gliding motility proteins are involved in the assembly of fully functional FAs, for example, proteins encoded in the G1 cluster affect AglZ localization in multiple clusters along the cell body (Nan *et al*., 2010b), suggesting that the cytoplasmic, IM and periplasmic proteins of motility complexes are essential for recruiting AglZ-YFP to FAs. To find out whether the G2 OM complex is required for proper AglZ-YFP localization or the assembly of FAs, deletion mutants of each gene from the G2 cluster carrying an AglZ-YFP fusion were generated and analyzed on the microscope.

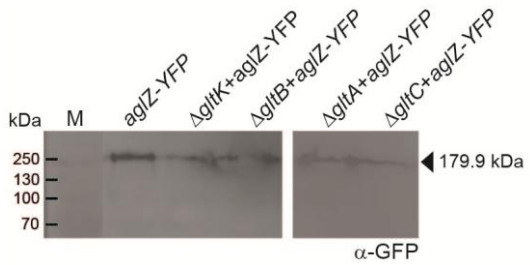

Figure 28. Immunoblot analysis of strains expressing AglZ-YFP fusion.
Immunoblot analysis of AglZ-YFP stability in G2 mutants using GFP primary antibodies. Bands corresponding to the fusion protein are marked with grey triangle and calculated molecular mass. M indicates protein ladder.

AglZ-YFP was expressed from its native site in the genome. Strains were analyzed by immunoblot to check for proper accumulation of the fusion proteins. AglZ-YFP was detected in *gltK*, *gltB*, *gltA* and *gltC* deletion mutants at levels comparable to WT, suggesting that the fusion is stable in these strains (Figure 28).

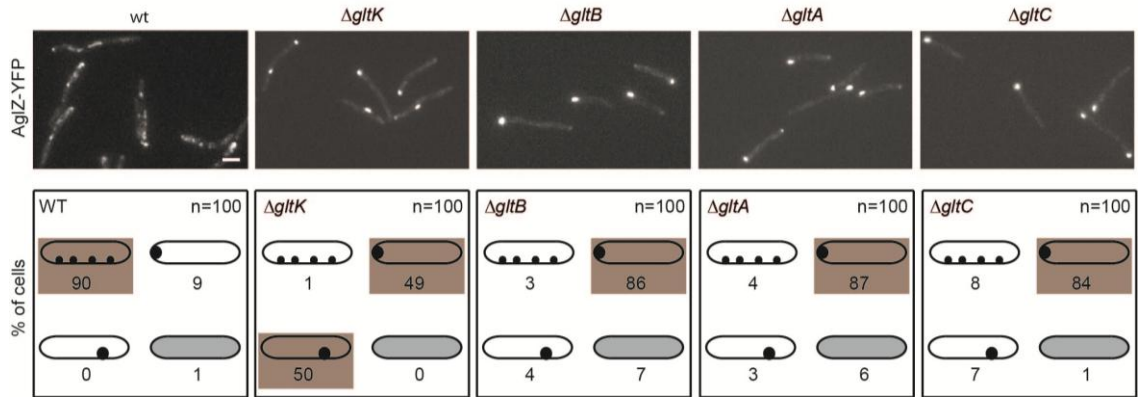

Figure 29. AglZ-YFP localizes to FAs in a G2 proteins dependent manner.
Analysis of AglZ-YFP localization by fluorescence microscopy. Quantification of the expression patterns of 100 representative cells is indicated in cartoons under the microscopy images. The major AglZ-YFP localization pattern/s in each strain is marked with brown box. Scale bar = 2 μm.

Fluorescence microscopy revealed that in WT cells, AglZ-YFP localizes to multiple clusters referred to as FAs, and to a polar cluster at the leading cell pole in a majority of the cells (Figure 29). In contrast, deletion of *gltK* leads to drastic changes in the localization of AglZ-YFP. In the majority of cells, FAs are not visible, and only one big cluster of AglZ-YFP is situated at the cell pole or elsewhere within the cell body (Figure 29). Cells lacking *gltB*, *gltA* and *gltC* showed similar abnormal AglZ-YFP localization and we could observe accumulation of the fusion protein into one big cluster located at the cell pole.

AglZ-YFP polar localization in these mutants suggests that the G2 proteins not only depend on FA components for correct localization, but they are also involved in the assembly of FAs.

2.4.5 Localization of AglQ is abnormal in the absence of the G2 proteins

AglQ is a critical component of the AglQRS motor complex. Previous studies suggested that the AglQRS complex assembles a proton channel in the IM that powers the gliding motility machinery (Sun *et al*., 2011b). A point mutation in AglQ altering the amino acid residue essential for the binding of H^+ within the lumen of the channel causes loss of function by the motor complex, resulting in non-motile FAs, providing strong evidence that single cell movement is driven by the AglQRS complex (Sun *et al*., 2011b). Deletion of *aglQ* affects GltD (a periplasmic protein encoded in the G1 cluster) localization, preventing the normal formation of multiple clusters, but interestingly, it did not affect AglZ localization (Luciano *et al*., 2011). To continue our investigation on the localization dependencies of gliding motility proteins, we generated strains in each G2 mutant expressing an *aglQ-mCherry* fusion. To analyze the stability of the fusion proteins, immunoblot analysis was performed. AglQ-mCherry accumulated at levels comparable to WT in each single G2 deletion mutant, indicating that the protein is stable (Figure 30).

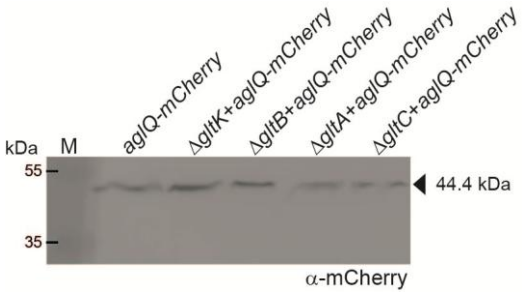

Figure 30. Immunoblot analysis of strains expressing AglZ-YFP fusion.
Immunoblot with mCherry primary antibodies. Bands corresponding to the fusion protein are marked with a grey triangle which also indicates the calculated molecular mass. M indicates protein ladder with marked molecular masses in kDa.

Microscopy analysis of AglQ-mCherry localization in WT cells revealed multiple clusters spread along the cell body (Figure 31). Similar to AglZ-YFP, AglQ-mCherry clusters remained fixed relative to the substratum in the moving

cells. Furthermore, AglQ also occasionally displayed diffuse membrane localization at frequencies similar to those of GltB and GltA. Interestingly, in the absence of *gltK,* AglQ-mCherry clusters were still visible in the cells (Figure 31). Analysis of AglQ localization in Δ*gltB*, Δ*gltA* and Δ*gltC* revealed the same localization pattern of multiple AglQ clusters formed within the cells.

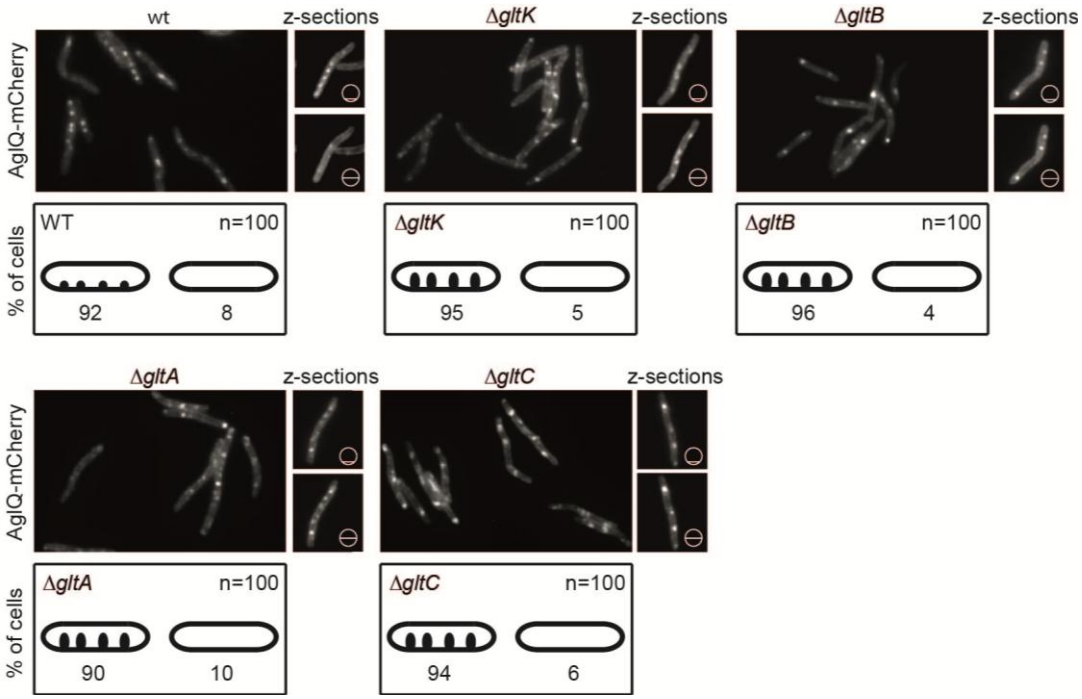

Figure 31. AglQ localization depends on G2 proteins.
Localization of AglQ-mCherry in WT and G2 mutants. Small panels on the right show unprocessed fluorescent micrographs of specific z sections, their z positions are indicated by a barred circle. Scale bar = 2 µm.

We decided to investigate AglQ-mCherry clusters by analyzing fluorescent images from different z-layers of the cells. We discovered that AglQ-mCherry clusters in the WT were focused on the ventral side of the cell, close to the gliding surface (Figure 31, z-sections). In contrast, in each single mutant of the G2 genes, the AglQ-mCherry clusters were visible in multiple focal planes, suggesting that the proteins were not focused into FA complexes on the ventral side of the cell, but instead were distributed along width of the cell in the IM. We propose that AglQ clusters form ring structures in the IM so that the clusters at FA sites are elongated towards the middle or to the dorsal side of the cell. Taken together, the fluorescence microscopy data suggest that the G2 proteins are important for the correct assembly of FAs.

2.5 GltB and GltA belong to FAs

The observation that GltA and GltB localize and behave in the same manner as AglZ and AglQ supports the hypothesis that G2 proteins are part of FA complexes. To further confirm or rule out this prediction we decided to compare the co-localizations of GltB- or GltA-mCherry and AglZ-YFP in WT, Δ*gltB,* or Δ*gltA* genetic backgrounds. GltB- and GltA-mCherry fusions were expressed under control of the native promoter at the Mx8 *attB* site, whereas AglZ-YFP was expressed from its native site. The accumulation of AglZ, GltB and GltA fusions in strains was checked by immunoblot analysis. GltB- and GltA-mCherry fusions were detected at sizes corresponding to the calculated molecular masses using mCherry antibodies; however, some additional degradation bands were visible on the immunoblots (Figure 32). Similarly, AglZ-YFP was found to accumulate in all strains, but some degradation products were detected by GFP antibodies. Microscopy analysis of the strains revealed that GltA and GltB colocalize with internal clusters of AglZ that are distributed along the x-axis of the cell body, but not with the polar clusters of AglZ (Figure 33).

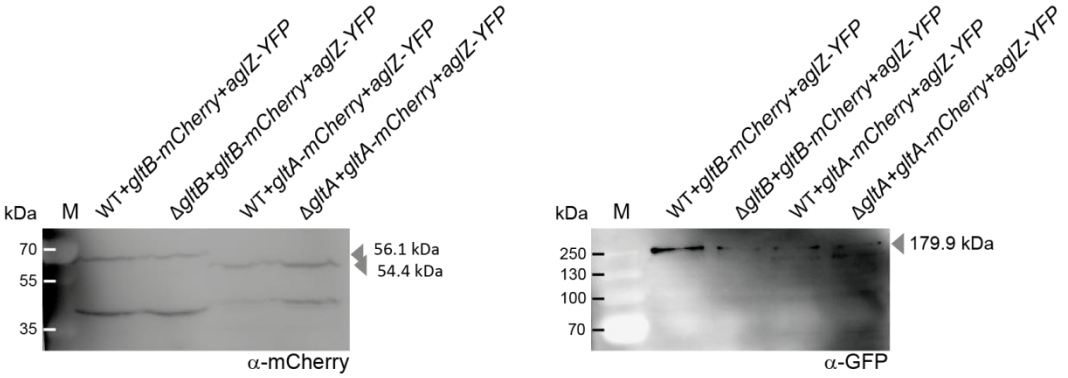

Figure 32. Imunoblot analysis of strains harboring *gltB*, *gltA* and *aglZ* fusions.
Immunoblot analysis of mCherry and YFP fusions using mCherry and GFP antibodies, respectively. The correct bands of fusion proteins are indicated with grey arrowheads with given calculated molecular masses in kDa. M corresponds to protein ladder with marked molecular masses on the left side of the blots.

Our next goal was to analyze the dynamics of AglZ, GltB and GltA clusters and test whether colocalization was stable over time. For this purpose time-lapse movies of moving cells were generated. Analysis revealed that all three proteins behaved in the same manner with colocalization remaining stable

over time and the clusters staying stationary with respect to the substratum in moving cells. As previously observed, AglZ-YFP colocalizes with GltB- and GltA-mCherry except at the polar AglZ clusters at the leading cell pole. These data strongly indicates that G2 proteins form a cell envelope complex in the FAs and belong to the same gliding machinery as AglZ and AglQ, since AglQ-mCherry was colocalized with AglZ-YFP in previous studies (Sun *et al*., 2011b).

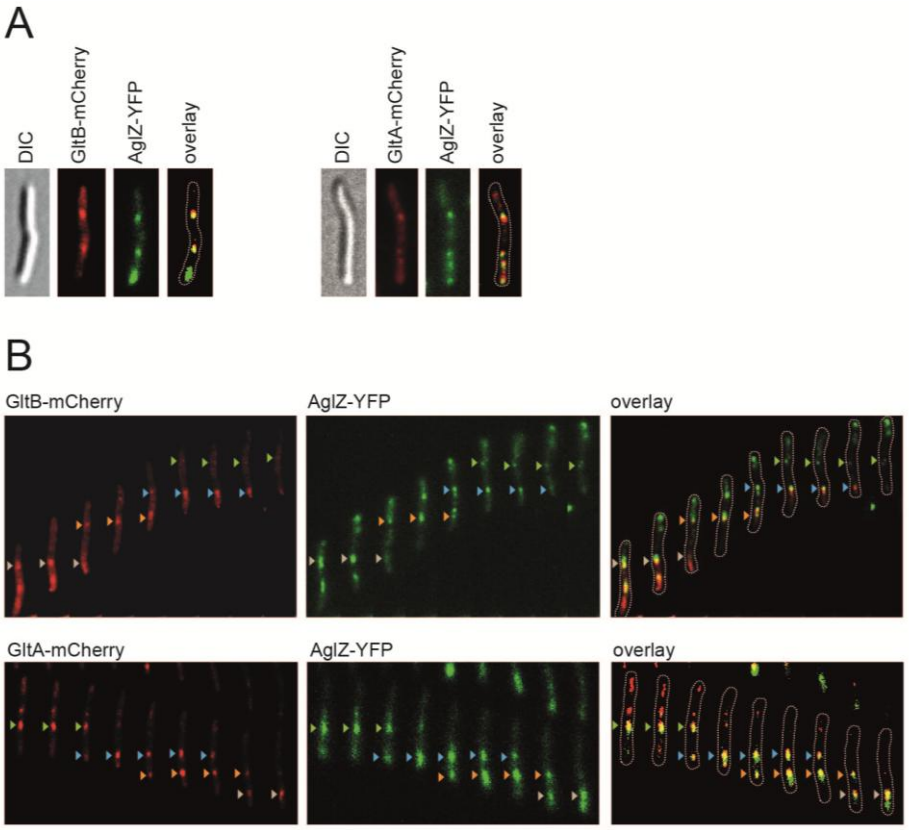

Figure 33. GltB and GltA are components of the gliding motility complexes.
(A) Fluorescent images representing AglZ-YFP and GltB-mCherry or GltA-mCherry colocalization. (B) AglZ-YFP colocalizes with GltB-mCherry and GltA-mCherry in moving cells. One colored triangles indicate position of the same cluster corresponding to the chimeric proteins colocalizing during cell movement.

3 Discussion

Bacteria have evolved more than one mechanism for movement over surfaces. Some utilize flagella in a manner described as swarming motility. T4P have also been shown to mediate surface motility. In this mechanism, pili extend from a cell pole and then attach to the surface followed by their retraction, which pulls the cell forward. Social motility (S-motility) in *M. xanthus* is mediated by T4P, but this organism also utilizes a second form of surface motility known as adventurous motility (A-motility) characterized by single cell movement. A-motility is a type of gliding motility, which has also been observed in *Flavobacterium jonsoniae* and *Mycoplasma spp*. The proposed models for gliding motility in these species differ in the structure of the motility machinery, but also in the way how cell behaves during movement. In *Flavobacterium,* gliding motility depends on the rapid movement of filaments composed of cell-surface adhesions such as SprB along the OM, which results in a left-handed cell rotation (Nakane *et al*., 2013). In contrast, in *Mycoplasma spp,* gliding motility is suggested to rely on the movements of the “leg” protein, extending from the cell surface, which binds to polysaccharides on the gliding surface and then retracts similarly to T4P (Miyata, 2010). Most importantly, both models involve extracellular structures that bind firmly to the gliding surface. In contrast, *M. xanthus* cells do not appear to have any extracellular structures while moving by gliding motility.

Although the study of gliding motility of *M. xanthus* has been ongoing for over two decades, the mechanism underlying this process is not fully understood. The working model of gliding motility in *M. xanthus* has changed significantly over the years. The first model was built around the slime polymer deposited at the lagging cell pole, and the slime hydration was thought to be sufficient to propel the cell via extrusion from polarly localized nozzles (Wolgemuth *et al.*, 2002a). However, more recent studies did not support this model, and a new model in which gliding motility is mediated by clusters that are fixed to the substratum and distributed along the cell body in a manner similar to eukaryotic focal adhesions was proposed (Wolgemuth et al., 2002a, Mignot et al., 2007). Most recently a third model was proposed that describes gliding motility via helically distributed clusters that are not fixed to the

substratum, but instead push on and deform the peptidoglycan layer and OM, which exerts force onto gliding surface and generates transverse waves that propagate towards the trailing cell pole (Nan *et al*., 2011). Slime is no longer considered to play a direct role in generating force for movement, but it still constitutes an important part of this system by promoting adhesion of the cell body to the gliding surface (Ducret *et al*., 2012). So far, multiple components of the gliding motility machinery have been experimentally characterized including cytoplasmic, IM, and periplasmic proteins. Most importantly, the AglQRS proton channel, which is a member of a ubiquitous family of bacterial motors (Mot/Tol/Exb), was identified as the energy-providing motor enabling gliding motility (Sun *et al*., 2011b). Previous bioinformatics analyses support that the gliding motility machinery includes OM proteins and thus the potential for an envelope complex that spans the IM and OM (Luciano *et al*., 2011).

In the studies described here, we analyzed the four proteins encoded in the G2 cluster identified in the bioinformatics study using genetic and biochemical tools and fluorescence microscopy. Our data demonstrate that these four proteins (GltK, GltB, GltA and GltC) localize to the periplasm and OM as predicted from bioinformatic analyses. The three proteins are dependent on each other for stability, and furthermore, interaction studies strongly indicate that GltB, GltA and GltC form a complex in the cell envelope. Localization studies revealed that GltBAC localize to FAs. Moreover, the G2 proteins and previously characterized gliding motility components are interdependent; both classes of proteins must be intact for proper assembly of the others into FAs. Thus, the GltBAC complex is the first characterized OM complex involved in gliding motility and the formation of FAs in *M. xanthus*.

3.1 The G2 proteins are essential for gliding motility

Transposon mutagenesis screens were carried out in the initial searches for genes essential to gliding motility (Youderian *et al*., 2003, Yu & Kaiser, 2007). In those studies, over 50 genes were identified; however, the functional role in motility of most of the identified genes was not established. Two proteins identified by these previous screens, GltK and GltC, attracted our special

attention when found again in the independent screenings performed by Keilberg (MPI, Marburg). Bioinformatic analyses revealed that *gltK* and *gltC* flank two genes *gltB* and *gltA*, and together they constitute the G2 cluster, which was hypothesized to be a part of the gliding motility machinery (Luciano *et al*., 2011).

The results from the transposon based screens were confirmed by motility assays carried out on in-frame deletion mutants of each individual gene transcribed in the G2 cluster. All four deletion mutants exhibited normal S-motility, while gliding motility was severely impaired. The gliding motility phenotype was complemented by introducing a native copy of the gene at the Mx8 *attB* site under control of the native promoter showing that motility phenotype did not result from polar effects. With these experiments the G2 cluster encoding four proteins was added to the pool of genes essential for gliding motility.

3.2 FAs span the entire cell envelope

In the focal adhesion model of gliding motility, the FA complexes span the entire cell envelope, assemble on the ventral side of the cell, and fix to the substratum in moving cells (Mignot *et al*., 2007). The alternative motor cargo model of gliding motility describes complexes that localize in a helical pattern and span only the IM (Nan *et al*., 2011). Furthermore, in both models protein complexes involved in gliding motility are suggested to be connected to the MreB actin cytoskeleton from the cytoplasmic side by an MglA/AglZ complex and in the focal adhesion model extracellularly to the gliding surface by interacting with the slime polymers deposited at FA sites (Ducret *et al*., 2012). We sought to distinguish between the two current models by investigating the localization of the G2 proteins via fractionation and fluorescence microscopy analyses. Based on bioinformatic analysis, we predicted that the G2 proteins form an OM associated envelope complex. This localization would suggest that they are part of FAs, since the motor cargo model does not involve OM proteins. To reinvestigate the structure and stability of the FAs including the GltBAC proteins, we started with fractionation experiments. We showed that

GltB, GltA and GltK are in the OM or associated with OM proteins, while GltC is a periplasmic protein, in agreement with our bioinformatic predictions. GltK is a predicted lipoprotein with a type II signal sequence (Pathak & Wall, 2012). Based on the OMV localization and secondary structure of GltK and the fact that it is transferred between cells, we postulate that GltK is associated with the OM. But is it faced to the periplasm or to the ECM? We did not perform any experiments that could answer this question; however, the CglB and CglD lipoproteins of *M. xanthus,* which are similarly transferred between the cells and are essential for gliding motility, have been predicted to contain two domains frequently found in ECM proteins: a von Willebrand domain characteristic for proteins involved in cell adhesion, and a cysteine rich domain. Unfortunately, neither domains characteristic for extracellular proteins nor domains characteristic for binding or hydrolyzing/synthesizing the peptidoglycan layer were identified within the GltK secondary structure. To find out how exactly GltK is positioned in the OM, the protein topology would have to be determined in future experiments. One of the common methods is a cysteine accessibility assay, which is based on labeling cysteine residues in intact cells (van Geest & Lolkema, 2000). Another experiment that might resolve GltK localization is cell shaving using Proteinase K, which digest ECM proteins as well as OM proteins while proteins anchored in the OM in the periplasm remain intact.

Fractionation experiments were followed by an analysis of protein stability because protein accumulation dependencies can suggest which proteins belong to the same protein complexes. Interestingly, GltB and GltA were shown to stabilize each other and to be essential for the accumulation of GltC in the cells. The pull down experiments with purified proteins revealed direct interaction between the GltB, GltA and GltC proteins, providing strong evidence for the existence of a GltBAC periplasmic and OM complex, which excludes the motor cargo model. We did not detect a direct interaction between GltK and other proteins encoded in the G2 cluster. However, GltK may interact with G2 proteins periodically, indirectly, or only with the full FA complex. Moreover, in pull down experiments MalE tagged versions of proteins were used, which might block interaction sites in the case of GltK. Based on the protein stability, fractionation and pull down data, we were able to show that

GltB, GltA and GltC build a complex in the cell envelope; however, we failed to connect GltK to the other G2 proteins. Another option for checking direct protein interactions would be crosslinking performed on OMVs using formaldehyde, since GltK, GltB and GltA were found to accumulate in OMVs. Alternatively, immunoprecipitation using WT cell lysate and specific G2 proteins antibodies could be performed.

We continued our investigation of G2 proteins using fluorescence microscopy. GltB, GltA and GltC were fused C-terminally to mCherry in order to maintain their N- terminal signal peptide sequences, and their localizations were analyzed. We discovered that all three proteins, GltB, GltA and GltC, localized in multiple clusters distributed along the cell body, which strongly supports the focal adhesion model, since motor cargo model describes helical localization pattern of proteins involved in gliding motility. More detailed analysis of the protein clusters by time lapse movies revealed that they behaved in the same manner as AglQ-mCherry or AglZ-YFP clusters in moving cells (Mauriello *et al*., 2009, Sun *et al*., 2011b), suggesting that the observed GltBAC clusters are most probably FAs. Additional colocalization studies revealed that AglZ-YFP colocalizes with GltB-mCherry and GltA-mCherry in multiple internally distributed clusters in moving cells, indicating that the GltBAC envelope complex is part of the FAs. Although we failed to connect all of the G2 proteins, as GltK seemed to be independent of the other G2 proteins, we successfully identified the missing OM element of the FAs by giving strong evidence that the protein complexes involved in gliding motility span the whole cell envelope. At present, the GltBAC complex seem to be the outermost component of FAs making them potential candidates for anchoring FAs to the substratum.

During the analysis of data obtained from fluorescence microscopy, we observed some differences in the percentages of cells displaying multiple cluster localization of fusion proteins in WT and deletion backgrounds. These results suggest that the protein level in the cell is important. We propose that in WT cells, in which the protein levels are higher in comparison to the deletion background, there is a higher possibility that the interaction sites in protein complexes are already occupied, and in consequence the proteins start to localize randomly in the cell envelope. In this case we expect an increase in the

strength of the background fluorescence signal, which obscures the visibility of the protein clusters.

In the focal adhesion model, FAs are formed and focused on the ventral side of the cell close to the gliding surface. This hypothesis was previously confirmed by localization studies on the periplasmic GltD protein in which the localization of GltD-mCherry clusters in different z layers of the cells were analyzed (Luciano *et al*., 2011). The GltD clusters were clearly visible when the focal plane was focused closer to the substratum. Since our data support the focal adhesion model as a mechanism of gliding motility, we investigated the localization of the FAs in different z layers of the cells. In agreement with previous data, we observed GltB and GltA clusters focused at the ventral region of the cell close to the gliding surface. Furthermore, when the focal plane was focused in the middle or dorsal region of the cell, the fluorescence signal was visible around the cell periphery consistent with envelope localization, but not in distinct clusters, confirming that GltB and GltA clusters are specifically to surface associated FAs. However, a direct connection between the G2 proteins and components of FAs or the secreted slime remains to be established. These data suggest that the proteins which function in gliding motility localize specifically to protein complexes in the cell envelope and constitute the motility machinery. This machinery is connected from one side to bacterial cytoskeleton and from the other side to substratum moving with a directed manner through all cell compartments towards the lagging cell pole.

3.3 GltB and GltA are recruited to FAs

MglA-GTP was suggested to recruit components of the gliding motility machinery to FAs at the leading cell pole and to stabilize FAs by interacting directly with MreB and AglZ (Hot *et al*., in submission). Studies on protein localization showed that the formation of motility complexes fixed to the gliding surface by AglQ-mCherry, GltI-YFP and AglZ-YFP depends on *mglA* and thus, MglA is required for the assembly and localization of FAs. The same study showed that *aglZ* and *gltI* affect MglA localization to FAs, suggesting that all three proteins act in one complex, which is essential for the formation of FAs. In

addition, a main factor involved in the stability and the recruitment of the proteins to FAs is MreB. This idea was promoted by studies which showed that a reduced polymerization of MreB caused by the A22 compound inhibits gliding motility and the assembly of new FAs, while also disrupting the existing FAs (Mauriello *et al*., 2010b).

To discover whether GltB and GltA are recruited to FAs by MglA and AglZ, we first analyzed the stability of the G2 proteins in cells lacking components of FAs. Using immunoblot analysis we were able to show that GltB and GltA accumulation was not affected in cells carrying *aglZ, mglA* or *aglQ* deletions, which supports that the protein stability of GltB and GltA does not depend on these FA components. Interestingly, fluorescence microscopy revealed a uniform distribution of GltB-mCherry and GltA-mCherry around the cell periphery in cells lacking *mglA*. Moreover, the *aglQ* and *aglZ* in-frame deletion mutants also showed a negative effect on GltB and GltA cluster formation in the cells. These data indicate that although GltB and GltA accumulate independently of other FA components, they are not able to form protein complexes at FA sites in the absence of IM and cytoplasmic proteins that are integral components of FAs. These findings suggest that the internal part of FAs must be first assembled to enable recruitment of GltB and GltA to the gliding motility machinery.

To further investigate dependencies among the G2 proteins, the localization of GltB and GltA was analyzed in the individual mutants of the G2 cluster genes. Interestingly, although GltB and GltA were stable in the absence of GltK, we observed that cells lacking *gltK* did not show any GltB and GltA clusters. It seems that GltK is involved in the assembly of the outermost part of FAs without which gliding motility machinery is incomplete and hence non-functional. Similarly, mutant strains lacking the other G2 genes showed a diffused envelope localization of GltB and GltA. These results indicate that the G2 proteins are crucial for the stability/assembly of OM part of the FAs, namely the GltBAC complex. Furthermore GltK was found to affect cluster formation of GltB and GltA, which indicates a connection of GltK to the GltBAC complex and therefore FAs.

3.4 Each protein involved in the gliding motility machinery is essential for the formation of stable and fully functional FAs in the cells

The T4P system in *M. xanthus* is assembled in the outside-in manner beginning with PilQ oligomerization and its insertion into the OM at the cell poles (Friedrich *et al*., 2014). The T4P machinery is assembled at the leading cell pole and spans the cell envelope similarly to FAs. In the case of gliding motility, it was suggested that MglA-GTP in a cytoplasmic complex with MreB, AglZ and GltI recruits gliding motility components and stimulates the formation of FAs at the leading cell pole, which then travel in a directed manner along the cell body towards the lagging cell pole during cell movement (Hot *et al*, in submission). The data presented here indicate that FAs are assembled in an inside-out manner starting with the assembly of the MglA, AglZ and GltI complex in the cytoplasm, based on the observation that the localization of OM proteins GltB and GltA to the FAs depends on the more internal FA components.

But does the assembly of FAs really start in the cytoplasm and continue to the OM? To answer this question we investigated whether the localization dependencies of the gliding motility proteins are bidirectional given that the effect of *gtlB* and *gltA* on cytoplasmic or IM FA components had not been investigated. In previous studies, mutual effects of MglA, GltI and AglZ on the localization to the FAs was shown (Hot *et al*., in submission) (Mauriello *et al*., 2010b, Nan *et al*., 2010b). Furthermore AglQ affected GltD localization to multiple clusters, in turn a *gltF* deletion resulted in polar AglZ-YFP localization and loss of FAs (Nan *et al*., 2010b, Luciano *et al*., 2011). To summarize, many proteins involved in gliding motility showed close relationships, suggesting that the formation of FAs does not depend only on the cytoplasmic proteins.

In this study, we showed that AglZ-YFP localization is strongly disrupted in cells lacking the G2 genes, resulting in the loss of FAs. In the majority of the cells lacking G2 components, AglZ-YFP no longer formed multiple internal clusters as seen in WT, but instead displayed diffuse localization and one unipolar cluster. In contrast, we observed a normal localization of AglQ-mCherry

in the absence of *gltKBAC*; however after more detailed analysis, we observed that the AglQ clusters were not focused on the ventral side of the cell. Instead, the clusters were visible in the envelope in each z layer of the cell suggesting that AglQ localized around the cell body in round structures rather than remaining focused at the ventral side of the cells, which is typical of FAs. We hypothesize that protein complexes formed by AglQ can still recognize the place for the gliding machinery, but they require the G2 proteins to pull them down to FAs, otherwise they are forming a ring structures along circumferential body of the cell. These observations strongly suggest that G2 proteins are essential for structural and functional aspects of the FAs. These results also indicate that each FA component, regardless of its cytoplasmic, IM, periplasmic or OM localization, is crucial for the formation/stability of fully functional FAs. The data indicate that there is no directionality in the assembly process of FAs, it seems that absence of any component regardless of its subcellular localization inhibits formation of FAs.

3.5 Reversals and cell polarity in gliding motility

M. xanthus cells stop and reverse their direction of movement on average every 15 min with the old leading cell pole becoming the new lagging cell pole and *vice versa* in an event known as a reversal (Blackhart & Zusman, 1985). *M. xanthus* reversals are controlled by a chemosensory-like signal transduction cascade, the Frz system, and also by RomR, MglA and MglB (Leonardy *et al*., 2007, Zhang *et al.*, 2010, Keilberg *et al*., 2012). The signal is transduced through the Frz proteins and the response regulator RomR down to MglA, which regulates the two motility systems, the cell polarity and the reversal frequency period in *M. xanthus* cells. Cell polarity is defined by the localizations of MglA (leading cell pole) and MglB (lagging cell pole) with synchronous pole-to-pole switching of these two proteins during a reversal; however, the exact mechanism establishing cell polarity remains unknown. It was shown that MglA in an active state (MglA-GTP) facilitates the assembly of FAs at the leading cell pole. MglB stimulates MglA-GTP conversion to an inactive MglA-GDP at the lagging cell pole (Leonardy *et al.*, 2010). This results in the disassembly of the FAs because MglA-GDP is not able to interact with MreB, and thus dissociates

from FAs making them unstable and leading to their dispersion (Hot *et al*, in submission).

The polarity switch effects the localization of proteins dependent on cell polarity, thus they must be relocated or degraded and synthesized anew. This phenomenon applies also to FAs. Because FAs are assembled at the leading cell pole and move in a directed manner from the leading cell pole towards the lagging cell pole, during a reversal, the old FAs must be first disassembled and then FA components must be regrouped in the cell to be ready at the leading cell pole to form new FAs, so the cell movement can occur in the new direction. The analysis of time-lapse movies revealed that clusters of GltB- and GltA-mCherry fusions appear close to the leading cell pole and disappear at the lagging cell pole, which is in agreement with previous data of other FA components. We also observed cells in which GltB- and GltA-mCherry clusters, shortly before cell reversal, disappeared in concert with the appearance of new clusters at the leading cell pole when the cell started and continued movement in the new direction. This is consistent with previous observation that showed the dispersal of AglZ-YFP clusters shortly before reversals (Mignot *et al*., 2007). Time lapse microscopy analyses of GltB- and GltA-mCherry localizations confirm that FAs move with a directed manner, always forming at the leading cell pole and traveling along the cell body in the direction of the lagging cell pole where they are disassembled. Thus any change in cell polarity results in total disassembly of gliding motility machinery and relocation of the gliding components to the new site of action.

Because GltB and GltA do not localize exclusively into multiple clusters, but are also diffuse in the cell envelope, we speculate that GltB and GltA molecules that are released from FAs at the lagging cell pole become diffusely localized in the OM with the potential for later recruitment to new FAs. Following this idea it would be worth to analyze whether GltB and GltA molecules which exhibit diffuse localization pattern are dynamic in the membrane. The common experiment for checking protein dynamics is FRAP (Fluorescence recovery after photobleaching). The principle of this assay is to flash a very intense light onto one cell spot, which will photobleach the molecules. The bleached spot is analyzed in terms of fluorescent recovery over time. Results from this

experiment might lead to a gliding motility model that includes highly dynamic GltB and GltA molecules in the OM, which can be recruited at the leading cell pole to the FAs after their deactivation/dispersion at the lagging cell pole.

3.6 Slime and OM material/vesicles in gliding motility

In previous studies, slime was suggested to be an important factor involved in gliding motility. It was shown that the A-motility slime referred to as gliding slime is deposited at FA sites underneath the cell body based on Wet-SEEC Microscopy (Ducret *et al*., 2012) and was suggested to promote adhesion of FAs to the substrate. Furthermore, it has been already shown that during gliding motility cells follow slime paths visible on the substratum. It is thought that the slime is composed of polysaccharides or glycoconjugate components since it can be stained with a fluorescent-derived lectins; however, the exact function and composition of the gliding motility slime is not known. To understand better how single cells move on a surface, the slime deposit role has to be established. So far, the best candidates that could connect FAs to the gliding slime directly or indirectly are GltB and GltA, integral OM proteins of FAs.

Previous studies discovered that *M. xanthus* cells deposit outer membrane material in the form of OMVs, which can form chains and membrane tubes observed to interconnect the cells (Remis *et al.*, 2014). OMVs are the OM derivatives produced constitutively during growth by Gram-negative bacteria. Furthermore, OMVs of *M. xanthus* were found to contain active proteases, phosphatases, hydrolases and secondary metabolites as well as proteins that are transferred between the cells (Evans *et al.*, 2012). The outer membrane material deposited by cells was shown to colocalize with gliding slime, suggesting that during gliding motility, cells share some of their OM, which remains attached to the slime polymer. In these studies, we confirmed the OMV localization of GltB previously published by Kahnt *et al*. (2010). Furthermore, GltA and GltK were also found in OMVs. Interestingly, during microscopy analyses of strains expressing GltB- and GltA-mCherry fusions, we observed fluorescent trails remaining behind cells during their movement on hard agar.

The fluorescent trails could represent OMVs that have been deposited; however, further experiments are needed to clarify this observation. One of the experiments that could give a clear answer whether fluorescence trails are formed by OMVs is EM in order to visualize possible OMV remnants. The presence of OMVs in the slime trails might play a role in intercellular signaling what for example could promote the tendency of single cells to follow the slime trails left by other cells. Further OMVs might serve as a protein secretion system that removes the excess of OM proteins arisen as a result of FAs disassembly at the lagging cell pole.

The OM tubes/vesicles were suggested to be involved in the protein transfer between the cells (Wall *et al.*, 1998, Nudleman *et al.*, 2005, Ducret *et al*., 2013). GltK is one of the lipoproteins which were shown to be transferred between the cells, in agreement with its OMV localization. Previously, GltB and GltA were not investigated in terms of protein transfer. Interestingly, during microscopic analysis of strains carrying GltB and GltA mCherry fusions, we observed that cells were not only leaving fluorescence trails in their wake, but also connected with other cells by fluorescent OM extensions/tubes, suggesting that these proteins might be also transferred between the cells. Furthermore, we also investigated whether GltB and GltA fusions can be transported between the cells, however the obtained results were not conclusive; the conditions for the protein transfer assay need to be optimized.

3.7 Function of the G2 proteins

The next goal of future work would be to find the precise function of the G2 proteins. In this study we showed that GltKBAC play an important role in single cell motility by contributing to the formation of the FAs. However, two questions arise: 1) Are these four proteins purely structural elements of the gliding motility machinery or do they also play a role in the attachment of the FAs to the gliding surface? And 2) Are they related to the slime composition or production?

GltB and GltA are integral OM proteins, and bioinformatic analysis of the secondary structure revealed that these two proteins contain internal as well as

external loops that could be potentially involved in interactions with other proteins or polymers, suggesting that they might connect the FAs directly or indirectly to the substrate (Kristin Wuichet). We think that most probably G2 proteins interact with ECM proteins that contain lectin binding domains, which then interact with gliding slime directly, fixing the fully assembled FA complexes to the gliding surface. In the future, it would be important to determine the precise topology of GltB and GltA. The knowledge of the proteins' structures might help us resolve their function in gliding motility. The information about the orientation of extra-membranous domains could be used in experiments deleting or substituting these parts in GltB or GltA, to further investigate whether topology changes cause any defects occur in gliding motility. A common approach to investigate protein topology is a chemical modification of cysteine residues (van Geest & Lolkema, 2000). Based on the bioinformatics, GltB and GltA contain a few cysteine residues in the predicted loops, which are crucial for a differentiation between loops that are situated outside of the cell and those that are located in the periplasm. The data obtained from investigation of the protein topology could be used in follow up experiments deleting/substituting extra-membranous domains of the proteins. Such studies could potentially result in stable proteins that can assemble as part of the FA complex, but are non-functional in motility. Thus, the effect of non-functional GltB and GltA on FA attachment to the surface or FA assembly, stability or dynamics and slime production could be investigated in detail.

Interestingly, proteins encoded in the G2 cluster are homologs of the NfsABC proteins involved in compact spore coat production during sporulation in *M. xanthus* (Muller *et al*., 2010, Muller *et al*., 2012). Although Nfs proteins were not predicted to encode any known carbohydrate hydrolyzing domain, they were shown to regulate composition of the polysaccharide chains in the polymer exported out of the cell by Wzy-like machinery (Carina Holkenbrink, personal communication) (Muller *et al*., 2010). This polymer is a component of the spore coat and its exact composition is crucial for the formation of a dense polymer layer around the spore membrane, playing the role of a protective shield. Furthermore, it was suggested that the Nfs complex and the FAs are paralogous complexes that utilize energy created by the same motor complex

AglQRS, which switches machineries when cells enter the developmental stage and start the sporulation process (Wartel *et al*., 2013).

The collected knowledge about Nfs and Glt proteins suggests that the G2 proteins might have a similar function as the Nfs proteins, which would be the regulation of gliding slime composition. Although gliding slime production was shown not to be effected by *gltE, gltD* or *aglQ* mutants and to be Wza-independent (Ducret *et al*., 2012), the OM components of FAs, namely GltB and GltA, might be still involved in the regulation of slime composition or production. Consideration of a possible role of the G2 proteins in regulating slime composition resulted in a careful analysis of GltKBAC proteins using bioinformatic tools. Unfortunately, no domains characteristic for polymer cleavage or transport were identified for any of the proteins encoded in the G2 cluster, however these results do not rule out the possibility that the G2 proteins could have some function or reaction related with gliding slime.

Another goal would be to find a direct connection of the G2 proteins to the rest of the components of the FAs and/or to the slime. What are their interaction partners? Are there any other proteins involved in gliding motility machinery? An approach to identify new interaction partners of the G2 proteins by affinity pull down did not result in any strong candidates. In the experiments, MalE-tagged proteins were used, and although we detected some envelope proteins, which were not identified before to be required for the gliding motility, we were not able to reproduce the results. Furthermore, the detergents which greatly solubilize the OM were not compatible with the amylose matrix used in the experiments.

Undoubtedly, our data strongly suggest that FAs are built as one protein complex spanning the cell envelope. Future research in the field is required to answer important questions: How do the FAs cope with movement through the membranes and peptidoglycan layer? And how do they interact with the gliding surface? So far no proteins which would be essential for gliding motility and involved in the synthesis or hydrolysis of PG were characterized suggesting that additional selective screenings are needed to identify the missing components of gliding machinery. However another possibility which could handle the PG problem might be the model in which protein complexes formed in the IM would

push and exert the force on the PG layer transducing the energy to the complex in the OM which would bind to the gliding surface. The exerted force on the PG would be the linker between the inner and outer module.

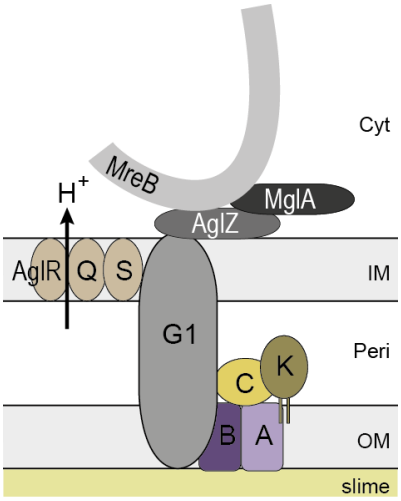

Figure 34. Model of the FA including the G2 proteins.
Motor proteins AglRQS, MreB actin cytoskeleton, MglA and AglZ are shown. G2 proteins are represented as K, B, A, C. The grey G1 box represents GltD, GltE, GltF, GltG, GltH, GltI and GltJ encoded in G1 cluster. Cyt, IM, Peri and OM stands for cytoplasm, inner membrane, periplasm and outer membrane, respectively.

3.8 Gliding motility model

This study helped to distinguish between two models currently proposed for gliding motility. The motor cargo model hypothesizes the helical localization of machinery components and the absence of OM components. We find that GltB and GltA are part of the membrane components and form multiple clusters on the ventral side of the cell, both of which support the focal adhesion model and refute the motor cargo model. Moreover, the data from this work indicate that the motility complexes are assembled at the leading cell pole and stay fixed to the substratum resulting in their directed movement towards the lagging cell pole in the moving cells where they are disassembled, which is in agreement with focal adhesion model. In contrast, motility complexes in motor cargo model are stable over the time and travel along helical loop in two opposite directions in the cell.

Summarizing, the OM components (GltBAC) of the FAs were successfully characterized in this study; however, a direct connection of GltBAC to other components of the FAs and slime was not established (Figure 34). Because gliding motility was proposed to be facilitated by the adhesion of FAs to the gliding slime polysaccharides, we speculate that the G2 proteins are

involved directly or indirectly in the anchoring of FAs to the substratum and that they play a role in the interaction between the FAs and the slime polymers deposited on the gliding surface based on the obtained results in this study. Unfortunately, neither the slime composition nor the slime deposition machinery has been identified, which makes it problematic to perform experimental test to determine if the G2 proteins interact with the gliding slime polymers or regulate its composition. Overall, these results strongly support the focal adhesion model as the mechanism that drives gliding motility, wherein G2 proteins constitute the outermost platform of FAs that could be involved in anchoring the whole complex to the substratum.

4 Material and Methods

4.1 Chemicals and equipment

All the reagents, enzymes, antibiotics and kits used in this work are listed with their supplier in the Table 2. The devices, their application and manufacturer as well as software for data analysis are described in Table 3.

Table 2. Reagents, enzymes, antibiotics and kits

Reagents	**Supplier**
Chemicals	Roth (Karlsruhe), Merck (Darmstadt), Sigma-Aldrich (Taufkirchen)
Media components, agar	Roth (Karlsruhe), Merck (Darmstadt), Difco (Heidelberg), Invitrogen (Darmstadt)
SDS-PAGE size standards	MBI Fermentas (St. Leon-Rot)
Agarose gel electrophoresis size standards	Bioline (Luckenwalde)
Oligonucleotides	Eurofins MWG Operon (Ebersberg), Invitrogen (Karlsruhe)
Rabbit antisera	Eurogentec (Seraing, Belgium)
Anti-GFP monoclonal antibody	Roche (Mannheim)
Rabbit anti-mouse IgG	Roche (Mannheim)
Goat anti-rabbit IgG, goat anti-rabbit IgG DyLight 549	Pierce/Thermo Scientific (Dreieich)
Luminata Western HRP Substrate	Merck Millipore (Darmstadt)
PageRuler Plus Prestained Protein Ladder	Thermo Scientific (Dreieich)
SuperSignal chemiluminescence detection	Pierce/Thermo Scientific (Dreieich)
HyperLadder I	Bioline (Luckenwalde)
2-log DNA Ladder	New England Biolabs (NEB) (Frankfurt a. M.)

Enzymes	
Antarctic Phosphatase	New England Biolabs (Frankfurt a. M.)
Phusion High-Fidelity DNA Polymerase	Thermo Scientific (Dreieich)
T4 DNA Ligase	Fermentas (St. Leon-Rot)
5 PRIME MasterMix	5 PRIME GmbH (Hamburg)
restriction enzymes	Fermentas (St. Leon-Rot), New England Biolabs (Frankfurt a. M.)
Antibiotics	
Kanamycin sulfate, chloramphenicol, ampicillin sodiumsulfate, gentamycin sulfate, oxytetracycline dehydrate, tetracycline hydrochloride	Roth (Karlsruhe)
Kits	
DNA purification (chromosomal DNA)	Epicentre Biotechnologies (Wisconsin,USA)
DNA purification (Plasmid DNA), PCR purification, Gel purification	Zymo Research (Freiburg), Qiagen (Hilden)
cDNA Archive kit	Applied Biosystems (Darmstadt)
RNA purification	RNeasy kit (Qiagen

Table 3. Equipment

Application	**Device**	**Manufacturer**
Cell disruption	Branson Sonifier 250	G. Heinemann (Schwäbisch Gmünd)
Centrifugation	RC 5B plus, Ultra Pro 80, Multifuge 1 S-R, Biofuge frasco, Biofuge pico, Avanti J-26 XP, Optima L-90K, Centrifuge 5424 R	Sorvall/Thermo Scientific (Dreieich), Heraeus/Thermo Scientific (Dreieich), Beckman Coulter (Krefeld), Eppendorf (Hamburg)
PCR	Mastercycler personal Mastercycler epgradient	Eppendorf (Hamburg)

Thermomixer	Thermomixer compact	Eppendorf (Hamburg)
DNA illumination and documentation	E-BOX VX2 imaging system	PeqLab (Eberhardzell)
DNA illumination	UVT_20 LE	Herolab (Wiesloch)
Electroporation	GenePulser Xcell	Bio-Rad (Munchen)
Protein electrophoresis	Mini-PROTEAN® 3 cell	Bio-Rad (Munchen)
Western blotting	TE77 semi-dry transfer unit TransBlot®Turbo™Transfer System	Amersham Biosciences (Munchen), Bio-Rad (München)
Chemiluminescence detection	Luminescent image analyzer LAS-4000	Fujifilm (Düsseldorf)
Imaging	Leica DMI6000B with Hamamatsu Flash 4.0 camera Leica DM6000B light microscope with the Cascade II camera MZ75 stereomicroscope with Leica DFC280 camera	Leica Microsystems (Wetzlar)
Determination of optical densities or nucleic acids absorption	Ultrospec 2100 pro Spectrophotometer Nanodrop ND-1000 UV-Vis spectrophotometer	Amersham Biosciences (Munchen) Nanodrop (Wilmington)
Size exclusion chromatography	ÄKTA purifier	Amersham Biosciences (Freiburg)
Identification of proteins	4800 plus MALDI TOF/TOF Analyzer	Applied Biosystems (Darmstadt)
Fluorescence microscopy data analysis	Metamorph® v 7.5 and v 7.7 Image-Pro® 6.2	Molecular Devices (Union city, CA) MediaCybernetics (Bethesda, MD)
Checking sequences, sequence alignments	Vector NTI advance software, suite 11	Invitrogen (Darmstadt)

4.2 Media

E. coli cells were cultivated in Luria-Bertani (LB) liquid media or on LB agar plates with 1% agar concentration. *M. xanthus* cells were cultivated in CTT media or on CTT agar plates with 1.5% or 0.5% agar concentration. Motility assays of *M. xanthus* cells were performed on A- or S-motility plates. Slides

with A50 microscopy agar were used for the microscopy experiments. Composition of media is described in Table 4.

Table 4. Growth media for *E. coli* and *M. xanthus*

Media	**Composition**
E. coli	
Luria-Bertani (LB)	1% (w/v) tryptone, 0.5% (w/v) yeast extract, 1% (w/v) NaCl
LB agar plates	LB medium, 1% (w/v) agar
M. xanthus	
CTT	1% (w/v) BactoTM casitone, 10 mM Tris-HCl pH 8.0, 1 mM potassium phosphate buffer pH 7.6, 8 mM $MgSO_4$
CTT agar plates	CTT medium, 1.5% agar
CTT soft agar	CTT medium, 0.5% agar
Motility assays	
A-motility plates (Hodgkin and Kaiser, 1977)	0.5% CTT, 1.5% agar
S-motility plates (Hodgkin and Kaiser, 1977)	0.5% CTT, 0.5% agar
Microscopy	
A50 microscopy agar	10 mM MOPS pH 7.2, 10 mM $CaCl_2$, 10 mM $MgCl_2$, 50 mM NaCl, 1.5% or 0.7% (w/v) agar

The appropriate antibiotics were added to cultures when needed (Table 5). For the protein induction IPTG was added and for the selection Xgal and Galactose were added.

Table 5. Additives used for *E. coli* and *M. xanthus*

Additive	Final concentration	Dissolved in
E. coli		
Ampicillin sodium sulfate	100 µg/ml	H_2O
Chloramphenicol	30 µg/ml	99.99 % ethanol
Kanamycin sulfate	50 µg/ml	H_2O
Tetracyclin	15 µg/ml	99.99 % ethanol
IPTG	0.1 mM	H_2O
Xgal	40 µg/ml	DMF
M. xanthus		
Kanamycin sulfate	50 µg/ml	H_2O
Oxytetracycline	10 µg/ml	99.99% methanol
Galactose	2%	H_2O

4.3 Microbiological methods

4.3.1 *E. coli* strains

Table 6 . *E. coli* strains used in this study

Strain	Relevant characteristics	Source or reference
Top10	F- *mcrA* Δ(*mrr-hsdRMS-mcrBC*), *80lacZΔM15ΔlacX74, recA1, deoR, araD139* Δ(*ara-leu*)*7697, galU, galK, rpsL* Str^R *endA1, nupG*	Invitrogen (Darmstadt)
Rosetta 2 (DE3)	F^-*ompT hsd*S_B($r_B^-m_B^-$) *gal dcm*(DE3) pRARE2(Cm^R)	Novagen/Merck (Darmstadt)
BTH101	F-, *cya-99, araD139, galE15, galK16, rpsL1* (Str^r), *hsdR2, mcrA1, mcrB1*	Euromedex (Strasbourg/France)

4.3.2 *M. xanthus* strains

Table 7. *M. xanthus* strains used in this study

Strain	Relevant characteristics	Source or reference
DK1622	wild type	(Kaiser 1979)
DK1300	Δ*sglG*	(Hodgkin and Kaiser 1979)
DK1217	Δ*aglB*	(Hodgkin and Kaiser 1979)
MxH2265	Δ*aglZ*	(Yang *et al*. 2004)
SA5923	Δ*aglQ*	(Hot PhD thesis, 2013)
SA4420	Δ*mglA*	(Leonardy *et al*. 2010)
SA3921	Δ*gltK*	(Keilberg PhD thesis, 2013)
SA3922	Δ*gltB*	(Keilberg PhD thesis, 2013)
SA3923	Δ*gltA*	(Keilberg PhD thesis, 2013)
SA3924	Δ*gltC*	(Keilberg PhD thesis, 2013)
SA3377	*aglZ-yfp*	(Leonardy, 2010)
SA4452	*aglQ-mCherry*	(Hot PhD thesis, 2013)
SA5209	Δ*agmP*	This work
SA5242	Δ*gltK*/P_{nat}-*gltK* (pBJA31)	This work
SA5239	Δ*gltB*/P_{nat}-*gltB* (pBJA32)	This work
SA5228	Δ*gltA*/P_{nat}-*gltA* (pBJA33)	This work
SA5246	Δ*gltC*/P_{nat}-*gltC* (pBJA34)	This work
SA5245	WT/P_{nat}-*gltB-mCherry* (pBJA35)	This work
SA5269	Δ*gltK*/P_{nat}- *gltB-mCherry* (pBJA35)	This work
SA5227	Δ*gltB*/P_{nat}- *gltB-mCherry* (pBJA35)	This work
SA5284	Δ*gltA*/P_{nat}- *gltB-mCherry* (pBJA35)	This work
SA5256	Δ*gltC*/P_{nat}- *gltB-mCherry* (pBJA35)	This work
SA5235	WT/P_{nat}-*gltA-mCherry* (pBJA36)	This work
SA5261	Δ*gltK*/P_{nat}- *gltA-mCherry* (pBJA36)	This work

SA5289	Δ*gltB*/P$_{nat}$- *gltA-mCherry* (pBJA36)	This work
SA5229	Δ*gltA*/P$_{nat}$- *gltA-mCherry* (pBJA36)	This work
SA5255	Δ*gltC*/P$_{nat}$- *gltA-mCherry* (pBJA36)	This work
SA5247	Δ*aglZ*/P$_{nat}$- *gltB-mCherry* (pBJA35)	This work
SA5254	Δ*aglQ*/P$_{nat}$- *gltB-mCherry* (pBJA35)	This work
SA5288	Δ*mglA*/P$_{nat}$- *gltB-mCherry* (pBJA35)	This work
SA5252	Δ*aglZ*/P$_{nat}$- *gltA-mCherry* (pBJA36)	This work
SA5249	Δ*aglQ*/P$_{nat}$- *gltA-mCherry* (pBJA36)	This work
SA5260	Δ*mglA*/P$_{nat}$- *gltA-mCherry* (pBJA36)	This work
SA5243	WT/P$_{nat}$-*gltC-mCherry* (pBJA37)	This work
SA5283	Δ*gltK*/P$_{nat}$- *gltC-mCherry* (pBJA37)	This work
SA5264	Δ*gltB*/P$_{nat}$- *gltC-mCherry* (pBJA37)	This work
SA5266	Δ*gltA*/P$_{nat}$- *gltC-mCherry* (pBJA37)	This work
SA5244	Δ*gltC*/P$_{nat}$- *gltC-mCherry* (pBJA37)	This work
SA5267	Δ*gltK*/*aglZ-yfp* (pSL65, integration at the native site, Km^R)	This work
SA5268	Δ*gltB*/*aglZ-yfp* (pSL65, integration at the native site, Km^R)	This work
SA5273	Δ*gltA*/*aglZ-yfp* (pSL65, integration at the native site, Km^R)	This work
SA5259	Δ*gltC*/*aglZ-yfp* (pSL65, integration at the native site, Km^R)	This work
SA5285	Δ*gltK*/*aglQ-mCherry* (pEH53, integration at the native site)	This work
SA5257	Δ*gltB*/*aglQ-mCherry* (pEH53, integration at the native site)	This work
SA5278	Δ*gltA*/*aglQ-mCherry* (pEH53, integration at the native site)	This work
SA5258	Δ*gltC*/*aglQ-mCherry* (pEH53, integration at the native site)	This work
SA5250	WT/P$_{nat}$-*gltB-mCherry*/*aglZ-yfp* (pBJA35, pSL65 integration at the native site, Km^R)	This work

SA5253	Δ*gltB* /P$_{nat}$-*gltB-mCherry*/*aglZ-yfp* (pBJA35, pSL65 integration at the native site, Km^R)	This work
SA5251	WT/P$_{nat}$-*gltA-mCherry*/*aglZ-yfp* (pBJA36, pSL65 integration at the native site, Km^R)	This work
SA5287	Δ*gltA* /P$_{nat}$-*gltA-mCherry*/*aglZ-yfp* (pBJA36, pSL65 integration at the native site, Km^R)	This work

4.3.3 Cultivation and storage of *E. coli* and *M. xanthus*

E. coli strains were grown shaking with 220 rpm in liquid LB media or on plates at 37°C. If it was needed appropriate antibiotics were added. The optical densities of cultures were determined photometrically at 600 nm.

M. xanthus cells were cultivated on CTT agar plates at 32°C in dark. For the *M. xanthus* culturing in liquid CTT media, cells were harvested from the plate, resuspended in volume of 1 ml and then transferred to the bigger volume of media. Liquid cultures were incubated shaking with 220 rpm at 32°C. Antibiotics were used when required. The optical densities of *M. xanthus* cultures were determined photometrically at 550 nm.

For the short time storage *E. coli* and *M. xanthus* strains were kept on plates at 4°C and 18°C, respectively. For the long time storage the cultures were grown to exponentially phase. To 1.5 ml of *E. coli* and *M. xanthus* cultures the glycerol was added to the final concentration of 15% and 3.5%, respectively. The glycerol stocks were snap freezed in liquid nitrogen and stored at -80°C.

4.3.4 Motility assays for *M. xanthus*

To analyze the motility phenotype of *M. xanthus* strains, the cells were grown to exponentially phase, harvested and concentrated to 7×10^9 cells/ml in CTT media. 5 µl of that cell suspension were spotted on 0.5% CTT plates supplemented with 0.5% or 1.5% agar to test for S- and A-motility, respectively. Plates were incubated at 32°C in dark for 24h. The bacterial colony edges were imaged by MZ75 stereomicroscope with Leica DFC280 camera and Leica DM6000B light microscope with the Cascade II camera.

4.3.5 BACTH system

The bacterial two-hybrid system (BACTH) was used to characterize protein-protein interactions *in vivo*. The principle of BACTH is the catalytic domain of the adenylate cyclase (CyaA) from *Bordetella pertusis* which consists of two complementary fragments T18 and T25. The experiments were performed according to the informations enclosed by the manufacturer (Euromedex). Proteins of interest x and y were co-expressed as fusions with the T25 and T18 fragments in the reporter strain BTH101 lacking *cyaA*. Interaction between x and y proteins leads to the heterodimerization of these hybrid proteins what results in functional complementation between T25 and T18 fragments and, therefore, cAMP synthesis. cAMP in a complex with the catabolite activator protein (CAP) regulates gene expression in *E. coli* including genes involved in lactose and maltose catabolism.

The BTH101 cells were co-transformed with the two recombinant plasmids and plated on indicator media LB/X-Gal/IPTG with addition of kanamycin and ampicilin to reveal resulting Cya^+ phenotype. Plates were incubated for 48h at 30°C; three representative clones from each transformation plate were resuspended in 50 µl of LB media and spotted on fresh LB/X-Gal/IPTG plates containing appropriate antibiotics. The pictures of the plates were taken after 48h incubation at 30°C. The blue colonies indicate positive interaction, while white colonies no interaction. The empty plasmids pKNT25 and pUT18C served as a negative control. The plasmids pKT25-zip and pUT18C-zip that encode for fusion proteins T25-zip and T18-zip (leucine zipper motifs appended to the T18 and T25 fragments) served as a positive control.

4.4 Molecular biological methods

4.4.1 Oligonucleotides and plasmids

Table 8. Oligonucleotides used in this study

Name	**Sequence (5'-3')**
M13 forward	CTGGCCGTCGTTTTAC
M13 revers	CAGGAAACAGCTATGAC

agmPA	ATCGGAAGCTTAGAACAAGGACGGCCTGGAG
agmPB	CGCGCCTGCGACGACACGGAGTGACGCCGCCCGCCGCAC
agmPC	CGTGTCGTCGCAGGCGCGGGGGCCGAGCAAAGGT
agmPD	ATCGGTCTAGATTCGCGCCGCGCACCGAGCG
agmPE	CCAGGACTTCGAGCGCACCT
agmPF	ATGCGCGCGTAGGCGGAGCCCATCA
Pnat fw	ATCGGAAGCTTCTTCATGGGACCTCTGACCT
Pnat rv	ATCGGCATATGCGGAGGCTCCGTGAGGG
nat 39 fw	ATCGGCATATGTTGAACCGCCCCAAGTTGCT
2539malErv	ATCGGTCTAGATCATTCCGAGTCCCTCCCCG
nat 39rv	ATCGGTCTAGATTCCGAGTCCCTCCCCG
mCh fw	ATCGGTCTAGATTCCGAGTCCCTCCCCG
mCherryEcoRI rv	ATCGGGAATTCTTACTTGTACAGCTCGTCCA
nat 40 fw	ATCGGCATATGATGAAGCGTTTCTTCCGTGTGC
2540malErv	ATCGGTCTAGATCATGACTCGGACCCGAAGA
nat 40rv	ATCGGTCTAGATGACTCGGACCCGAAGA
nat 41 fw	ATCGGCATATGATGCGCTCCTTCCGGCTCAT
2541malErv	ATCGGTCTAGATTACATCGCCTCGGCGGACT
nat 41rv	ATCGGTCTAGACATCGCCTCGGCGGACT
PnatO rv	ATCGGCATCTAGATGGGACCTCTGACCT
PnatO fw	ATCGGAAGCTTATCCGGAGGCTCCGTGAGGG
agmOmChforw	ATCGGTCTAGAATGTTCGTGCGAACCGCCCT
agmOrvIPTG	ATCGGGGTACCTCAATCCGGGATGAGCGCGC
extf1	GGAAAGGTGGCGTTCCTCAA
extrv1	GCCCACGCGCAGGCTGACGC
extfnew2	CGGTGGATCACGCTGCGCACGGAGCTGCGT

extrvnew2	GTTCTTGAAGAGGCTGACGGCCACGTCCAG
ext3_fw	GGACATCATCCTGGAGCGCA
ext3_rv	GCGAACAGACCGATGGCGAG
extf4	GCGCTGGGGGGCTGGCTCTTC
extrv4	CCTTCGCGCCGCGCACCGAG
extf0	GCACGGCTTGCCAATCTCGC
extrv0	TTCCAATGGCTCGTCCGCGG
41int_fw	GTGGCCGTCAGCCTCTTCAA
41int_rv	AGCCGGAGGATGCGCTCCAGGATGA
agmPG	AGTCTCTGCCGCTGCTCTTCCT
agmPH	AATCGCCGCGAAGAGCCAAC
MXAN_2539G	GCGTCCAGCGGAAGGTTTAC
MXAN_2539H	TGGAGTTGAGGAACGCCACC
MXAN_2540G	TCTCCGGCCACGTCTTCCTCAA
MXAN_2540H	TCAGCCAGCAGCGACACCTT
agmOmalEfw	ATCGGGAATTCTGTGAGGTGGCCAGCGAGATTG
agmOmalErv	ATCGGTCTAGATCAATCCGGGATGAGCGCGC
2539malEfw	ATCGGGAATTCCAGAGCCAGGAAGGCATGGG
2540malEfw	ATCGGGAATTCCAGACCACCGAAGAGGCGGA
2541malEfw	ATCGGGAATTCCAGAACTTCGAGGGCCTGGA
ds2541forwC	ATCGGGAATTCGCAGAACTTCGAGGGCCTGGA
2541rev	ATCGGAAGCTTCATCGCCTCGGCGGACTGGA
2539stoprev	ATCGGCTCGAGTCATTCCGAGTCCCTCCCCG
BTH2538dspforw	ATCGGTCTAGAGATTGGCAAGCCGTGCGCGCTGGTGCGAAAG
BTH2538stoprevNEW	ATCGGGAATTCATCAATCCGGGATGAGCGCGCCGGCGCAGAAGA

BTH2538rev	ATCGGGAATTCCTATCCGGGATGAGCGCGCCGG
BTH2541dspforw	ATCGGTCTAGAGCTGGACCTCTCCGGCCAGTCCA
BTH2541stoprev	ATCGGGAATTCATTACATCGCCTCGGCGGACT
BTH2541rev	ATCGGGAATTCCTCATCGCCTCGGCGGACTGGA
AglQcheckmChfw	CTACGTGGCTGGCCAGAAGT
AglQcheckmChrv	CGCGAAGTTGATGTTGTTGT
aglZ-gfprev	CCACCAGGATGGGCTTGTCCATCCG
attP left	GGGAAGCTCTGGGTACGAA
attB right	GGAATGATCGGACCAGCTGAA
attB left	CGGCACACTGAGGCCACATA
2538forw	ATCGGAAGCTTGTGCCCCATCCCCCCTTTGT
2538stoprev	ATCGGCTCGAGTCAATCCGGGATGAGCGCGC
ds2539forwC	ATCGGGAATTCGCAGAGCCAGGAAGGCATGGG
2539rev	ATCGGAAGCTTTTCCGAGTCCCTCCCCGTCG
ds2540forw	ATCGGAAGCTTTTCGCCCAGACCACCGAAGA
2540stoprev	ATCGGCTCGAGTCATGACTCGGACCCGAAGA

Table 9. Sequencing primers

Name	**Description**	**Sequence (5'-3')**
M13 uni (-43)	sequencing primer for pBJ114 and pSWU30	AGGGTTTTCCCAGTCACGACGTT
M13 rev (-49)	sequencing primer for pBJ114 and pSWU30	GAGCGGATAACAATTTCACACAGG
T7	sequencing primer for pET24b$^+$ and pET45b$^+$	TAATACGACTCACTATAGGG
T7 term	sequencing primer for pET24b$^+$ and pET45b$^+$	CTAGTTATTGCTCAGCGGT
malE	sequencing primer for pMal-c2x	GGTCGTCAGACTGTCGATGAAGCC

M13 uni (-21)	sequencing primer for pMal-c2x	TGTAAAACGACGGCCAGT
pGEX-for	sequencing primer for pGEX-4T1	GGAGCAGACAAGCCCGTCAGG
pGEX-rev	sequencing primer for pGEX-4T1	CAGGCTTTACACTTTATGCTTCCGGC
pSWUfw	sequencing primer for pSWU30	GGATGTGCTGCAAGGCGATTAAGTTGG
pSWUrv	sequencing primer for pSWU30	GCTTTACACTTTATGCTTCCGGCTCG
Intmxan_2541	Internal sequencing primer for mxan_2541	TACCGCAACGAGTTCCGCTA

Table 10. Plasmids used in this study

Plasmid	**description**	**reference**
pSWU30	Vector for integration at *attB* site, Tet^R	
pBJ114	Vector for in-frame deletion constructs, Km^R	(Julien *et al.*, 2000)
pET24b$^+$	Expression vector, T7 promoter, C-term. His_6-tag, Km^R	Merck Millipore
pET45b$^+$	Expression vector, T7 promoter, N-term. His_6-tag, Amp^R	Merck Millipore
pMal-c2x	Expression vector, *tac* promoter, N-term. MBP-tag, Amp^R	New England biolabs
pSL65	Vector for insertion of pBJ113 *aglZ*(C-terminal fragment of 345aa)-*yfp* at the *aglZ* native site	Laboratory collection
pEH53	Vector for insertion of *mCherry* at the *aglQ* native site	Laboratory collection
pGEX-4T1	Expression vector, *tac* promoter, N-term. GST-tag, Amp^R	GE-Healthcare
pCHYC	Vector for *mCherry* amplification	
pBJA9	pET 24b$^+$ - *gltC*	This work
pBJA1	pET 45b$^+$ - *gltK*	This work
pBJA3	pET 45b$^+$ - *gltA*	This work
pBJA10	pET 24b$^+$ - *gltB*	This work

pBJA25	pMal-c2x – *gltC*	This work
pBJA26	pMal-c2x – *gltK*	This work
pBJA27	pMal-c2x – *gltB*	This work
pBJA28	pMal-c2x – *gltA*	This work
pBJA29	pGEX-4T1 - *gltB*	This work
pBJA38	pBJ114 – *agmP* in-frame deletion	This work
pBJA31	pSWU30 – P_{nat}-*gltK*	This work
pBJA32	pSWU30 – P_{nat}-*gltB*	This work
pBJA33	pSWU30 – P_{nat}-*gltA*	This work
pBJA34	pSWU30 – P_{nat}-*gltC*	This work
pBJA35	pSWU30 – P_{nat}-*gltB-mCherry*	This work
pBJA36	pSWU30 – P_{nat}-*gltA-mCherry*	This work
pBJA37	pSWU30 – P_{nat}-*gltC-mCherry*	This work
pBJA39	pUT18 - $gltK_{24\text{-}171}$	This work
pBJA40	pUT18C - $gltK_{24\text{-}171}$	This work
pBJA41	pKNT25 - $gltK_{24\text{-}171}$	This work
pBJA42	pKT25 - $gltK_{24\text{-}171}$	This work
pBJA43	pUT18 - $gltC_{30\text{-}674}$	This work
pBJA44	pUT18C - $gltC_{30\text{-}674}$	This work
pBJA45	pKNT25 - $gltC_{30\text{-}674}$	This work
pBJA46	pKT25 - $gltC_{30\text{-}674}$	This work

4.4.2 Plasmid construction

Genomic DNA of *M. xanthus* DK1622 was used to amplify DNA fragments or genes whereas plasmid DNA was used to generate the *mCherry* gene by PCR. Plasmid constructs were transformed to *E. coli* TOP10 cells. The purified plasmid DNA was sent for sequencing to verify the correct sequence of

the plasmids. Sequencing was performed by the company Eurofins MWG Operon (Ebersberg). Sequences were analyzed using program ContigExpress of the VectorNTI advance suite 11 software (Invitrogen).

Plasmids **pBJA1**, **pBJA3**, **pBJA9** and **pBJA10** were used for the His_6-GltK, $GltB_{20-275}$-His_6, His_6-$GltA_{20-257}$ and $GltC_{25-674}$-His_6 overexpression. Primer pairs 2538forw/2538stoprev, ds2539forwC/2539rev, ds2540forw/2540stoprev and ds2541forwC/ 2541rev were used to amplify the fragments of *gltK*, *gltB*, *gltA* and *gltC* which were digested and cloned at the *EcoR*I/*Hind*III sites of pET $24b^+$ (*gltB*, *gltC*) and *Hind*III/*Xho*I sites of pET $45b^+$ (*gltK*, *gltA*).

To overexpress MalE-GltK, MalE-GltB, MalE-GltA and MalE-GltC the plasmids **pBJA26**, **pBJA27**, **pBJA28** and **pBJA25** were constructed. Genes were amplified using the primer pairs agmOmalEfw/agmOmalErv ($gltK_{17-171}$), 2539malEfw/2539malErv ($gltB_{20-276}$), 2540malEfw/2540malErv ($gltA_{22-257}$) and 2541malEfw/2541malErv ($gltC_{25-674}$), digested with respective enzymes and cloned at *EcoR*I and *Xba*I sites of pMal-c2x.

To construct **pBJA29** for GST-GltB overexpression, the $gltB_{20-276}$ fragment was generated using 2539malEfw and 2539stoprev primers, digested with *EcoR*I and *Xho*I and cloned into pGEX-4T1.

The plasmid **pBJA38** was generated for the construction of the *agmP* in-frame deletion mutant in DK1622 *M. xanthus* which is described in 4.4.3. The upstream and downstream regions of *agmP* were amplified using primer pairs agmPA/agmPB and agmPC/agmPD. The AB and CD DNA fragments were fused by overlap PCR reaction. Resulting AD fragment was digested with *Hind*III and *Xba*I and ligated to pBJ114.

The complementation construct **pBJA31** for *gltK* was generated by amplifying the 277bp fragment upstream from the *gltK* open-reading frame which served as a native promoter (PnatO fw/PnatO) and *gltK* gene (agmOmChforw/agmOrvIPTG). In the first step of cloning *gltK* native promoter (P_{nat}) was digested with *Hind*III and *Xba*I and ligated to pSWU30. In the next step *gltK* was cloned at *Xba*I and *Kpn*I sites of pSWU30-P_{nat}.

The plasmids **pBJA32**, **pBJA33** and **pBJA34** were generated for gene complementation. Primers Pnat fw and Pnat rv were used to amplify 277bp

fragment upstream from the *gltB* open-reading frame which served as promoter for *gltBAC* operon. The other PCR products corresponded to *gltB* (nat39 fw /2539malErv), *gltA* (nat40 fw /2540malErv) and *gltC* (nat41 fw /2541malErv). The promoter region was digested with *Hind*III and *Nde*I while gene products were digested with *Nde*I and *Xba*I. Both DNA fragments were ligated in one step at *Hind*III and *Xba*I sites of pSWU30.

To localize GltB, GltA and GltC in the cells the following mCherry-fusion constructs **pBJA35**, **pBJA36** and **pBJA37** were generated. pCHYC served as a template to amplify *mCherry* gene using mCh fw, mCherryEcoRI rv primers. The *mCherry* fragment was cloned at the *Xba*I and *EcoR*I sites of the previously prepared pBJA32, pBJA33 and pBJA 34 constructs.

To check for direct protein-protein interactions the plasmids **pBJA39**, **pBJA40**, **pBJA41**, **pBJA42**, **pBJA43**, **pBJA44**, **pBJA45** and **pBJA46** were constructed for BACTH system. The plasmids were generated by amplifying $gltK_{24\text{-}171}$, $gltK_{24\text{-}170}$ using primers BTH2538dspforw and BTH2538stoprevNEW (pBJA40, pBJA42), BTH2538dspforw and BTH2538rev (pBJA39, pBJA41) as well as by amplifying $gltC_{30\text{-}674}$, $gltC_{30\text{-}673}$ using primers BTH2541dspforw and BTH2541stoprev (pBJA44, pBJA46), BTH2541dspforw and BTH2541rev (pBJA43, pBJA45). The gene products were digested with *Xba*I and *EcoR*I and cloned into pKT25 (pBJA42, pBJA46), pKNT25 (pBJA41, pBJA45), pUT18 (pBJA39, pBJA43) and pUT18C (pBJA40, pBJA44) vector.

4.4.3 Construction of in-frame deletions

In-frame deletion mutants were constructed by two-step homologous recombination as previously described (Figure 35) (Shi *et al.*, 2008). Briefly, the upstream and downstream flanking regions of approximately 500bp of gene of interest were amplified using AB and CD primer pairs. B and C primers were designed to contain compatible ends essential for the fusion of AB and CD fragments in a PCR reaction using A and D primers. AB and CD fragments served as a template to generate the full-length in-frame deletion fragment. A and D primers posses restriction sites allowing for cloning the AD fragment into pBJ114 vector. The correct pBJ114AD construct which was checked by sequencing was transformed into *M. xanthus* DK1622 to construct strains by

homologous recombination. pBJ114 vector encodes for kanamycin resistance. Thus, for the clone selection, *M. xanthus* cells were plated on CTT agar plates containing kanamycin. The plasmid integration was checked by PCR reaction using E (binds upstream of A primer) and F (binds downstream of D primer), E and M13forward (binds to pBJ114), F and M13reverse (binds to pBJ114) primer pairs. If possible one clone resulted from an up- and downstream plasmid integration was used for the second step of homologous recombination.

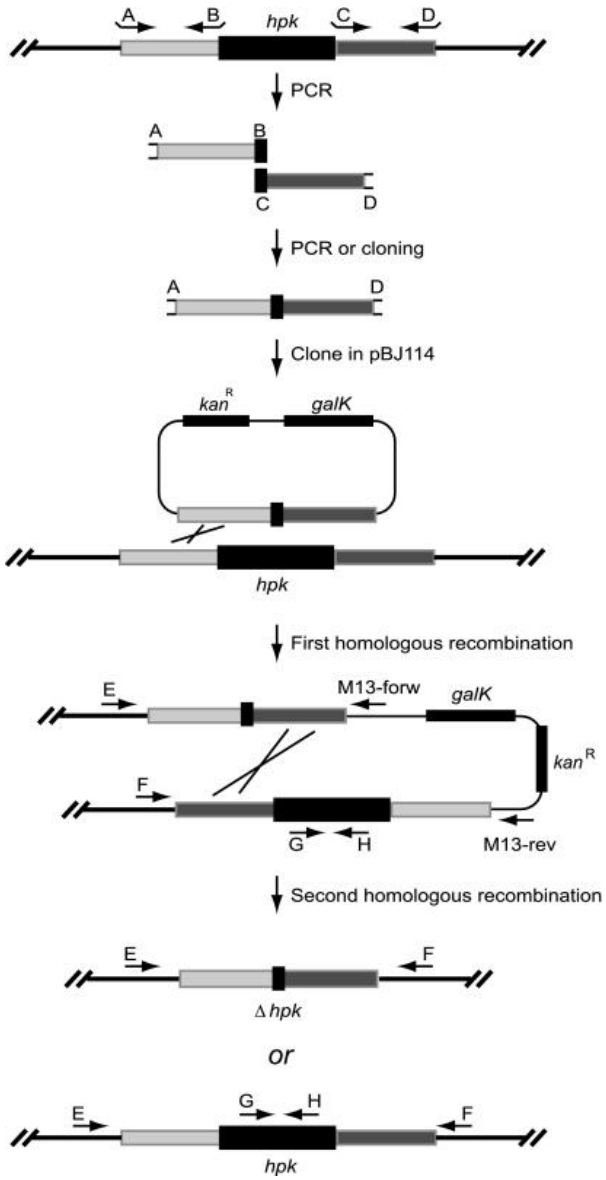

Figure 35. Strategy for in-frame deletion mutants construction. First homologous recombination leads to up- or downstream plasmid integration in the genomic region of interest. Second homologous recombination enables loop out of vector (reconstitution) or vector with the region of interest (in-frame deletion). Details in the text. The figure is reproduced from Shi *et al*. (2008).

The pBJ114 plasmid encodes for *galK* gene which is a counter-selection marker. The product of *galK* (galactokinase) phosphorylates galactose to galactose-1-phosphat which is toxic for *M. xanthus* cells in high levels. Only

cells which “loop out” the plasmid are able to grow on galactose rich media. To select for the in-frame deletion mutants the cells were grown in CTT liquid media to reach the exponentially phase. 100µl and 10µl of cells were mixed with 4ml of soft agar and plated on CTT agar plates enriched with 2% galactose (Sigma/Roth). The transformants which were galactose resistant and kanamycin sensitive were checked by PCR reaction using E and F, G (binds downstream of B primer) and H (binds upstream of C primer) primer pairs. The EF fragment was longer for the WT in comparison to the deletion mutant, while GH fragment was amplified only in the WT. Thus, EF and GH PCR products helped to distinguish between WT and in-frame deletion.

4.4.4 DNA isolation from *E. coli* and *M. xanthus*

Plasmid DNA from *E. coli* was isolated using the QIAprep Spin Miniprep Kit (Qiagen) or Zyppy™ Plasmid Miniprep Kit (Zymo) in accordance to the instructions supplied by the manufacturer. Genomic DNA from *M. xanthus* was isolated using MasterPure DNA preparation Kit (Epicentre) according to the instructions supplied by the manufacturer. Concentration and purity of DNA was determined with the Nanodrop ND-1000 spectrophotometer (Nanodrop, Wilmington). Crude genomic DNA for colony PCR was prepared by resuspending cell pellet in 50 µl of ddH_2O, boiling for 10 min and centrifuging the sample for one minute at 13000 rpm. 3 µl of resulting supernatant was taken for the PCR reaction.

4.4.5 Polymerase Chain Reaction (PCR)

For the amplification of specific DNA fragments, the Phusion High-Fidelity DNA Polymerase was used in a reaction volume of 50 µl. The colony PCR was performed in a volume of 20 µl using 5 PRIME MasterMix. The composition of the PCR reaction mix was prepared as described in Table 11.

Table 11. PCR reaction mix

Component	Volume	Final concentration
PCR for cloning		
Genomic DNA or plasmid DNA	1 µl	~ 100 ng
10 µM primer (each)	1 µl	0.5 µM
10 mM dNTPs	1 µl	
5 x Phusion GC buffer	4 µl	1x
5 x enhancer	4 µl	1x
Phusion DNA polymerase	0.2 µl	
ddH2O		-
Check PCR		
Crude genomic DNA	3 µl	~ 200 ng
10 µM primer (each)	1 µl	0.5 µM
5 PRIME MasterMix	8 µl	
DMSO	1 µl	5 % (v/v)
ddH2O	6 µl	-

The PCR programs used in this study are represented in Table 12. PCR conditions were modified in terms of the predicted primer annealing temperature and expected product sizes.

Table 12. PCR programs

Step	Temperature	Time	
Standard/check PCR			
Initial denaturation	94°C	3 min	
denaturation	94°C	30 sec	30x
Primer annealing	5˚C below predicted melting temperature	30 sec	
elongation	72°C	1 min/kb	
Final elongaation	72°C	5 min	

hold	4°C	∞	
Touch down PCR			
Initial denaturation	94°C	3 min	
denaturation	94°C	30 sec	9x
Primer annealing	70°C	30 sec	
elongation	72°C	30 sec	
denaturation	94°C	30 sec	9x
Primer annealing	60°C	30 sec	
elongation	72°C	30 sec	
denaturation	94°C	30 sec	20x
Primer annealing	55°C	30 sec	
Elongation	72°C	30 sec	
Final elongaation	72°C	5 min	
hold	4°C	∞	

PCR products were analyzed by agarose gel electrophoresis. Correct PCR products were purified using the NucleoSpin® Gel and PCR Clean-up kit (Macherey-Nagel) or excised from the gel and then purified using the Zymoclean Gel DNA recovery kit (Zymo Research).

4.4.6 Reverse transcription PCR

Total RNA of *M. xanthus* was isolated using the hot phenol extraction method (Overgaard *et al.*, 2006). Briefly, the cell pellet from 10 ml of exponentially growing *M. xanthus* culture was resuspended in 600 µl ice cold solution 1 (0.3 M sucrose, 0.01 M NaAc, pH 4.5) and 300 µl were transferred to 1.5 ml tubes containing 300 µl hot (65°C) solution 2 (2% SDS, 0.01 M NaAc, pH 4.5). The cell lysis was performed twice with equal volume of hot phenol extraction (saturated acid phenol pH<6.0 at 65°C), once with equal volume of phenol: chloroform extraction (5:1), and once with equal volume of chloroform: isoamyl alcohol extraction (24:1). RNA was precipitated with 1/10 volume of 3 M NaAc, pH 4.5 and two volumes of 96% ethanol for 30 min at -20°C and

centrifuged at 13000 rpm for 30min at 4°C. RNA pellet was washed twice with 500 µl of ice cold 75% ethanol, dried at RT and resuspended in 50 µl RNase-free H_2O. RNA samples were stored at -80°C.

For the cDNA synthesis RNA was treated with DNase I (Ambion) and purified with the RNeasy kit (Qiagen). cDNA was synthesized from 1 µg of RNA using the High capacity cDNA Archive kit (Applied Biosystems) and random hexamer primers according to the instructions enclosed by manufacturer. The *gltBAC* locus was mapped by performing PCR reactions using DNA, RNA and cDNA as templates and primers listed in Table 8.

4.4.7 Agarose gel electrophoresis

Nucleic acid fragments were separated by size on 1% agarose gels with 0.01% (v/v) ethidium bromide in TBE buffer (Invitrogen) at 120V. DNA samples were mixed with 5 x DNA loading buffer (32.5 % saccharose, 5 mM EDTA, 5 mM Tris-HCl pH 7.5, 0.15 % bromophenol blue). As a DNA marker the HyperLadder I (Bioline) or the 2-log DNA ladder (NEB) were used. Gels were imaged using the E-BOX VX2 imaging system from PeqLab.

4.4.8 DNA restriction and ligation

DNA (0.5-2 µg) was incubated with the restriction endonucleases for 2h at 37°C according to the manufacturer's recommendations. Restricted DNA was purified using the DNA Clean & Concentrator kit (Zymo Research).

Ligation reactions were conducted with T4 DNA ligase (NEB). DNA fragments were ligated into vectors with 3- to 5-fold molar excess of insert DNA. Normally ~80 ng of vector was used in one ligation reaction which was performed at RT for 5h or overnight at 18°C. T4 DNA ligase was inactivated at 65°C for 10 min.

4.4.9 Preparation and transformation of electrocompetent *E. coli* cells

To prepare electrocompetent *E. coli* cells, the overnight culture was used to inoculate 1 L of LB media. Cultures were grown with shaking at 230 rpm at

37°C to an OD_{600} of 0.5 - 0.7. The cells were harvested by centrifugation at 5000 rpm for 20 min at 4°C and the cell pellet was resuspended in 1 L cold sterile 10% glycerol. The cells were centrifuged again at the same conditions and the washing procedure was repeated three times with 500 ml, 250 ml and 40 ml cold sterile 10% glycerol. The final cell pellet was resuspended in 2 ml of cold, sterile 10% glycerol, aliquoted à 50 µl, frozen in liquid nitrogen and stored at -80°C.

For transformation cells were thawed on ice, 10 µl of the ligation reaction was dialyzed against sterile water (VSWP membrane from Millipore) for 20 min and added to 50 µl cells and mixed gently. The mixture was transferred into an electroporation cuvette (Bio-Rad, Munchen) and pulsed with 1.8 kV, 25 µF and 200 Ω. To allow phenotypic expression 1 ml of LB media was added to the cuvette and mixed with cells. The cell suspension was transferred to sterile microcentrifuge tube and incubated shaking at 230 rpm for 1h at 37°C. 100 µl of cells were plated on LB agar plates supplemented with the appropriate antibiotics. The plates were incubated overnight at 37°C. Grown colonies were transferred to the fresh agar plates and checked for the presence of the plasmid containing the insert by restriction digestion.

4.4.10 Preparation and transformation of chemical competent *E. coli* cells

To prepare chemical competent *E. coli* cells, the overnight culture was used to inoculate 200 ml of LB media. Cultures were grown with shaking at 230 rpm at 37°C to an OD_{600} of 0.5 - 0.7. The cells were harvested by centrifugation at 5000 rpm for 20 min at 4°C and resuspended in 50 ml 50 mM CaCl2. The cells were centrifuged again at the same conditions and the washing procedure was repeated. The final cell pellet was resuspended in 50 ml icecold 50 mM CaCl2/10% glycerol, aliquoted à 200 µl, frozen in liquid nitrogen and stored at -80°C.

For transformation cells were thawed on ice, 10 µl of the ligation reaction were added to 200 µl cells and mixed gently. After 30 min incubation on ice cells were transferred to 42°C for 2 min for heat shock. Then, the cells were transferred on ice and incubated for 5 min. To allow phenotypic expression 800 µl of LB media was added and mixed with the cells. Transformations were

incubated shaking at 230 rpm for 1h at 37°C and after that centrifuged at 5000 rpm at RT for 5 min. The supernatant was carefully discarded, the cells were resuspended in the residual supernatant and plated on LB agar plates supplemented with the appropriate antibiotics. The plates were incubated overnight at 37°C. Grown colonies were transferred to fresh agar plates and checked for the presence of the insert containing plasmid by restriction digestion.

4.4.11 Transformation of *E. coli* cells for BACTH system

The chemical competent cells of BTH101 *E. coli* were prepared and transformed as described in 4.4.9. For one transformation two plasmids were added to the cells one encoding for the T25 fragment (derivatives of pKNT25 or pKT25) and the other one encoding for the T18 fragment (derivatives of pUT18 or pUT18C). Normally ~20 ng of each vector was used in one transformation. The cell suspension was plated on rich LB media in the presence of X-Gal (40 µg/ml), 0.5 M IPTG, 100 µg/ml ampicillin and 50 µg/ml kanamycin.

4.4.12 Preparation and transformation of electrocompetent *M. xanthus* cells

M. xanthus cells were grown overnight with shaking at 230 rpm at 32°C to an OD_{550} of 0.5-0.9. For one transformation 1.5 ml of cells were transferred to a sterile Eppendorf tube and centrifuged at 13000 rpm at RT for 1 min. The cell pellet was resuspended in 1 ml sterile ddH_2O and centrifuged at 13000 rpm at RT for 2 min. The washing procedure was repeated as described above. The resulting cell pellet was resuspended in 40 µl sterile ddH_2O. The cell suspension was immediately used for electroporation.

Normally, 0.1 µg (for the integration at the chromosomal Mx8 attachment site) or 1 µg (for the integration at the endogenous site) of plasmid DNA was dialyzed against sterile water (VSWP membrane from Millipore) for 20 min and added to 40 µl cells and mixed gently. The mixture was transferred into an electroporation cuvette (Bio-Rad, Munchen) and pulsed with 0.65 kV, 25 µF and 400 Ω. 1 ml of CTT media was added and mixed with cells, the cell suspension was transferred to a 25 ml Erlenmyer flask containing 1.5 ml of CTT media and

incubated with shaking at 230 rpm at 32°C for 5 h. Then, 1 ml and 100 µl of the culture were mixed with 4 ml of soft agar and plated on CTT agar plates supplemented with appropriate antibiotics. The plates were incubated for 5-10 days at 32°C in the dark. Grown colonies were transferred to fresh agar plates. Plasmid integration was verified by colony PCR.

4.5 Biochemical methods

4.5.1 Purification of proteins

To purify MalE-GltK, MalE-GltB, GST-GltB, MalE-GltA, MalE-GltC and GltC-His, the plasmids pBJA26, pBJA27, pBJA29, pBJA28, pBJA25, pBJA9 were introduced into *E. coli* Rosseta 2 (DE3)/pLysS strain (Novagen). The cultures were grown in 1l LB medium containing appropriate antibiotics at 37°C to an OD_{600} of 0.5-0.7. The protein expression was induced by addition of IPTG to a final concentration of 0.1 mM. Proteins were expressed overnight at 18°C. The cells were harvested by centrifugation at 5.000 rpm for 10 min at RT and resuspended in 40 ml lysis buffer with added protease inhibitors (Complete Protease Inhibitor Cocktail Tablets from Roche). For MalE- and GST-tagged proteins we used CB1 buffer (20 mM Tris-HCl pH7.4, 200 mM NaCl, 1 mM DTT, 1 mM EDTA) while for His-tagged proteins the lysis buffer (50 mM NaH_2PO_4, 300 mM NaCl pH 7.5, 1 mM DTT). Cells were disrupted by sonication (large tip, duty cycle 50 %, output control 5, 4 x 2 min) and centrifuged at 13000 rpm for 30 min at 4°C to collect cell debris. The supernatant was taken for the protein purification. All proteins used in pull down experiments were purified under native conditions. MalE-tagged proteins were purified using amylose beads (Biolabs), His_6-tagged proteins were purified using Ni^{2+}-NTA-agarose columns (Qiagen) and GST-tagged proteins were purified using a glutathione-Sepharose column (Novagen) as recommended by the manufacturers. The supernatant was incubated with appropriate amounts of the beads with gentle shaking at 4°C for 1h. The mixture was loaded on a Pierce centrifuge column. MalE-tagged proteins were eluted with CB2 buffer (20 mM Tris-HCl pH7.4, 200 mM NaCl, 1 mM DTT, 1 mM EDTA, 10 mM maltose), His-tagged proteins were eluted with elution buffer (50 mM NaH_2PO_4, 300 mM NaCl, 250 mM imidazole, pH 8.0) and GST-tagged proteins were eluted with CB1 buffer enriched with 10 mM

glutathione. The purified proteins were dialyzed against CB1 buffer containing 10% glycerol using the Slide-A-Lyzer Dialysis Cassettes, frozen in liquid nitrogen and stored at -80°C. The protein concentration was determined by Bradford as described in 4.5.3 while protein purity was verified by SDS-PAGE.

To purify His_6-GltK, GltB-His_6 and His_6-GltA the plasmids pBJA1, pBJA10, pBJA3 were introduced into *E. coli* Rosseta 2 (DE3)/pLysS strain (Novagen). The cultures were grown as described before. Cells were resuspended in 40 ml buffer A (50 mM NaH_2PO_4, 300 mM NaCl pH 7.5, 1 mM DTT) with addition of protease inhibitors, sonicated and harvested as described before. The cell pellet was resuspended in 40 ml buffer B (100 mM NaH_2PO_4, 10 mM Tris, 8 M Urea; pH 8) and incubated overnight at 4°C. The mixture was centrifuged at 13000 rpm for 30 min at 4°C to dispose cell debris. The resulting supernatant was incubated with the equilibrated Ni^{2+}-NTA agarose gently shaking at 4°C for 1h. The mixture was loaded on a Pierce centrifuge column. After collecting the flow through the column was washed twice with 20 ml buffer C (buffer B; pH 6.3). The proteins were eluted with buffer D (buffer B, pH 5.9) and buffer E (buffer B, pH 4.5). The purified proteins were dialyzed against buffer B containing 10% glycerol, frozen in liquid nitrogen and stored at -80°C. The protein concentration and purity was determined as described before.

4.5.2 SDS polyacrylamide gel electrophoresis (SDS-PAGE)

To separate proteins under denaturing conditions SDS-PAGE (Laemmli, 1970) with 12% polyacrylamide gels was performed. To denature proteins, the protein samples were mixed with 2x loading buffer (20% (v/v) glycerol, 100 mM Tris-HCl pH 6.8, 4% (w/v) SDS, 200 mM β-mercaptoethanol, 0.2% (w/v) bromophenol blue) and heated at 95°C directly before loading on the gel. Gel electrophoresis was performed in Bio-Rad electrophoresis chambers (Bio-Rad, München) at 100-120 V in 1x Tris/Glycine SDS (TGS) running buffer from Bio-Rad. Size of proteins was determined by comparison to the protein marker, the PageRuler Prestained Protein Ladder from Fermentas. Proteins were visualized by staining with PageBlue protein staining solution (Pierce) containing coomassie G-250. Destaining was performed by washing in water.

4.5.3 Determination of protein concentration by Bradford (Bradford, 1976)

To determine protein concentrations the Bradford reagent (Bio-Rad) was used. The protein standard curve was generated using bovine serum albumin (BSA). The reaction samples to measure protein concentration were prepared in duplicates by mixing 980 µl of 1:5 dilution of the Bradford reagent and 20 µl of the sample. After 10 min incubation at RT in the dark, the absorbance was measured at 595 nm with the Ultrospec 2100 pro spectrophotometer (Amersham Biosciences, München). Using the linear slope of the standard curve the protein concentrations were measured.

4.5.4 Immunoblot analysis

Western blotting was performed using standard procedures (Sambrook, 1989). Protein solutions or proteins from cell extracts (approximately $7x10^7$ cells per lane) were separated in the gel by SDS-PAGE as it was described in 4.5.2 and transferred to a nitrocellulose membrane using Hoefer TE77 semi-dry blotting apparatus (Amersham Biosciences, München) with constant current of 0.8 mA/cm^2. Buffers used in the transfer reactions are listed in Table 13. The membranes were blocked with TTBS buffer (0.05% (v/v) Tween 20, 20 mM Tris-HCl, 137 mM NaCl pH 7) supplemented with 5% (w/v) non-fat milk powder for 1h at 4°C. Next, membranes were washed with TTBS buffer and incubated with primary antibodies in TTBS buffer containing 2% (w/v) non-fat milk powder overnight at 4°C. Dilutions of primary antibodies are listed in Table 14. After overnight incubation membranes were washed two times with TTBS buffer and incubated with secondary anti-rabbit immunoglobulin G peroxidase conjugate (Sigma) in a dilution of 1:15000 for 1h at 4°C. Next, membranes were washed twice with TTBS buffer and the Luminata Western HRP Substrate (Merck Millipore) was added. To visualize signals the membrane was developed using luminescent image analyzer LAS-4000 (Fujifilm).

Table 13. Composition of buffers used in immunoblot transfer reaction

Membrane side (anode)		**Gel side (kathode)**	
Chemicals per 1 liter H_20	**Final concentration**	**Chemicals per 1 liter H_20**	**Final concentration**
3,03 g Tris	25 mM	6,06 g Tris	50 mM
14,4 g glycine	192 mM	28,8 g glycine	384 mM
0,1 g SDS	0,01%	2,0 g SDS	0,2%
250 ml methanol	25%	100 ml methanol	10%

Table 14. Dilutions of primary antibodies used in immunoblot analysis

antibody	α-GltK	α-GltB	α-GltA	α-GltC	α-PilB	α-PilC	α-PilQ	α-mCherry
dilution	1:5000	1:5000	1:5000	1:5000	1:5000	1:5000	1:10.000	1:15.000

4.5.5 Antibody production

The antibodies α-PilB, α-PilC and α-PilQ were produced and described previously (Jakovljevic *et al*., 2008, Friedrich *et al*., 2014, Bulyha *et al*., 2009). For the α-GltK, α-GltB, α-GltA and α-GltC antibodies production the proteins His_6-GltK, GltB-His_6, His_6-GltA and GltC-His_6 were purified as described in 4.5.1. Then, 1.3 mg of each purified protein was sent to Eurogentec (Belgium) for antibody production.

4.5.6 Size exclusion chromatography

Purified proteins were loaded on Hi Load 16/600 Superdex 200 prep grade column (SD200) (GE Healthcare) equilibrated with CB1 buffer using the ÄKTA purifier (Amersham Biosciences) and the unicorn 4.10 software. The standard curve was generated by loading on the column a mixture of ferritin (440kDa), aldolase (158 kDa), conalbumin (75 kDa), ovalbumin (44 kDa) and ribonuclease (13.7 kDa) (Figure 36). The void (V_0) volume was determined by running blue dextran over the column (GE Healthcare). The void volume represents the elution volume of molecules which pass straight through the column without entering the pores because they are larger in size than the

largest pores in the matrix. The determined V_0 for SD200 column is 47.2 ml. The total volume (V_t) represents the total volume of the column which is 120.6 ml for SD200, while the elution volume (V_e) represents the volume that is required to "elute" the molecule from the column, thus it determines the molecular size. The partition coefficient Kav which is essential for the preparation of calibration curve is calculated from the following formula:

$$\mathbf{Kav} = \frac{\boldsymbol{V_e} - \boldsymbol{V_0}}{\mathbf{V_t} - \mathbf{V_0}}$$

The formula from the calibration graph is used to calculate the molecular weight of the applied proteins from their Kav, calculated from their V_e.

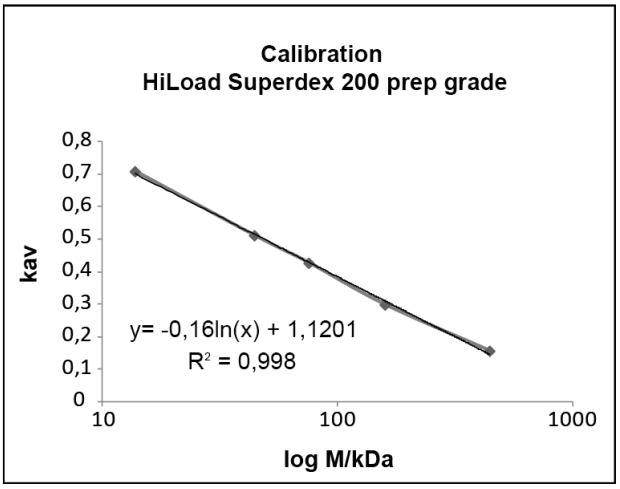

	ferritin	aldolase	conalbumin	ovalbumin	ribonuclease
M/kDa	440	158	75	44	13.7
Ve/ml	58.71	69.14	78.56	84.76	99.21
kav	0.16	0.30	0.43	0.51	0.71

Figure 36. Calibration curve from HiLoad Superdex 200 prep grade size exclusion column.
Y axis represents the partition coefficient Kav, while the x axis represents the logarithm of the molecular weight M. The formula of the logarithmic trendline is indicated on the graph. The proteins which were separated on the column are listed in the table below the graph with the given molecular weights (M), elution volume (Ve) and calculated partition coefficient (Kav).

4.5.7 Cell fractionation

Briefly, 100 ml of a *M. xanthus* culture was grown in CTT media to an OD_{550} of 0.7. Cells were harvested by centrifugation at 8000 rpm at RT for 10 min and resuspended in 2 ml 50 mM Tris-HCl pH 7.6 with addition of protease inhibitors tablet (Roche). Cell membrane was disrupted by sonication (small tip,

duty cycle 20 %, output control 2.5, 8 x 15 sec) and the sample was centrifuged at 5000 rpm at 4°C for 10 min to remove cell debris. For soluble fraction, the obtained supernatant was centrifuged at 25000rpm at 4°C for 30 min. The resulting supernatant served as a fraction of cytoplasmic and periplasmic proteins. The pellet containing the crude envelope fractions was washed with 50 mM Tris-HCl, resuspended in 2 ml 50 mM Tris-HCl pH 7.2, 2% Triton X 100, 10 mM $MgCl_2$ and incubated overnight gently shaking at 4°C. The resulting sample was enriched with membrane proteins. The soluble and membrane fraction was precipitated with four volumes of ice-cold acetone at -20°C overnight and resuspended in SDS-PAGE loading buffer.

Detergent-based methods to separate the IM from the OM using Triton X 100 did not work. To check for OM proteins OMVs were isolated. To isolate OMVs the cell culture was centrifuged at 8000 rpm for 10 min. The supernatant from the culture (1l) was passed through a 0.2 µl membrane filter (Millipore) and centrifuged at 36000 rpm for 2h at 4°C. The pellet was collected to one tube, centrifuged at 44000 rpm for 2h at 4°C and resuspended in 100 µl of SDS-PAGE loading buffer. The soluble, membrane and OMVs samples were analyzed in terms of quality by immunoblots using PilB, PilC and PilQ antibodies.

4.5.8 Pull down experiments

To test for direct protein-protein interactions pull down experiments with 300 µg of each protein in CB1 buffer were performed. The mixture of two fusion proteins harboring MalE-, His_6- or GST- tags was incubated with 1 ml amylose matrix (New England Biolabs) for 1-2h at 4°C and applied on the Pierce centrifuge column. A mixture of His_6- or GST-tagged protein and MalE served as a negative control. After washing the beads with 10 column volumes of buffer CB1, the elutions were performed using buffer CB2 (for MalE-tagged proteins) or CB1 complemented with 10 mM glutathione (for GST-tagged proteins). The samples of proteins mixture (L), flow through (FT), washing step (W) and elution (E) were analyzed by immunoblot analysis using α-GltK α-GltB α-GltA α-GltC and α-MalE antibodies (Biolabs) as described in 4.5.4. The taken volume for

analysis of W and E samples was ten times greater than the volume of L and FT samples.

4.6 Microscopy

DIC and fluorescence microscopy were performed as previously described (Leonardy *et al*., 2007). Briefly, cells from exponentially growing cultures were spotted on 1.5% agar pads with A50 buffer (10 mM MOPS pH 7.2, 10 mM $CaCl_2$, 10 mM $MgCl_2$, 50 mM NaCl) on a glass slide and covered with a cover slip. Cells were incubated at RT for 15 min to allow them to attach to the agar surface. Microscopic analysis was performed using a temperature-controlled Leica DMI6000B microscope with an adaptive focus control, a motorized stage and a Hamamatsu Flash 4.0 camera. Images were recorded with Leica MM AF software package and processed with Metamorph (Molecular Devices) and ImageJ 1.46r. For time-lapse recordings the intervals between the frames were one minute.

4.7 Bioinformatic analyses

Gene and protein sequences of *M. xanthus* were obtained from TIGR database (http://cmr.jcvi.org/tigr-scripts/CMR/CmrHomePage.cgi). Functional domains were identified using SMART database (http://smart.embl-heidelberg.de/). Alignment and analysis of selected sequences was performed using Vector NTI (Invitrogen). Transmembrane helices were predicted using the TMHMM Server v. 2.0 (http://www.cbs.dtu.dk/services/TMHMM/), while type I and II signal peptides were identified using SignalP 4.1 Server (http://www.cbs.dtu.dk/services/SignalP/) and LipoP 1.0 Server (http://www.cbs.dtu.dk/services/LipoP/), respectively.

5 References

Astling, D.P., J.Y. Lee & D.R. Zusman, (2006) Differential effects of chemoreceptor methylation-domain mutations on swarming and development in the social bacterium *Myxococcus xanthus*. *Mol Microbiol* **59**: 45-55.

Baker, M.D., P.M. Wolanin & J.B. Stock, (2006) Signal transduction in bacterial chemotaxis. *Bioessays* **28**: 9-22.

Baron, D.M., K.S. Ralston, Z.P. Kabututu & K.L. Hill, (2007) Functional genomics in *Trypanosoma brucei* identifies evolutionarily conserved components of motile flagella. *Journal of cell science* **120**: 478-491.

Bean, G.J., S.T. Flickinger, W.M. Westler, M.E. McCully, D. Sept, D.B. Weibel & K.J. Amann, (2009) A22 disrupts the bacterial actin cytoskeleton by directly binding and inducing a low-affinity state in MreB. *Biochemistry* **48**: 4852-4857.

Behmlander, R.M. & M. Dworkin, (1991) Extracellular fibrils and contact-mediated cell interactions in *Myxococcus xanthus*. *J Bacteriol* **173**: 7810-7820.

Berleman, J.E. & J.R. Kirby, (2009) Deciphering the hunting strategy of a bacterial wolfpack. *Fems Microbiol Rev* **33**: 942-957.

Berleman, J.E., J.J. Vicente, A.E. Davis, S.Y. Jiang, Y.E. Seo & D.R. Zusman, (2011) FrzS regulates social motility in *Myxococcus xanthus* by controlling exopolysaccharide production. *PLoS One* **6**: e23920.

Blackhart, B.D. & D.R. Zusman, (1985) Frizzy genes of *Myxococcus xanthus* are involved in control of frequency of reversal of gliding motility. *PNAS* **82**: 8767-8770.

Blatch, G.L. & M. Lassle, (1999) The tetratricopeptide repeat: a structural motif mediating protein-protein interactions. *Bioessays* **21**: 932-939.

Bowden, M.G. & H.B. Kaplan, (1998) The *Myxococcus xanthus* lipopolysaccharide O-antigen is required for social motility and multicellular development. *Mol Microbiol* **30**: 275-284.

Bradford, M.M., (1976) A rapid and sensitive method for the quantitation of microgram quantities of protein utilizing the principle of protein-dye binding. *Analytical biochemistry* **72**: 248-254.

Bulyha, I., S. Lindow, L. Lin, K. Bolte, K. Wuichet, J. Kahnt, C. van der Does, M. Thanbichler & L. Sogaard-Andersen, (2013) Two small GTPases act in concert with the bactofilin cytoskeleton to regulate dynamic bacterial cell polarity. *Developmental cell* **25**: 119-131.

Bulyha, I., C. Schmidt, P. Lenz, V. Jakovljevic, A. Hone, B. Maier, M. Hoppert & L. Sogaard-Andersen, (2009) Regulation of the type IV pili molecular machine by dynamic localization of two motor proteins. *Mol Microbiol* **74**: 691-706.

Bustamante, V.H., I. Martinez-Flores, H.C. Vlamakis & D.R. Zusman, (2004) Analysis of the Frz signal transduction system of *Myxococcus xanthus* shows the importance of the conserved C-terminal region of the cytoplasmic chemoreceptor FrzCD in sensing signals. *Mol Microbiol* **53**: 1501-1513.

Charest, P.G. & R.A. Firtel, (2007) Big roles for small GTPases in the control of directed cell movement. *The Biochemical journal* **401**: 377-390.

Clausen, M., V. Jakovljevic, L. Sogaard-Andersen & B. Maier, (2009) High-force generation is a conserved property of type IV pilus systems. *J Bacteriol* **191**: 4633-4638.

Cole, C., J.D. Barber & G.J. Barton, (2008) The Jpred 3 secondary structure prediction server. *Nucleic acids research* **36**: W197-201.

Craig, L. & J. Li, (2008) Type IV pili: paradoxes in form and function. *Current opinion in structural biology* **18**: 267-277.

Craig, L., M.E. Pique & J.A. Tainer, (2004) Type IV pilus structure and bacterial pathogenicity. *Nat Rev Microbiol* **2**: 363-378.

Cuthbertson, L., I.L. Mainprize, J.H. Naismith & C. Whitfield, (2009) Pivotal roles of the outer membrane polysaccharide export and polysaccharide copolymerase protein families in export of extracellular polysaccharides in gram-negative bacteria. *Microbiology and molecular biology reviews : MMBR* **73**: 155-177.

Domian, I.J., K.C. Quon & L. Shapiro, (1997) Cell type-specific phosphorylation and proteolysis of a transcriptional regulator controls the G1-to-S transition in a bacterial cell cycle. *Cell* **90**: 415-424.

Dubnau, D., (1999) DNA uptake in bacteria. *Annu Rev Microbiol* **53**: 217-244.

Ducret, A., B. Fleuchot, P. Bergam & T. Mignot, (2013) Direct live imaging of cell-cell protein transfer by transient outer membrane fusion in *Myxococcus xanthus*. *Elife* **2**.

Ducret, A., M.P. Valignat, F. Mouhamar, T. Mignot & O. Theodoly, (2012) Wet-surface-enhanced ellipsometric contrast microscopy identifies slime as a major adhesion factor during bacterial surface motility. *PNAS* **109**: 10036-10041.

Dworkin, M. & H. Voelz, (1962) The formation and germination of microcysts in *Myxococcus xanthus*. *Journal of general microbiology* **28**: 81-85.

Esue, O., M. Cordero, D. Wirtz & Y. Tseng, (2005) The assembly of MreB, a prokaryotic homolog of actin. *The Journal of biological chemistry* **280**: 2628-2635.

Evans, A.G.L., H.M. Davey, A. Cookson, H. Currinn, G. Cooke-Fox, P.J. Stanczyk & D.E. Whitworth, (2012) Predatory activity of *Myxococcus xanthus* outer-membrane vesicles and properties of their hydrolase cargo. *Microbiol-Sgm* **158**: 2742-2752.

Francetic, O., N. Buddelmeijer, S. Lewenza, C.A. Kumamoto & A.P. Pugsley, (2007) Signal recognition particle-dependent inner membrane targeting of the PulG Pseudopilin component of a type II secretion system. *J Bacteriol* **189**: 1783-1793.

Friedrich, C., I. Bulyha & L. Sogaard-Andersen, (2014) Outside-in assembly pathway of the type IV pilus system in *Myxococcus xanthus*. *J Bacteriol* **196**: 378-390.

Garner, E.C., R. Bernard, W. Wang, X. Zhuang, D.Z. Rudner & T. Mitchison, (2011) Coupled, circumferential motions of the cell wall synthesis machinery and MreB filaments in *B. subtilis*. *Science* **333**: 222-225.

Hager, A.J., D.L. Bolton, M.R. Pelletier, M.J. Brittnacher, L.A. Gallagher, R. Kaul, S.J. Skerrett, S.I. Miller & T. Guina, (2006) Type IV pili-mediated secretion modulates *Francisella* virulence. *Mol Microbiol* **62**: 227-237.

Harshey, R.M., (1994) Bees arent the only ones - swarming in gram-negative bacteria. *Mol Microbiol* **13**: 389-394.

Hartzell, P. & D. Kaiser, (1991) Function of Mgla, a 22-Kilodalton protein essential for gliding in *Myxococcus xanthus*. *J Bacteriol* **173**: 7615-7624.
Henrichsen, J., (1983) Twitching Motility. *Annu Rev Microbiol* **37**: 81-93.
Herrington, D.A., R.H. Hall, G. Losonsky, J.J. Mekalanos, R.K. Taylor & M.M. Levine, (1988) Toxin, Toxin-Coregulated Pili, and the Toxr Regulon Are Essential for Vibrio-Cholerae Pathogenesis in Humans. *J Exp Med* **168**: 1487-1492.
Hodgkin, J. & D. Kaiser, (1979) Genetics of gliding motility in *Myxococcus xanthus* (Myxobacterales) - genes-controlling movement of single cells. *Mol Gen Genet* **171**: 167-176.
Hoiczyk, E., (2000) Gliding motility in cyanobacteria: observations and possible explanations. *Arch Microbiol* **174**: 11-17.
Hot, E.G., M.; Alcor, D.; Ducret, A.; Jakobczak, B.; Keilberg D.; E. Macia, S. Lacas Gervais, L. Faure, P. Lenz, M. Franco, L. Søgaard-Andersen, T. Mignot (in submission) The small G-protein MglA connects the motility machinery to the MreB actin cytoskeleton at bacterial focal adhesions.
Inclan, Y.F., S. Laurent & D.R. Zusman, (2008) The receiver domain of FrzE, a CheA-CheY fusion protein, regulates the CheA histidine kinase activity and downstream signalling to the A- and S-motility systems of *Myxococcus xanthus*. *Mol Microbiol* **68**: 1328-1339.
Inclan, Y.F., H.C. Vlamakis & D.R. Zusman, (2007) FrzZ, a dual CheY-like response regulator, functions as an output for the Frz chemosensory pathway of *Myxococcus xanthus*. *Mol Microbiol* **65**: 90-102.
Jakovljevic, V., S. Leonardy, M. Hoppert & L. Sogaard-Andersen, (2008) PilB and PilT are ATPases acting antagonistically in type IV pilus function in *Myxococcus xanthus*. *J Bacteriol* **190**: 2411-2421.
Jarrell, K.F. & M.J. McBride, (2008) The surprisingly diverse ways that prokaryotes move. *Nat Rev Microbiol* **6**: 466-476.
Julien, B., A.D. Kaiser & A. Garza, (2000) Spatial control of cell differentiation in *Myxococcus xanthus*. *PNAS* **97**: 9098-9103.
Kahnt, J., K. Aguiluz, J. Koch, A. Treuner-Lange, A. Konovalova, S. Huntley, M. Hoppert, L. Sogaard-Andersen & R. Hedderich, (2010) Profiling the outer membrane proteome during growth and development of the social bacterium *Myxococcus xanthus* by selective biotinylation and analyses of outer membrane vesicles. *J Proteome Res* **9**: 5197-5208.
Kaiser, D., (1979a) Social gliding is correlated with the presence of pili in *Myxococcus xanthus*. *PNAS* **76**: 5952-5956.
Kaiser, D., (1979b) Social gliding is correlated with the presence of pili in *Myxococcus xanthus*. *Proc. Natl. Acad. Sci. USA* **76**: 5952-5956.
Katz, B.Z., E. Zamir, A. Bershadsky, Z. Kam, K.M. Yamada & B. Geiger, (2000) Physical state of the extracellular matrix regulates the structure and molecular composition of cell-matrix adhesions. *Molecular biology of the cell* **11**: 1047-1060.
Kearns, D.B., (2010) A field guide to bacterial swarming motility. *Nat Rev Microbiol* **8**: 634-644.
Keilberg, D., K. Wuichet, F. Drescher & L. Sogaard-Andersen, (2012) A response regulator interfaces between the Frz chemosensory system and the MglA/MglB GTPase/GAP module to regulate polarity in *Myxococcus xanthus*. *Plos Genet* **8**: e1002951.

Kimura, Y., S. Yamashita, Y. Mori, Y. Kitajima & K. Takegawa, (2011) A *Myxococcus xanthus* bacterial tyrosine kinase, BtkA, is required for the formation of mature spores. *J Bacteriol* **193**: 5853-5857.

Krogh, A., B. Larsson, G. von Heijne & E.L. Sonnhammer, (2001) Predicting transmembrane protein topology with a hidden Markov model: application to complete genomes. *Journal of molecular biology* **305**: 567-580.

Laemmli, U.K., (1970) Cleavage of structural proteins during assembly of head of bacteriophage-T4. *Nature* **227**: 680-&.

Leonardy, S., G. Freymark, S. Hebener, E. Ellehauge & L. Sogaard-Andersen, (2007) Coupling of protein localization and cell movements by a dynamically localized response regulator in *Myxococcus xanthus*. *Embo J* **26**: 4433-4444.

Leonardy, S., M. Miertzschke, I. Bulyha, E. Sperling, A. Wittinghofer & L. Sogaard-Andersen, (2010) Regulation of dynamic polarity switching in bacteria by a Ras-like G-protein and its cognate GAP. *Embo J* **29**: 2276-2289.

Li, Y., V.H. Bustamante, R. Lux, D. Zusman & W. Shi, (2005a) Divergent regulatory pathways control A and S motility in *Myxococcus xanthus* through FrzE, a CheA-CheY fusion protein. *J Bacteriol* **187**: 1716-1723.

Li, Y., R. Lux, A.E. Pelling, J.K. Gimzewski & W. Shi, (2005b) Analysis of type IV pilus and its associated motility in *Myxococcus xanthus* using an antibody reactive with native pilin and pili. *Microbiology* **151**: 353-360.

Licking, E., L. Gorski & D. Kaiser, (2000) A common step for changing cell shape in fruiting body and starvation-independent sporulation of *Myxococcus xanthus*. *J Bacteriol* **182**: 3553-3558.

Luciano, J., R. Agrebi, A.V. Le Gall, M. Wartel, F. Fiegna, A. Ducret, C. Brochier-Armanet & T. Mignot, (2011) Emergence and modular evolution of a novel motility machinery in bacteria. *Plos Genet* **7**.

Maier, B., L. Potter, M. So, H.S. Seifert & M.P. Sheetz, (2002) Single pilus motor forces exceed 100 pN. *PNAS* **99**: 16012-16017.

Mattick, J.S., (2002a) Type IV pili and twitching motility. *Ann. Rev. Microbiol.* **56**: 289-314.

Mattick, J.S., (2002b) Type IV pili and twitching motility. *Annu Rev Microbiol* **56**: 289-314.

Mauriello, E.M., F. Mouhamar, B. Nan, A. Ducret, D. Dai, D.R. Zusman & T. Mignot, (2010a) Bacterial motility complexes require the actin-like protein, MreB and the Ras homologue, MglA. *Embo J* **29**: 315-326.

Mauriello, E.M.F., F. Mouhamar, B. Nan, A. Ducret, D. Dai, D.R. Zusman & T. Mignot, (2010b) Bacterial motility complexes require the actin-like protein, MreB and the Ras homologue, MglA. *Embo J* **29**: 315-326.

Mauriello, E.M.F., B.Y. Nan & D.R. Zusman, (2009) AglZ regulates adventurous (A-) motility in *Myxococcus xanthus* through its interaction with the cytoplasmic receptor, FrzCD. *Mol Microbiol* **72**: 964-977.

McBride, M.J., (2000) Bacterial gliding motility: mechanisms and mysteries. *Asm News* **66**: 203-210.

McBride, M.J., (2001) Bacterial gliding motility: multiple mechanisms for cell movement over surfaces. *Annu Rev Microbiol* **55**: 49-75.

McBride, M.J., R.A. Weinberg & D.R. Zusman, (1989) "Frizzy" aggregation genes of the gliding bacterium *Myxococcus xanthus* show sequence

similarities to the chemotaxis genes of enteric bacteria. *PNAS* **86**: 424-428.

Miertzschke, M., C. Koerner, I.R. Vetter, D. Keilberg, E. Hot, S. Leonardy, L. Sogaard-Andersen & A. Wittinghofer, (2011) Structural analysis of the Ras-like G protein MglA and its cognate GAP MglB and implications for bacterial polarity. *Embo J* **30**: 4185-4197.

Mignot, T., (2007) The elusive engine in Myxococcus xanthus gliding motility. *Cell Mol Life Sci* **64**: 2733-2745.

Mignot, T., J.W. Shaevitz, P.L. Hartzell & D.R. Zusman, (2007) Evidence that focal adhesion complexes power bacterial gliding motility. *Science* **315**: 853-856.

Miyamoto, S., S.K. Akiyama & K.M. Yamada, (1995a) Synergistic roles for receptor occupancy and aggregation in integrin transmembrane function. *Science* **267**: 883-885.

Miyamoto, S., H. Teramoto, O.A. Coso, J.S. Gutkind, P.D. Burbelo, S.K. Akiyama & K.M. Yamada, (1995b) Integrin function: molecular hierarchies of cytoskeletal and signaling molecules. *The Journal of cell biology* **131**: 791-805.

Miyata, M., (2010) Unique centipede mechanism of *Mycoplasma* gliding. *Annu Rev Microbiol* **64**: 519-537.

Muller, F.D., C.W. Schink, E. Hoiczyk, E. Cserti & P.I. Higgs, (2012) Spore formation in *Myxococcus xanthus* is tied to cytoskeleton functions and polysaccharide spore coat deposition. *Mol Microbiol* **83**: 486-505.

Muller, F.D., A. Treuner-Lange, J. Heider, S.M. Huntley & P.I. Higgs, (2010) Global transcriptome analysis of spore formation in *Myxococcus xanthus* reveals a locus necessary for cell differentiation. *BMC genomics* **11**: 264.

Nakane, D. & M. Miyata, (2007) Cytoskeletal "jellyfish" structure of *Mycoplasma mobile*. *PNAS* **104**: 19518-19523.

Nakane, D., K. Sato, H. Wada, M.J. McBride & K. Nakayama, (2013) Helical flow of surface protein required for bacterial locomotion. *Biophys J* **104**: 639a-639a.

Nan, B., E.M. Mauriello, I.H. Sun, A. Wong & D.R. Zusman, (2010a) A multi-protein complex from Myxococcus xanthus required for bacterial gliding motility. *Mol Microbiol* **76**: 1539-1554.

Nan, B.Y., J.N. Bandaria, A. Moghtaderi, I.H. Sun, A. Yildiz & D.R. Zusman, (2013) Flagella stator homologs function as motors for myxobacterial gliding motility by moving in helical trajectories. *PNAS* **110**: E1508-E1513.

Nan, B.Y., J. Chen, J.C. Neu, R.M. Berry, G. Oster & D.R. Zusman, (2011) Myxobacteria gliding motility requires cytoskeleton rotation powered by proton motive force. *PNAS* **108**: 2498-2503.

Nan, B.Y., E.M.F. Mauriello, I.H. Sun, A. Wong & D.R. Zusman, (2010b) A multi-protein complex from *Myxococcus xanthus* required for bacterial gliding motility. *Mol Microbiol* **76**: 1539-1554.

Nudleman, E., D. Wall & D. Kaiser, (2005) Cell-to-cell transfer of bacterial outer membrane lipoproteins. *Science* **309**: 125-127.

Nudleman, E., D. Wall & D. Kaiser, (2006) Polar assembly of the type IV pilus secretin in *Myxococcus xanthus*. *Mol Microbiol* **60**: 16-29.

Nunn, D.N. & S. Lory, (1991) Product of the *Pseudomonas aeruginosa* gene pilD is a prepilin leader peptidase. *PNAS* **88**: 3281-3285.

O'Connor, K.A. & D.R. Zusman, (1991a) Analysis of *Myxococcus xanthus* cell types by two-dimensional polyacrylamide gel electrophoresis. *J Bacteriol* **173**: 3334-3341.

O'Connor, K.A. & D.R. Zusman, (1991b) Development in *Myxococcus xanthus* involves differentiation into 2 cell-types, peripheral rods and spores. *J Bacteriol* **173**: 3318-3333.

O'Toole, G.A. & R. Kolter, (1998) Flagellar and twitching motility are necessary for *Pseudomonas aeruginosa* biofilm development. *Mol Microbiol* **30**: 295-304.

Overgaard, M., S. Wegener-Feldbrugge & L. Sogaard-Andersen, (2006) The orphan response regulator DigR is required for synthesis of extracellular matrix fibrils in *Myxcoccus xanthus*. *J Bacteriol* **188**: 4384-4394.

Pathak, D.T. & D. Wall, (2012) Identification of the *cglC*, *cglD*, *cglE*, and *cglF* genes and their role in cell contact-dependent gliding motility in *Myxococcus xanthus*. *J Bacteriol* **194**: 1940-1949.

Pathak, D.T., X. Wei, A. Bucuvalas, D.H. Haft, D.L. Gerloff & D. Wall, (2012) Cell contact-dependent outer membrane exchange in myxobacteria: genetic determinants and mechanism. *Plos Genet* **8**: e1002626.

Patryn, J., K. Allen, K. Dziewanowska, R. Otto & P.L. Hartzell, (2010) Localization of MglA, an essential gliding motility protein in *Myxococcus xanthus*. *Cytoskeleton* **67**: 322-337.

Pelicic, V., (2008) Type IV pili: e pluribus unum? *Mol Microbiol* **68**: 827-837.

Petersen, T.N., S. Brunak, G. von Heijne & H. Nielsen, (2011) SignalP 4.0: discriminating signal peptides from transmembrane regions. *Nature methods* **8**: 785-786.

Postle, K. & R.J. Kadner, (2003) Touch and go: tying TonB to transport. *Mol Microbiol* **49**: 869-882.

Raymond, K.N., E.A. Dertz & S.S. Kim, (2003) Enterobactin: An archetype for microbial iron transport. *PNAS* **100**: 3584-3588.

Razin, S., D. Yogev & Y. Naot, (1998) Molecular biology and pathogenicity of mycoplasmas. *Microbiology and molecular biology reviews : MMBR* **62**: 1094-1156.

Reichenbach, H., (1999) The ecology of the myxobacteria. *Environmental microbiology* **1**: 15-21.

Remis, J.P., D. Wei, A. Gorur, M. Zemla, J. Haraga, S. Allen, H.E. Witkowska, J.W. Costerton, J.E. Berleman & M. Auer, (2014) Bacterial social networks: structure and composition of *Myxococcus xanthus* outer membrane vesicle chains. *Environmental microbiology* **16**: 598-610.

Remmert, M., D. Linke, A.N. Lupas & J. Soding, (2009) HHomp-prediction and classification of outer membrane proteins. *Nucleic acids research* **37**: W446-W451.

Rice, P., I. Longden & A. Bleasby, (2000) EMBOSS: the European Molecular Biology Open Software Suite. *Trends in genetics : TIG* **16**: 276-277.

Ridley, A.J. & A. Hall, (1992) The small GTP-binding protein rho regulates the assembly of focal adhesions and actin stress fibers in response to growth factors. *Cell* **70**: 389-399.

Rosenberg, E., K.H. Keller & M. Dworkin, (1977) Cell Density-Dependent Growth of *Myxococcus xanthus* on Casein. *J Bacteriol* **129**: 770-777.

Sambrook, J., Fritsch, E.F., Maniatis, T., (1989) *Molecular cloning. A laboratory manual.* Cold Spring Harbor, N.Y., Cold Spring Harbor Laboratory Press.

Scheurwater, E.M. & L.L. Burrows, (2011) Maintaining network security: how macromolecular structures cross the peptidoglycan layer. *Fems Microbiol Lett* **318**: 1-9.

Seto, S., A. Uenoyama & M. Miyata, (2005) Identification of a 521-kilodalton protein (Gli521) involved in force generation or force transmission for *Mycoplasma mobile* gliding. *J Bacteriol* **187**: 3502-3510.

Shi, W. & D.R. Zusman, (1993) The two motility systems of *Myxococcus xanthus* show different selective advantages on various surfaces. *Proc. Natl. Acad. Sci. USA* **90**: 3378-3382.

Shi, X.Q., S. Wegener-Feldbrugge, S. Huntley, N. Hamann, R. Hedderich & L. Sogaard-Andersen, (2008) Bioinformatics and experimental analysis of proteins of two-component systems in *Myxococcus xanthus*. *J Bacteriol* **190**: 613-624.

Shimkets, L.J., (1999a) Intercellular signaling during fruiting-body development of *Myxococcus xanthus*. *Annu. Rev. Microbiol.* **53**: 525-549.

Shimkets, L.J., (1999b) Intercellular signaling during fruiting-body development of *Myxococcus xanthus*. *Annu Rev Microbiol* **53**: 525-549.

Shrivastava, A., J.J. Johnston, J.M. van Baaren & M.J. McBride, (2013) *Flavobacterium johnsoniae* GldK, GldL, GldM, and SprA are required for secretion of the cell surface gliding motility adhesins SprB and RemA. *J Bacteriol* **195**: 3201-3212.

Shrivastava, A., R.G. Rhodes, S. Pochiraju, D. Nakane & M.J. McBride, (2012) *Flavobacterium johnsoniae* RemA is a mobile cell surface lectin involved in gliding. *J Bacteriol* **194**: 3678-3688.

Siewering, K., S. Jain, C. Friedrich, M.T. Webber-Birungi, D.A. Semchonok, I. Binzen, A. Wagner, S. Huntley, J. Kahnt, A. Klingl, E.J. Boekema, L. Sogaard-Andersen & C. van der Does, (2014) Peptidoglycan-binding protein TsaP functions in surface assembly of type IV pili. *PNAS* **111**: E953-961.

Skerker, J.M. & H.C. Berg, (2001) Direct observation of extension and retraction of type IV pili. *PNAS* **98**: 6901-6904.

Spormann, A.M., (1999) Gliding motility in bacteria: Insights from studies of *Myxococcus xanthus*. *Microbiology and molecular biology reviews : MMBR* **63**: 621-+.

Stock, A.M., V.L. Robinson & P.N. Goudreau, (2000) Two-component signal transduction. *Annual review of biochemistry* **69**: 183-215.

Sudo, S.Z. & M. Dworkin, (1969) Resistance of vegetative cells and microcysts of *Myxococcus xanthus*. *J Bacteriol* **98**: 883-887.

Sun, H., Z. Yang & W. Shi, (1999) Effect of cellular filamentation on adventurous and social gliding motility of *Myxococcus xanthus*. *PNAS* **96**: 15178-15183.

Sun, M., M. Wartel, E. Cascales, J.W. Shaevitz & T. Mignot, (2011a) Motor-driven intracellular transport powers bacterial gliding motility. *Proc Natl Acad Sci U S A* **108**: 7559-7564.

Sun, M.Z., M. Wartel, E. Cascales, J.W. Shaevitz & T. Mignot, (2011b) Motor-driven intracellular transport powers bacterial gliding motility. *PNAS* **108**: 7559-7564.

Tudyka, T. & A. Skerra, (1997) Glutathione S-transferase can be used as a C-terminal, enzymatically active dimerization module for a recombinant

protease inhibitor, and functionally secreted into the periplasm of *Escherichia coli*. *Protein Sci* **6**: 2180-2187.

Uenoyama, A., A. Kusumoto & M. Miyata, (2004) Identification of a 349-kilodalton protein (Gli349) responsible for cytadherence and glass binding during gliding of *Mycoplasma mobile*. *J Bacteriol* **186**: 1537-1545.

Uenoyama, A. & M. Miyata, (2005) Identification of a 123-kilodalton protein (Gli123) involved in machinery for gliding motility of *Mycoplasma mobile*. *J Bacteriol* **187**: 5578-5584.

van den Ent, F., L.A. Amos & J. Lowe, (2001) Prokaryotic origin of the actin cytoskeleton. *Nature* **413**: 39-44.

van Geest, M. & J.S. Lolkema, (2000) Membrane topology and insertion of membrane proteins: Search for topogenic signals. *Microbiology and molecular biology reviews : MMBR* **64**: 13-+.

van Teeffelen, S., S. Wang, L. Furchtgott, K.C. Huang, N.S. Wingreen, J.W. Shaevitz & Z. Gitai, (2011) The bacterial actin MreB rotates, and rotation depends on cell-wall assembly. *PNAS* **108**: 15822-15827.

Wachi, M., M. Doi, S. Tamaki, W. Park, S. Nakajima-Iijima & M. Matsuhashi, (1987) Mutant isolation and molecular cloning of mre genes, which determine cell shape, sensitivity to mecillinam, and amount of penicillin-binding proteins in Escherichia coli. *J Bacteriol* **169**: 4935-4940.

Wall, D., S.S. Wu & D. Kaiser, (1998) Contact stimulation of Tgl and type IV pili in *Myxococcus xanthus*. *J Bacteriol* **180**: 759-761.

Wartel, M., A. Ducret, S. Thutupalli, F. Czerwinski, A.V. Le Gall, E.M. Mauriello, P. Bergam, Y.V. Brun, J. Shaevitz & T. Mignot, (2013) A versatile class of cell surface directional motors gives rise to gliding motility and sporulation in *Myxococcus xanthus*. *PLoS biology* **11**: e1001728.

Wei, X., D.T. Pathak & D. Wall, (2011) Heterologous protein transfer within structured myxobacteria biofilms. *Mol Microbiol* **81**: 315-326.

Wei, X., C.N. Vassallo, D.T. Pathak & D. Wall, (2014) Myxobacteria produce outer membrane enclosed tubes in unstructured environments. *J Bacteriol*.

Wireman, J.W. & M. Dworkin, (1977) Developmentally induced autolysis during fruiting body formation by *Myxococcus xanthus*. *J Bacteriol* **129**: 798-802.

Wolgemuth, C., E. Hoiczyk, D. Kaiser & G. Oster, (2002a) How myxobacteria glide. *Curr Biol* **12**: 369-377.

Wolgemuth, C., E. Hoiczyk, D. Kaiser & G. Oster, (2002b) How myxobacteria glide. *Curr. Biol.* **12**: 369-377.

Xie, H., M.A. Pallero, K. Gupta, P. Chang, M.F. Ware, W. Witke, D.J. Kwiatkowski, D.A. Lauffenburger, J.E. Murphy-Ullrich & A. Wells, (1998) EGF receptor regulation of cell motility: EGF induces disassembly of focal adhesions independently of the motility-associated PLCgamma signaling pathway. *Journal of cell science* **111 (Pt 5)**: 615-624.

Yang, R., S. Bartle, R. Otto, A. Stassinopoulos, M. Rogers, L. Plamann & P. Hartzell, (2004a) AglZ is a filament-forming coiled-coil protein required for adventurous gliding motility of Myxococcus xanthus. *J Bacteriol* **186**: 6168-6178.

Yang, R.F., S. Bartle, R. Otto, A. Stassinopoulos, M. Rogers, L. Plamann & P. Hartzell, (2004b) AglZ is a filament-forming coiled-coil protein required

for adventurous gliding motility of *Myxococcus xanthus*. *J Bacteriol* **186**: 6168-6178.

Youderian, P., N. Burke, D.J. White & P.L. Hartzell, (2003) Identification of genes required for adventurous gliding motility in *Myxococcus xanthus* with the transposable element mariner. *Mol Microbiol* **49**: 555-570.

Yu, R. & D. Kaiser, (2007) Gliding motility and polarized slime secretion. *Mol Microbiol* **63**: 454-467.

Zaidel-Bar, R., C. Ballestrem, Z. Kam & B. Geiger, (2003) Early molecular events in the assembly of matrix adhesions at the leading edge of migrating cells. *Journal of cell science* **116**: 4605-4613.

Zhang, Y., M. Franco, A. Ducret & T. Mignot, (2010) A bacterial Ras-like small GTP-binding protein and its cognate GAP establish a dynamic spatial polarity axis to control directed motility. *PLoS biology* **8**.

Zhang, Y., M. Guzzo, A. Ducret, Y.Z. Li & T. Mignot, (2012) A dynamic response regulator protein modulates G-protein-dependent polarity in the bacterium *Myxococcus xanthus*. *Plos Genet* **8**: e1002872.

Zusman, D.R., (1982) "Frizzy" mutants: a new class of aggregation-defective developmental mutants of *Myxococcus xanthus*. *J Bacteriol* **150**: 1430-1437.

Zusman, D.R., A.E. Scott, Z. Yang & J.R. Kirby, (2007) Chemosensory pathways, motility and development in *Myxococcus xanthus*. *Nat Rev Microbiol* **5**: 862-872.

Erklärung

Hiermit versichere ich, dass ich die vorliegende Dissertation mit dem Titel „Identification and characterization of a novel cell-envelope subcomplex crucial for A-motility in *M. xanthus*“ selbstständig verfasst, keine anderen als die im Text angegebenen Hilfsmittel verwendet und sämtliche Stellen, die im Wortlaut oder dem Sinn nach anderen Werken entnommen sind, mit Quellenangaben kenntlich gemacht habe.

Die Dissertation wurde in der jetzigen oder einer ähnlichen Form noch bei keiner anderen Hochschule eingereicht und hat noch keinen sonstigen Prüfungszwecken gedient.

Ort, Datum

Beata Jakobczak